

THE ROLE OF TAU IN AMYLOID β PLAQUE GROWTH AND FORMATION

Dissertation

zur Erlangung des naturwissenschaftlichen Doktorgrades

an der Fakultät für Biologie

der Ludwig-Maximilians-Universität

München

vorgelegt von

Hazal Salihoglu

München, den 07.06.2019



Neyi arıyorsan O'sun sen.

What you seek is seeking you.

Was du suchst, sucht dich.

Mevlana (1207-1273)

Diese Dissertation wurde unter der Leitung von Prof. Dr. Jochen Herms am Institut für Neuropathologie der Ludwig-Maximilians-Universität angefertigt und von Prof. Dr. Wolfgang Enard an der Fakultät für Biologie vertreten.

Eidesstattliche Erklärung

Ich versichere hiermit an Eides statt, dass die vorgelegte Dissertation von mir selbständig und ohne unerlaubte Hilfe angefertigt ist. Hiermit erkläre ich, dass die Dissertation nicht ganz oder in wesentlichen Teilen einer anderen Prüfungskommission vorgelegt worden ist und ich mich anderweitig einer Doktorprüfung ohne Erfolg nicht unterzogen habe.

München, den 17.10.2018

Hazal Salihoglu

Erstgutachter: Prof. Dr. Wolfgang Enard

Zweitgutachter: Dr. rer. nat. Anja Horn-Bochtler

Tag der Abgabe: 06.11.2018

Tag der mündlichen Prüfung: 27.05.19

Table of Contents

ACKNOWLEDGEMENTS	1
DECLARATION.....	2
LIST OF FIGURES	3
ABBREVIATIONS	4
ABSTRACT	5
ABSTRAKT	6
AIM OF THE STUDY.....	7
INTRODUCTION	8
Alzheimer`s disease	8
Tau protein (MAPT)	13
The role of Tau in AD	18
Tau and axonal transport	21
Tau knockout mice.....	22
AD mice crossed on Tau deficient background	23
Plaque-associated dystrophies	25
BACE1 (β -site APP cleaving enzyme) protein	29
The role of BACE1 in dystrophies at plaques.....	30
The Alzheimer mouse model – APPPS1.....	31
The VGLUT1 ^{Venus} mouse line	32
MATERIALS AND METHODS	34
RESULTS.....	47
Tau expression is important for plaque growth and the formation of new plaques.47	
Plaques are less compact in tau deficient APPPS1 mice	49
Tau expression contributes to the formation of new plaques in close proximity of pre-existing plaques	50
Lack of Tau decreases BACE1 volume fraction around plaques	51
The decrease in BACE1 volume fraction around plaques was observed in Tau ^{-/-} x APPPS1 mice	53
Tau expression modulates APP-positive accumulations in peri-plaque dystrophies	54

Table of contents

Pre-synaptic transportation of VGLUT1 is not affected by absence of Tau	56
Tau deficiency does not affect the expression of APP, BACE and LAMP1 in pre-synaptic terminals.....	58
The anterograde transport of VGLUT1 within axonal dystrophies is not altered by lack of tau.....	59
Microglia activation at plaques is independent of the presence of tau	61
BACE1 protein levels are significantly reduced in the whole brains of Tau ^{-/-} x APPPS1	62
DISCUSSION	64
CONCLUSION	75
CONTRIBUTIONS.....	76
ACCEPTED PAPERS.....	77
CURRICULUM VITAE	79
REFERENCES	81

ACKNOWLEDGEMENTS

For making my PhD experience worthwhile I would like to thank all of the old and new PhD students and lab members and Jochen Herms for providing me the opportunity to pursue a life long awaited scientific career. I specially thank Elena Montagna for being my reliable friend, for being with me inside and outside of the lab and her sincere advice. Many thanks to Eva Rodrigues, Anna Jaworska, Viktoria Korzhova for making lunch- and coffee breaks and activities joyful and not just a necessary uptake of nutrition.

I thank Finn Peters for his collaboration and for his fruitful discussions and positive attitude. Also I would like to thank Severin Filser for his useful comments and corrections on my thesis.

My very very special thanks go to my parents (Nesrin Salihoglu, Mustafa Salihoglu) for their year's long effort to raise me as me. I am sincerely grateful to have them not only for their endless support and but also for being the most reliable humans in the universe. I also thank to my sister, Idil Salihoglu, for teaching me how to stay positive in also difficult moments. I thank my grandmother for teaching me how to be an independent woman in this world.

I would not be able to finish this challenging PhD journey without Arjan Dijke. Last but not least, I specially thank him for his endless patience for dealing with the cranky, sensitive and lost child who is me and for his smart jokes which I occasionally understand. I am so grateful to have him as being my lifelong best buddy.

DECLARATION

All work included in this thesis was performed at the Ludwig-Maximilians-University under the supervision of Prof. Dr. Jochen Herms.

For the project, Hazal Salihoglu performed most of the experimental procedures described. Dr. Finn Peters was involved in the analysis of some of the in vivo imaging data. Novartis performed some biochemical measurements (quantification of Abeta) in one mouse cohort.

I confirm that these statements about the contribution of Hazal Salihoglu are accurate.

Munich, 07. September 2018

Prof. Dr. Jochen Herms

LIST OF FIGURES

<i>Figure 1.</i>	10
<i>Figure 2:</i>	12
<i>Figure 3:</i>	16
<i>Figure 4.</i>	23
<i>Figure 5.</i>	32
<i>Figure 6.</i>	33
<i>Figure 7.</i>	40
<i>Figure 8.</i>	41
<i>Figure 9.</i>	45
<i>Figure 10.</i>	48
<i>Figure 11.</i>	50
<i>Figure 12.</i>	51
<i>Figure 13.</i>	52
<i>Figure 14.</i>	53
<i>Figure 15.</i>	54
<i>Figure 16.</i>	55
<i>Figure 17.</i>	57
<i>Figure 18.</i>	59
<i>Figure 19.</i>	60
<i>Figure 20.</i>	62
<i>Figure 21.</i>	63

ABBREVIATIONS

A β	Amyloid beta peptides
AD	Alzheimer`s Disease
Ach	Acetylcholine
ANOVA	Analysis of Variance
APP	Amyloid Precursor Protein
AV	Autophagolysosomes
A β	Amyloid Beta
BACE1	<i>β-site of APP cleaving enzyme</i>
CNS	Central Nervous System
CSF	Cerebrospinal fluid
DNA	Deoxyribonucleic acid
FAD	Familial Alzheimer`s Disease
FRAP	Fluorescence recovery after photobleaching
GFP	Green Fluorescent Protein
GSM	Gamma Secretase Modulator
KO	Knockout
LAMP1	Lysosomal-associated membrane protein 1
LTP	Long-term potentiation
MAPT	Microtubule-associated protein tau
MS	Mass spectrometry
NF	Neurofilamets
PBS	Phosphate-buffered saline
PCR	Polymerase chain reaction
PNS	Peripheral Nervous System
PS	Presenilin
PSD95	Postsynaptic density protein 95
RM	Repeated measure
Tg	Transgenic
TM	Transmembrane
VGLUT1	Vesicular glutamate transporter 1
WT	Wild type

ABSTRACT

Alzheimer`s disease (AD), a very complex neurodegenerative disease, is characterized histopathological through amyloid plaques (formed by accumulation of A β -peptides which are formed by consecutive cleavage of the APP protein) and neurofibrillary tangles (aggregates of hyperphosphorylated tau protein). Although these two protein accumulations are characteristic for this disease, a mechanistic link between them has yet to be established. In the current study, chronic *in vivo* two-photon microscopy was performed in a transgenic AD mouse model with lack of murine tau protein to monitor the impact of the tau protein on early and late β -amyloid pathology. The longitudinal approach allowed to assess the kinetics of growth and formation of individual plaques and associated axonal and presynaptic dystrophies. Lack of tau could not prevent but slowed down the progressive β -amyloid deposition and associated synaptic pathology significantly. Notably, the data revealed that the accumulation of APP and BACE1 in axonal and presynaptic dystrophies is tau-dependent. The observed findings suggest a new relation between the expression of tau and amyloid beta peptide pathology which may have profound implications for new strategies to hold the disease progression.

ABSTRAKT

Alzheimer ist eine komplexe neurodegenerative Erkrankung, die histopathologisch durch das Auftreten von β -amyloiden Plaques und neurofibrillären Tangles charakterisiert ist. Plaques entstehen durch Akkumulation des β -amyloiden Peptids ($A\beta$), welches durch sequenzielle Spaltung des APP-Proteins gebildet wird. Tangles bestehen aus hyperphosphoryliertem Tau Protein. Obwohl die Akkumulation dieser beiden Proteine für die Alzheimer-Krankheit charakteristisch ist, bleibt die mechanistische Verbindung zwischen ihnen bislang unklar. In der aktuellen Studie wurde der Einfluss des Tau-Proteins auf die frühe und späte $A\beta$ -Pathologie untersucht. Dafür wurde chronische in vivo Zwei-Photonen-Mikroskopie in einem transgenen Alzheimer Mausmodell mit deletiertem Tau-Gen durchgeführt. Der longitudinale Ansatz ermöglichte die Beurteilung der Wachstumskinetik und Bildungsrate einzelner Plaques und damit verbundener axonaler Dystrophien. In Abwesenheit von Tau wurde die fortschreitende $A\beta$ -Ablagerung und die damit verbundene synaptische Pathologie zwar nicht verhindert, jedoch verlangsamt. Bemerkenswerterweise zeigten die Daten, dass die Akkumulation von APP und BACE1 in axonalen und präsynaptischen Dystrophien Tau abhängig ist. Die beobachteten Ergebnisse deuten auf einen neuen Zusammenhang zwischen Tau und der $A\beta$ -Pathologie hin. Die Erkenntnisse könnten tiefgreifende Auswirkungen auf neue Strategien zur potentiellen Behandlung der Alzheimer-Erkrankung haben.

AIM OF THE STUDY

The hallmarks of Alzheimer's disease (AD) are amyloid plaque pathology by accumulation of β -amyloid ($A\beta$) peptides and neurofibrillary tangles by hyperphosphorylation of tau. The 'amyloid cascade' hypothesis represents a widely accepted concept for the description of the cellular events associated with AD. The prevalent amyloid cascade hypothesis postulates abnormal production and accumulation of β -amyloid ($A\beta$) as the most critical trigger in the development of Alzheimer's disease (AD) pathology. According to this classical view, $A\beta$ is an executor of tau pathology, which in turn affects neuronal and synaptic function, neuronal toxicity and degeneration. However, the relation between $A\beta$ and tau pathology throughout the disease development is not understood fully.

We aimed to investigate the dynamics of individual amyloid plaque growth and the development of associated presynaptic and axonal pathology by chronic, long-term *in vivo* two-photon imaging as well as immunohistochemistry. In order to tackle this question, we generated a $Tau^{-/-}$ x APPPS1 x VGlut1^{Venus} mouse line by crossing transgenic an Alzheimer mouse model APPPS1 mice (Radde et al., 2006) with VGLUT1^{Venus} mice (Herzog et al., 2011) and $Tau^{-/-}$ mice (Dawson et al., 2001).

INTRODUCTION

Alzheimer`s disease

Prevalence

Alzheimer`s disease is a progressive, unceasing, neurodegenerative disorder that affects wide areas of the cerebral cortex and hippocampus (Brettschneider et al., 2015). Abnormalities in the frontal and temporal regions are early signs of the disease, and they slowly progress to other areas of the neocortex at rates varying between individuals.

Alzheimer`s disease is a chronic and fatal neurodegenerative disease with long preclinical and prodromal phases (approximately 20 years) with an average clinical duration of 8–10 years. The disease has an estimated prevalence of 10–30% of the population >65 years of age with an incidence of 1–3%. Most common form in patients with Alzheimer`s disease (>95%) is the sporadic form, which is characterized by a late onset (80–90 years of age) (Kawas et al., 2000; Norton et al., 2014). The sporadic form develops due to failure to clear the amyloid- β ($A\beta$) peptide from the brain and depends on numerous genetic risk factors (Masters et al., 2015). Besides, co-morbidities such as cerebrovascular disease and hippocampal sclerosis are frequent at this age in those patients; which brings problems in incorrect diagnosis.

A small proportion of patients (<1%), on the other hand, carry inherited genetic mutations in presenilins, amyloid precursor protein (APP) production and processing of $A\beta$ (Terwel et al., 2002). The familial disease develops at a much younger age (mean age of ~45 years).

The current gold standard in biomarkers included positron emission tomography (PET) for brain $A\beta$ imaging and $A\beta$ and tau concentrations in the cerebrospinal fluid (CSF) biomarkers allow detecting AD 15-20 years before clinical onset (Jansen et al., 2015; Ossenkoppele et al., 2015). In most clinical respects, the sporadic and familial forms of Alzheimer`s disease are comparable, including the rate of disease progression and biomarker profiles (Shah et al., 2017). Many risk factors such as mid-life hypertension (RR: 1.61), mid- life obesity (RR: 1.60), physical inactivity (RR: 1.82), depression (RR: 1.65), smoking (RR: 1.59) and low educational attainment (RR: 1.59) are also involved in the disease (Norton et al., 2014). Several approved drugs ameliorate some of the symptoms

of Alzheimer's disease, but no current interventions can modify the underlying disease mechanisms. Management is focused on the support of the social networks surrounding the patient and the treatment of any comorbid illnesses, such as hypertension, diabetes and cerebrovascular disease.

Hallmarks

The neuropathological and neurochemical hallmarks of Alzheimer's disease can be listed as: synaptic, neuronal and memory loss (Götz et al., 2004); abnormality in specific neurotransmitters affecting cholinergic, monoaminergic and glutamatergic systems (Noetzli and Eap, 2013); the presence of abnormal proteinaceous deposits in neurons (noted as neurofibrillary tangles) (Glennner and Wong, 1984) and in the extracellular space (as cerebrovascular, diffuse and neuritic plaques) (Glennner and Wong, 1984).

In pathological levels, specific protein inclusions are observed in neurodegenerative disorders (Goedert, 2009). Two types of aberrant protein deposits were described in Alzheimer's disease: firstly intra-neuronal tau tangles and secondly extra-neuronal amyloid β peptides which are also seen in the walls of blood vessels (Brion et al., 1985; Masters et al., 1985). Recent studies propose that protein assemblies follow self-propagating features and alternative conformations, such as prions (Jucker and Walker, 2013). The direct or indirect mechanical relation between tangles and plaques remains elusive. On the other hand, tau inclusions correlate better with cognitive impairment than amyloid- β deposits (Arriagada et al., 1992).

A β plaques are encountered in basal temporal and orbitofrontal neocortex in the early stages of the AD (Braak and Braak, 1991; Thal et al., 2002). In the later stages, plaques are found in many brain regions such as throughout the neocortex, hippocampal formation, amygdala and basal ganglia (Braak and Braak, 1997). Tau inclusions are observed in locus coeruleus and entorhinal cortex. In later stages, tangles are also detected in the hippocampal formation and in the neocortex (**Figure 1**) (Morris et al., 2014).

Plaques and neurofibrillary lesions were revealed by electron microscopy to be composed of abnormal filaments whose diameter is of ~ 10 nm with the fine unbranched structure (Eisenberg and Jucker, 2012). Amyloid filaments form several proto-filaments with β -sheet structures stabilized through hydrogen bonds, predominantly in parallel form.

Amyloidogenic peptides in crystal structures complement each other across the sheet-sheet confirmation without water, in dry-steric zipper form (Sawaya et al., 2007; Eisenberg and Jucker, 2012).

Studying Alzheimer's disease mechanisms in humans will bring new insights into the pathogenesis, diagnosis, and treatment of the disease. Since it is a disease associated with memory decline, understanding the disease will eventually lead to understanding of memory. A β and tau are two elements contributing to Alzheimer's disease.

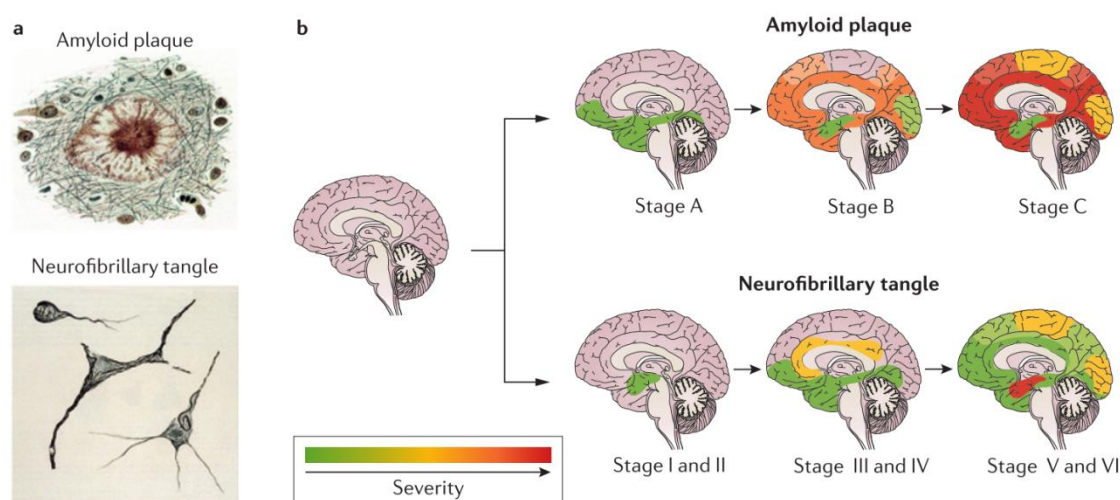


Figure 1. Amyloid plaques and neurofibrillary tangles progression. (A) Amyloid plaques and neurofibrillary tangles, from Spielmeyer's classic textbook 'Histopathologie des Nervensystems' using the Bielschowsky method of silver impregnation to visualize the aggregated proteins that constitute the extracellular plaques and intracellular neurofibrillary tangles. (B) In typical cases of Alzheimer's disease, A β deposition precedes neurofibrillary and neuritic changes with an apparent origin in the frontal and temporal lobes, hippocampus and limbic system (top row). Less commonly, the disease seems to emerge from other regions of the cerebral neocortex (parietal and occipital lobes) with relative sparing of the hippocampus. The neurofibrillary tangles and neuritic degeneration start in the medial temporal lobes and hippocampus and progressively spread to other areas of the neocortex (bottom row). A β deposition (stages A, B, and C) and neurofibrillary tangles (stages I–VI) are adapted from Braak and Braak. Image is used with a license details and the terms and conditions provided by Springer Nature and Copyright Clearance Center (Masters et al., 2015) (Licence # 4266481010097; Jan 12, 2018).

Amyloid cascade hypothesis:

The APP is a type 1 transmembrane glycoprotein (Masters and Selkoe, 2012) whose N-terminus is region located in the extracellular space and its C-terminus intracellular. N-terminal side of the APP is cleaved by β -secretase and successively by γ -secretase (for

reviews see (Goedert, 2015; Montagna et al., 2017). β -site APP cleaving enzyme 1 (β -secretase, BACE1) is a type I transmembrane aspartyl protease, whose active site is in the extracellular space. It is a rate-limiting factor in $A\beta$ peptide production by removing the extracellular fragment $sAPP\beta$ from APP. γ -Secretase is a membrane-embedded aspartyl protease. Although γ -secretase has several domains such as presenilin (PS; including PS1 and PS2), nicastrin, anterior pharynx defective 1 (APH-1), and presenilin enhancer 2 (PEN-2), PS domains are actively involved in APP cleavage (Zhang et al., 2014). The various isoforms of γ -secretase cleave APP at particular sites that produce $A\beta_{37}$, $A\beta_{38}$, $A\beta_{39}$, $A\beta_{40}$, $A\beta_{42}$, and $A\beta_{43}$ peptides (Golde et al., 2000; Selkoe, 2001). Approximately 90% of secreted $A\beta$ peptides are 40 aa long ($A\beta_{40}$) (Qi-Takahara et al., 2005). The second most common $A\beta$ species is $A\beta_{42}$, which is prone to aggregate. Consequently, $A\beta$ peptides spontaneously aggregate into soluble oligomers, which come together to form fibrils and plaques (**Figure 2**). Non-pathogenic form of APP, more explicitly P3, is produced by α -secretase and successively γ -secretase cleavage (Phinney et al., 1999).

Mutations in APP are located near the β - and γ -secretase cleavage sites as well as within $A\beta$ region (Benilova et al., 2012; Goedert, 2015). Mutations near the β -secretase cleavage site enhance production of $A\beta$, whereas those near the γ -secretase cleavage site increase the ratio of $A\beta_{42}$ to $A\beta_{40}$. Mutations within $A\beta$ region increase rates of aggregation, suggesting that familial AD is initiated by the aggregation of $A\beta$.

APP expressed on the cell surface is endocytosed. After endocytosis, endosomal $A\beta$ is produced and excreted to the extracellular space (Morris et al., 2014). $A\beta$ is a typical product of the APP metabolism and is generated at significant levels in neurons and low levels in other cell types. The neuronal function of APP is yet controversial, but it might be associated with synaptic plasticity. Multiple lines of evidence suggest that $A\beta$ accumulation and a change of conformation to forms with a high β -sheet structure is essential in Alzheimer's disease pathogenesis (Holtzman et al., 2002).

Plaques can be identified by light microscopy using methods specific for fibrillar amyloids such as thioflavin-S or Congo red staining. They can be classified into two main types: "primitive" and "cored" plaques. Primitive plaques are composed of extracellular wisps of amyloid woven among a dense cluster of dystrophic neurites; whereas cored plaques possess a large central mass of amyloid. Sometimes this amyloid core has a star-shaped

appearance with spokes of amyloid extending outward, surrounded by a cluster of dystrophic neurites and wisps of amyloid.

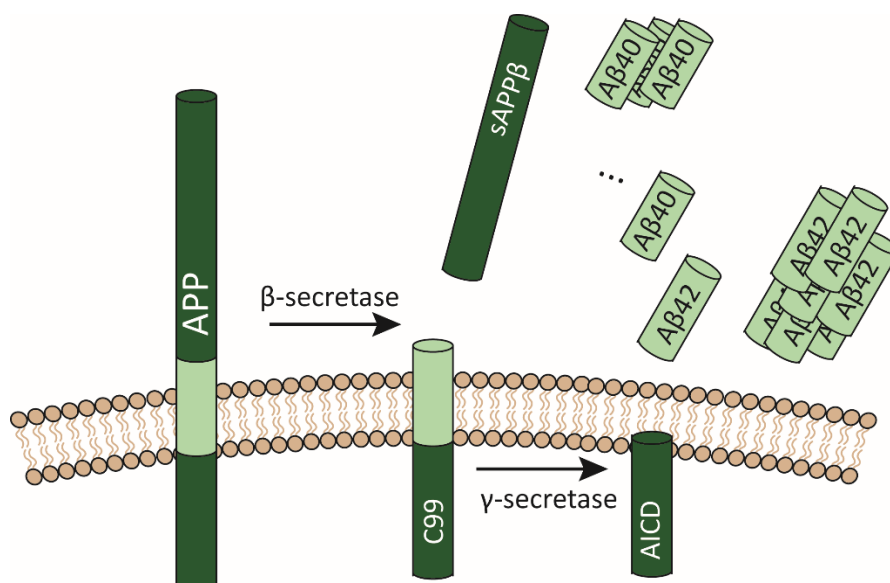


Figure 2: APP cleavage cascade in Alzheimer's disease. Combinatorial action of β and γ -secretases produce $A\beta$ species. Especially, $A\beta_{42}$ species are most prone to aggregate into plaques.

Types of plaques:

Diffuse plaques

Diffuse plaques generally have a diameter of 10–70 μm (Armstrong, 1999; Bussi re et al., 2004; Fiala, 2007; Blazquez-Llorca et al., 2017). The smallest primitive plaques contain clusters of mostly regular-looking neuronal and glial processes and a few dystrophic neurites in the neuropil. The density of synapses is markedly diminished in neuropil at the diffuse plaques (Dickson et al., 1989). Electron microscopy reveals many more microscopic neurotic plaques that cannot be examined with the light microscopy (Blazquez-Llorca et al., 2017).

Cored plaques

Cored plaques consist of a vast central mass of amyloid, which diverges from primitive plaques and they are often referred to as compact or "burnt-out". The amyloid core might have a star-shaped appearance with spikes of amyloid extending outward, and a spherical cluster of dystrophic neurites and extracellular wisps of amyloid as in the primitive/rudimentary plaques frequently surround it.

Ultrastructural studies report that this halo effect is created by glia encircling the core of the plaques (Kato et al., 1998; Stalder et al., 2001; Ye et al., 2003). Their cores are enveloped by one or two activated microglia, while large plaque cores are surrounded by processes from dozens of microglia and astrocytes (Ye et al., 2003).

Tau protein (MAPT)

Isoforms and expression pattern

Human *MAPT* (microtubule-associated protein tau) gene is located on chromosome 17, with length over 100 kb and a number of 16 exons. Tau protein expression is mainly identified in neurons and localized preferentially in axons. Tau protein was observed likewise in astrocytes and oligodendrocytes at low levels under non-disease conditions (Tashiro et al., 1997). However, varied types of glial cells such as oligodendrocytes and astrocytes may also express high level of tau protein in taupathies like supranuclear palsy or Pick's disease (Terwel et al., 2002; Kahlson and Colodner, 2015).

Tau isoforms containing an extra exon, exon 4a, are present in the peripheral nervous system (PNS) (Goedert et al., 1992). Isoforms without exon 10 are encountered in early developmental stages, whereas isoforms with alternative splicing of exon 2, 3 and 10 are expressed in adult brains. Due to alternative splicing, the adult brain contains six tau isoforms. These six tau protein isoforms range from 352 to 441 amino acids (**Figure 3**).

The shortest tau protein isoform (i.e., three-repeat tau with no amino-terminal inserts-ON3R) is present merely in the fetal human brain, whereas in the cerebral cortex of healthy adults, the amounts of three-repeat and four-repeat tau are equal to each other (Goedert and Jakes, 1990). This might imply that the different tau species must interact with specific subsets of proteins and execute specific cellular functions that are indispensable for development.

The expression of tau in grey matter is approximately twice as high as in the white matter and cerebellum. In parallel, *MAPT* mRNA expression in the frontal cortex (highest expression) and within the white matter (lowest) differs 1.5-fold. Tau protein expression is highest in the frontal cortex; lowest in the cerebellum and putamen (Trabzuni et al., 2012). In the cerebellum, ON3R isoform is determined as considerably lower compared with other regions. *MAPT* mRNA expression at the gene level and tau protein levels vary

in regional levels. The localized differences in the alternative mRNA splicing of *MAPT* might give rise to different roles of tau in various tauopathies (Spillantini and Goedert, 2013).

Although *Tau* is expressed in many forms in vertebrates, the isoform ratios are not conserved. For example, in the brain of adult chickens, tau isoforms with three, four, or five repeats are expressed and most adult rodents express the four-repeat isoform (Götz et al., 1995; Yoshida and Goedert, 2002).

Tau is expressed at high levels in murine brains. More specifically 0N4R isoform is the most predominant one in two-month-old adult mice. A study with subcellular fractionations showed how the different isoforms are distributed at subcellular level. 1N isoform is over-represented in the soluble nuclear fraction; also present in cell bodies and dendrites, but not in axons. The 0N isoform is mainly detected in cell bodies and axons, whereas nuclei and dendrites are only slightly stained with the 0N antibody. The 2N isoform is highly present in axons and in cell bodies, with a detectable localized in dendrites and a very slight expression in nuclei. While the 2N isoform was undetectable at P0, 2N isoform was mainly found localized to cell bodies and dendrites in the adult brain (Liu and Götz, 2013). The presence of 1N and 2N in dendrites and the absence of 1N tau in axons suggest not only isoform-specific functions, but also make tau more accepted as a post-synaptic molecule.

N-terminal half of tau protein contains a larger variability than at C-terminal tau (León-Espinosa et al., 2013). In parallel, the localization of threonine (or alanine) residues are concentrated in a higher proportion at the N-terminal region of tau protein (Avila et al., 2016). The C-terminal part shows more conserved residues among different species which indicates that these fewer variable regions could be essential for some of its functions.

Tau protein was considered being natively unfolded and not having strong secondary structure (α -helix or β -sheet) in solution (Schweers et al., 1994). Studies in fluorescence resonance energy transfer demonstrated that soluble WT tau monomers prefer a “paper clip” conformation by interactions of C-terminus with microtubule-binding repeats (MTBR) (Jeganathan et al., 2006). One of the major problems in structural studies is the flexible and intrinsically disordered nature of tau proteins. This type of proteins offers a

wide population of compact conformations with a highly dynamic structure and a complex network of long-range transient contacts, which is not amenable to be studied (Avila et al., 2016).

Domains

Tau protein isoforms consist of two main domains: projection domain at the amino-terminus as well as microtubule-binding domain at the carboxy-terminus. More precisely, projection domains encompass an amino-terminus region with a significant proportion of acidic residues and a proline-rich domain. The functions of the projection domain of Tau protein is determining the stabilizing and spacing between axonal microtubules (Chen et al., 1992), interactions with other proteins such as cytoskeletal elements, mitochondria or neuronal plasma membrane by establishing the link between actin and tubulin (Drubin and Kirschner, 1986; Jung et al., 1993). In short, this projection domain is important for tau protein binding to plasma membrane-associated proteins (Brandt et al., 1995).

In the microtubule-binding domain, three (Tau 3R) or four (Tau 4R) repetitive sequences are located. The repeats are formed by 31 or 32 similar, but not identical, residues. These repeats have mainly two parts: first, 18 residue sequences with a tubulin-binding capacity (Lee et al., 1989) and second, less conserved 13-14 sequences with inter-repeat residues (Goedert et al., 1989). Tau 4R isoform has higher affinity to microtubules, compared to Tau 3R (Goedert and Jakes, 1990; Scott et al., 1991), thus Tau 3R could be displaced by the other isoform. The mechanism of tau protein binding to the microtubules is explained by “Jaws-model”; which is not only three or four C-terminal repeats; but also flanking regions are fundamental in the Tau binding affinity to microtubules (Mandelkow et al., 1995)

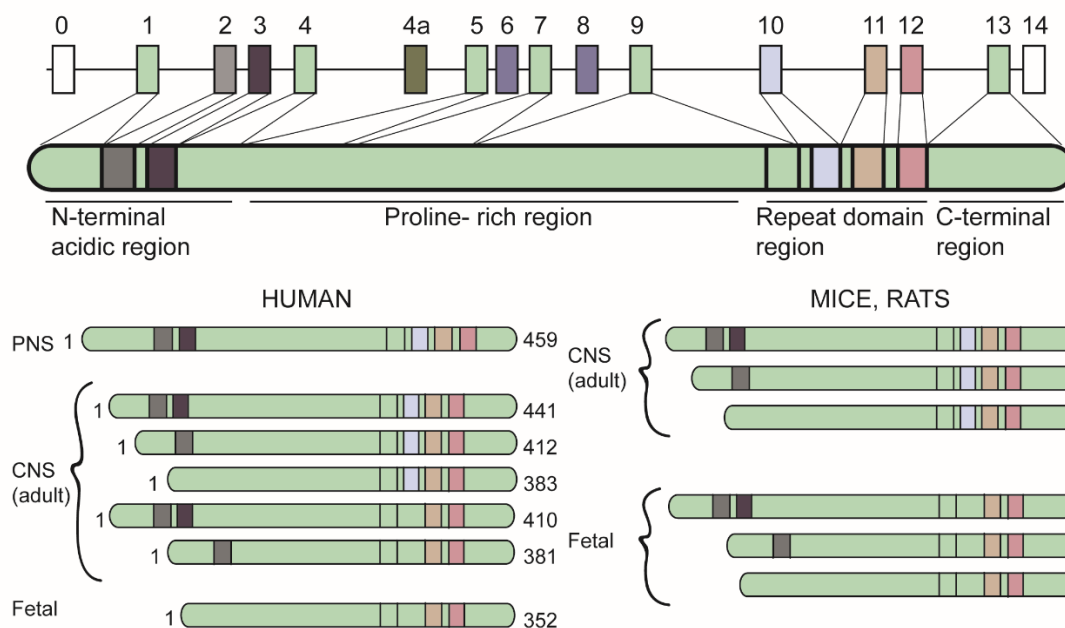


Figure 3: Structure of Tau gene and protein isoforms. Tau protein contains several regions such as an N-terminal acidic, a proline-rich repeat domain and C-terminal region. Tau isoforms vary in the N-terminal acidic region and in the number of repeat domain regions. Presence of various isoforms in humans, mice, and rats in PNS and CNS are illustrated.

Cellular and subcellular localization of the tau protein

Tau can bind to microtubules and to the plasma membrane. As pointed out above, murine tau protein isoforms have special sub-cellular distribution, including the nucleus, axons, dendrites and the cell body. This suggests that the particular distribution of each tau isoforms is likely to reflect unique functions (Liu and Götz, 2013).

The phosphorylation of tau proteins influences its cellular localization. Its proline-rich phosphorylation is predominantly present in the somatodendritic compartment and dephosphorylation of the proline-rich region predominantly occurs in distal axonal compartments. Carboxyl-terminal domain of tau is mainly phosphorylated in the distal axons.

Other MAPT Binding Proteins

Several MAPT interaction partners of functional importance have been identified in addition to microtubules. For example, actin or protein phosphatase 2A binds to tau, through tau repeats (Caceres et al., 1990; Bakota and Brandt, 2016), which inhibits the

neurite polarity. Mutations in the carboxy-terminal, non-microtubule binding region affect tau protein's bridging function of growing microtubules to the membrane within the growth cone. The stability of bridging and the axonal localization of tau are supported by membrane-associated proteins such as annexin A2 (Gauthier-Kemper et al., 2011). The proline-rich sequence in the amino terminus of tau (more definitely membrane-associated components) interacts with proteins containing SH3 domains (Hwang et al., 1996), such as FYN and SRC-family non-receptor tyrosine kinases (Lee et al., 1998). This advocates a mechanism for coupling extracellular signals to the cytoskeletal system; leading to cytoskeletal changes. In AD, this interaction is involved in conferring A β -toxicity at the post-synapses (Ittner et al., 2010).

Protein phosphatase 2A can be listed as the primary tau phosphatase, which regulates phosphorylation and development of tauopathies in AD (Sontag et al., 1999; Sontag and Sontag, 2014).

A recent study with tandem-mass labeling and quantitative mass-spectrometry identified 101 proteins that either directly or indirectly interact with tau and/or with the three isoforms (0N, 1N, and 2N) (Liu et al., 2016). Those 101 proteins were identified as membrane-bound proteins (51%), cytoplasmic (17%) and cytoskeletal proteins (12%). The biggest group of tau-interacting proteins, which are membrane-bound proteins can be more specifically categorized as mitochondrial proteins (40.4%), plasma membrane (25.5%) and vesicle membrane proteins (21.3%), endoplasmic reticulum/Golgi apparatus (10.6%) and the endosome (2.1%) (Liu et al., 2016). Some of the 0N-interacting proteins can be counted as: ATP synthase β -subunit, α -synuclein, β -synuclein, mitochondrial creatine kinase U-type (MtCK), creatine kinase B-type, synapsin 2 and synaptogyrin-3. Some 1N interacting proteins include as ATPase, neuromodulin, tropomyosin α -1 chain isoform 10, calmodulin and myelin basic protein isoform 3. 2N-interacting proteins: APOA1, APOE, synaptotagmin, syntaxin 1B and 14-3-3 ζ . Different ATPase subunits, cofilin-1, synaptophysin and DNMT1 are the proteins that bind to all isoforms (Liu et al., 2016). More importantly, exon 3 of a 2N isoform of tau protein was shown to have a distinct role compared to the other isoforms in neurological diseases due to their binding preference to disease-related proteins (Zhong et al., 2012).

Tau can interact with TIA1, a RNA binding protein, through a RNA intermediate (Vanderweyde et al., 2016). The interaction of tau with other proteins like ferritin and transferrin has been reported (Jahshan et al., 2016) and the residues 139–143 could be involved in the binding to heparin which is used as an anticoagulant (blood thinner). The residues 336–343 and 347–351 could be involved in chaperone-mediated autophagy (Wang et al., 2009).

Another protein involved in Alzheimer`s disease is APOE (Saunders et al., 1993). The interaction of tau and APOE has been shown in neurofibrillary tangles and with the method of co-IP and even under 2% SDS presence, which indicates that this interaction is strong and consistent (Liu et al., 2016). Tau - actin interactions may mediate neuronal degeneration by altering the organization and the dynamics of the actin cytoskeleton (Fulga et al., 2007).

Table 1: Tau interacting proteins are classified according to their function and subcellular localization

<i>Functional classes of identified proteins</i>	<i>Ratio</i>	<i>Subcellular localization of Tau interacting proteins</i>	<i>Ratio</i>
Energy metabolism	31%	Cytoplasmic	17%
Synaptic signalling	22%	Cytoskeletal	12%
Cytoskeleton processing	18%	Extracellular	8%
Regulation of protein phosphorylation	9%	Cytoplasmic/Nuclear	4%
Others	20%	Membrane-bound/Nuclear	2%
		Cytoplasmic/Membrane bound	2%
		Nuclear	2%
		Membrane-bound	51%
		Mitochondrial	40,4%
		Plasma membrane	25,50%
		Vesicle membrane	21,3%
		ER/ Golgi apparatus	10,6%
		Endosome	2,1%

The role of Tau in AD

The *MAPT* locus is involved in multiple neurodegenerative disorders, including progressive supranuclear palsy (Baker et al., 1999; Höglinger et al., 2011), corticobasal degeneration (Houlden et al., 2001), Parkinson's disease (Golbe et al., 2001) and

Alzheimer's disease (Trabzuni et al., 2012). In some of these diseases such as progressive supranuclear palsy, corticobasal degeneration and Pick's disease tau inclusions are also found in glial cells (Komori, 1999).

Senile plaques and neurofibrillary tangles are both hallmark lesions of Alzheimer's disease. The relationship between tau protein and amyloid beta protein in Alzheimer's disease has been studied extensively. However, the mechanistic link between them is incompletely understood.

About 5% of cases of frontotemporal dementia carry mutations in *MAPT*, which cause a toxic gain of function (Goedert et al., 2012). Most of the mutations are located in exons 9-12, the repeat domains and in the adjacent introns. Those mutations can affect either the protein expression level or the alternative splicing of the tau pre-mRNA. Single amino acid change/deletion might also affect the protein level as well as the interaction of tau with microtubules (Spillantini and Goedert, 2013). Other tau mutations involved in the assembly of tau into filaments increases the alternative mRNA splicing of exon 10 of *MAPT*, which influences the three-repeat to four-repeat isoform ratio.

The total tau levels in CSF were found approximately 300% higher in AD patients than in control subjects (Blennow et al., 2001). Increased concentrations of tau in CSF can predict the disease 15 years before symptoms developed, whereas global cognitive impairment starts 5 years before the disease prognosis (Spillantini and Goedert, 2013). However, total-tau level change in CSF may not be specific for AD, since they can be observed in patients with acute stroke, head trauma or Creutzfeldt-Jakob disease (Rosén et al., 2013).

Studies so far show that Tau takes a role in A β -induced neuronal dysfunction at multiple levels such as disassembly of microtubules (King et al., 2006; Jin et al., 2011; Zempel et al., 2013), cell-cycle re-entry (Seward et al., 2013), cell death (Rapoport et al., 2002; Leroy et al., 2012; Nussbaum et al., 2012), DNA double-strand break (Suberbielle et al., 2013), synaptic dysfunction (Roberson et al., 2011; Shipton et al., 2011), aberrant network excitability (Roberson et al., 2007; Ittner et al., 2010; Roberson et al., 2011), mortality (Roberson et al., 2007; Ittner et al., 2010; Roberson et al., 2011; Leroy et al., 2012), impaired axonal transport (Vossel et al., 2010), cytotoxicity and cognitive and behavioural alterations (Ittner et al., 2010; Roberson et al., 2011; Leroy et al., 2012).

Effect of tau protein on cytoskeletal disruption has been proven in non-neuronal cells after MAPT transfection. Tau confers acute hyper-sensitivity of microtubules to prefibrillar, extracellular A β via its active portion in the N-terminal fragment excluding microtubules binding region (King et al., 2006; Jin et al., 2011). Especially microtubule breakdown and microtubule poly-glutamylation occurring in dendrites is mediated by tau (tau missorting) and missorting of Tubulin-Tyrosine-Ligase-Like-6 (TTL6) into dendrites by tau-induced spastin, an MT-severing enzyme (Zempel et al., 2013).

Amyloid β was shown to be mitotic in vitro experiments (for review (Lee et al., 2009); which can induce cell-cycle mediated events in AD. Although most regions of the adult human brain do not possess dividing neurons, cortical neurons in AD brain commonly re-enter the cell cycle, but then die after exiting G0 of the cell cycle (Greene et al., 2007; Lee et al., 2009). Loss of cortical neurons in AD is explained by dying cells through this ectopic cell cycle re-entry (CCR) (Mucke et al., 2000; Arendt et al., 2010). It has also been shown that amyloid- β signals through tau to drive ectopic neuronal cell cycle re-entry in Alzheimer's disease (Seward et al., 2013).

Morphological analysis indicated that neurons expressing either mouse or human tau proteins degenerated in the presence of fibrillar A β , while tau-depleted neurons showed no signs of degeneration; suggesting that more dynamic microtubules might confer resistance to A β -mediated neurodegeneration (Rapoport et al., 2002). Similar results were also observed *in vivo* since AD mice crossed on TauKO background live longer (Roberson et al., 2007, 2011; Leroy et al., 2012; Nussbaum et al., 2012).

A β causes inhibition of long-term potentiation (LTP) and enhancement of long-term depression (LTD) in the hippocampus (Walsh et al., 2002). Tau protein is required not only for amyloid β -induced impairment of hippocampal long-term potentiation, but also for the induction of LTD in the hippocampus. During LTD, synaptic AMPA receptors (AMPA) are removed, so the synaptic efficiency is reduced and a shrinkage and elimination of synapses may occur (Collingridge et al., 2010). Especially, tau phosphorylation by GSK3 is required for LTD (Kimura et al., 2013). GSK3 is one the main tau kinase whose activation phosphorylates tau and eventually causes neurofibrillary tangles. In another study, lack of tau also reduced the active form of GSK3 β (Leroy et al., 2012). These results suggest that not only GSK3 affects tau activity, but also tau affects GSK3 (Avila et al., 2010).

The physiology data indicated that tau reduction corrects several abnormalities in multiple hippocampal sub-regions in Alzheimer mouse models, such as excitation/inhibition imbalance, field potentials, LTP and PPF (paired-pulse facilitation), in other words for synaptic plasticity (Roberson et al., 2011; Shipton et al., 2011).

Double-strand DNA breaks are observed in human amyloid precursor protein (hAPP) transgenic mice after exploration of novel environment as a behavioural test. Besides, increase in neuronal γ H2A.X foci (Crowe et al., 2011), which is a predictor of neuronal death and an early marker of nonlethal neuronal harm is observed in AD mice. It was shown that Tau reduction prevents the $A\beta$ -induced increase in neuronal γ H2A.X foci (Suberbielle et al., 2013).

$A\beta$ -oligomers induced axonal transport defect of mitochondria and anterograde transport of neurotrophin receptor TrKA could be prevented with tau reduction to almost wild-type level (Vossel et al., 2010).

Tau and axonal transport

Axonal transport is one of the perturbed mechanisms in tauopathies, though the available data seem controversial. It was shown in several models that tau overexpression results in axonal cargo depletion, slowing down the axonal transport and transport deficits.

Not only tau overexpression but also, an imbalance in 3R:4R tau isoform ratio in cultured neurons and mouse models impaired transport dynamics. Tau controls transport and subcellular mislocalization of APP intracellularly (Stamer et al., 2002; Mandelkow, 2003; Ebner et al., 2011). 3R isoform promotes the anterograde movement of APP vesicles by increasing trafficking distance and reducing retrograde transport velocities, while 4R isoform favors retrograde transport by slowing down the anterograde transport (Lacovich et al., 2017).

Studies performed in hippocampal neuronal culture showed that tau is taking an important role in mechanisms leading to $A\beta$ -induced neurodegeneration. Tau-depleted neurons are not only resistant to $A\beta$ -induced neurodegeneration, but also more persistent in dynamic microtubule formation (Rapoport et al., 2002).

Tau knockout mice

In order to understand the physiological functions of tau protein *in vivo*, several mouse strains with tau overexpression as well as tau deletion have been generated (**Figure 4**) (Ke et al., 2012). There are four different Tau knockout mice available. First TauKO was generated by Harada and colleagues (Harada et al., 1994). In 2001, two additional tau knockout lines have been generated. A first tau knockout mouse line was carrying GFP-encoding cDNA in exon 1 of *MAPT*, which resulted in the deletion of endogenous tau protein and expression of a GFP fusion protein with amino acids 1 to 31 of tau under the promoter of *MAPT* (Tucker et al., 2001). Fujio et al., 2007 reported another Tau^{-/-} line by inserting a selection cassette into exon 1 with FRT flank (flippase recognition target) recombination motifs allowing subsequent manipulation of the targeted *MAPT* gene (Fujio et al., 2007). And Dawson et al., 2001 reported another TauKO (B6.129X1-*Mapt*^{tm1Hnd/J}) whose construction was shown in **Figure 4**. In this study, we used B6.129X1-*Mapt*^{tm1Hnd/J} TauKO. Therefore, the phenotype of B6.129X1-*Mapt*^{tm1Hnd/J} is in focus.

B6.129X1-*Mapt*^{tm1Hnd/J} (Dawson et al., 2001):

Dawson et al., 2001 reported that hippocampal cell culture from TauKO mice show a significant delay in axonal and dendritic extensions, which was contrary to what was observed in the previous mouse lines. However, in E16 as well as in brains from newborn mice MAP1A was expressed twice as much in TauKO mice (Dawson et al., 2001). Old mice showed a significant decrease in P-MAP1B, P-GSK3 β , SMAI31, and acetylated α -tubulin (Ma et al., 2014) which might suggest an age-dependent role of the tau protein in the brain.

Tau knock-out mice showed a loss of excitatory synaptic proteins such as NR2B, Drebrin and post-synapses and pre-synapses like PSD-95, FYN, and Synaptophysin at 19-20 months old. At 8-9 months, tyrosine hydroxylase (TH) was significantly reduced in the substantia nigra (Ma et al., 2014). In another study, tau knockout mice had higher iron concentrations and dopaminergic nerve cell loss in the brain. Besides, increased quantification of Fe(II) and Fe(III) staining in the hippocampus; increased cellular APP, decreased surface APP were observed (Lei et al., 2012). This study suggested that lack of tau induces neurotoxic iron accumulation with an age-dependent manner by APP

trafficking. However, the same molecular changes were not reported in other studies with the same tau knockout line (Roberson et al., 2007; Morris et al., 2011b).

The subtle motor deficits at 3–3.5 months, like a decrease in latency to fall and to increase in descending/crossing the pole, and more slipped steps, but otherwise normal motor functions were independent of the TH levels in the striatum (Morris et al., 2011a, 2013). Interestingly, at 12–15 months the knock-out mice weighed more (with 21–22 month-old mice showing a trend) (Morris et al., 2013), suggesting that subtle motor deficits are related to an increased body weight. Worsened motor abilities and deficits in Morris water maze were detected in TauKO mice at age 12 and 24 months (Lei et al., 2012; Ma et al., 2014). However, no overt behavioral abnormalities were observed in another study at 10-12 months of age (Dawson et al., 2010).

In parallel, motor deficits in this strain (Dawson et al., 2010) by two different backgrounds at 12-months of age were investigated (Lei et al., 2014). The most pronounced phenotype was reported with C57BL/6/SV129 background compared C57BL/6, which could be due to the already-reported discrepancies in brain metal levels (Maynard et al., 2006)

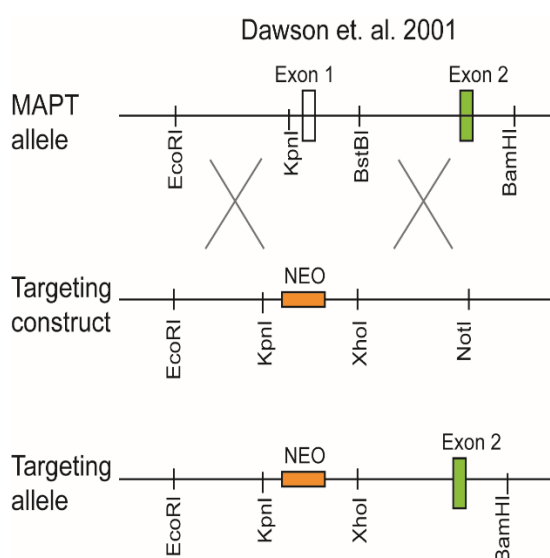


Figure 4. Generation of Tau knockout mice by targeting exon 1.

AD mice crossed on Tau deficient background

The role of tau in A β -induced neuronal dysfunction can occur via multiple mechanisms, such as DNA double-strand breaks (Suberbielle et al., 2013), cell-cycle reentry (Seward et al., 2013), cytoskeletal disruption (King et al., 2006; Zempel et al., 2013), cell death

(Rapoport et al., 2002; Leroy et al., 2012; Nussbaum et al., 2012), synaptic dysfunction (Roberson et al., 2011; Shipton et al., 2011), aberrant network excitability, mortality and cognitive and behavioural alterations (Roberson et al., 2007; Ittner et al., 2010; Roberson et al., 2011).

There are several pieces of evidence showing that a reduction of the endogenous tau level does not only prevent behavioral deficits in transgenic mice but also protects them against excitotoxicity (Roberson et al., 2007, 2011). Overall tau ablation has been considered as a possible therapeutic approach for AD (Morris et al., 2011a; DeVos et al., 2013; Holth et al., 2013; Gheyara et al., 2014). Therefore, understanding the enabling role of the tau protein in A β -induced neuronal dysfunction is important for the development of new therapies.

Several previous studies indicate, that tau is involved in synaptic effects of A β -induced neuronal dysfunction. Tau reduction prevents LTP impairment, NMDA receptor dysfunction and seizure activity in hAPP, hAPPJ9/Fyn and TASD41/Fyn mice (Roberson et al., 2007, 2011) (Roberson et al., 2011). Besides, increase in survival rate was observed in APP23 (Ittner et al., 2010), hAPP-J20 (Roberson et al., 2007), hAPPJ9/Fyn mice (Roberson et al., 2011). However, these changes did not affect A β plaque deposition, neuritic dystrophy and aberrant sprouting in hAPP-J20 (Roberson et al., 2007). Knowing that tau reduction prevents behavioral deficits, but not neuritic dystrophies it was argued with the fact that A β plaque deposition and neuritic dystrophies are formed first. In other words, tau acts downstream in the cascade of mechanism relevant in AD pathophysiology; while A β plaque deposition and neuritic dystrophies are located upstream of the cascade.

Tau ablation was reported to change A β levels in mouse models. In the APP^{sw} mouse model, lack of Tau reduces neuritic plaques in 10 and 12 months of age, while increasing soluble A β 40 and 42 levels (Dawson et al., 2010). In the APPxPS1 mouse model (Leroy et al., 2012), these results were observed to be inconsistent with the findings from hAPPJ20, hAPPJ9, hAPPJ9/FYN, and TASD41/FYN mice.

In regard to GSK3 β and tau protein interaction, many studies have focused on the part of phosphorylation of tau by GSK3 β regulation. However, growing evidence suggests that endogenous tau also regulates GSK3 β levels and activity. In heat-shock-induced neuronal

injury (Miao et al., 2010) and APPPS1 AD models (Leroy et al., 2012), for example, tau reduction decreases GSK3 β activity.

Non-microtubule binding domain of tau has been shown to play a role in A β -induced deficits in mitochondrial anterograde axonal transport through different factors such as activation of axonal phosphotransferases, glycogen synthase kinase 3 (GSK3), protein phosphatase 1 (PP1), neuronal activity and through NMDAR signalling (Miao et al., 2010; Vossel et al., 2010; Kanaan et al., 2011; Leroy et al., 2012).

Electrophysiological experiments showed similar NMDA/AMPA receptor currents, synaptic transmission and synaptic plasticity between wild-type and tau knockout mice (Roberson et al., 2011; Shipton et al., 2011). AD mouse model with Tau deficient background are more resistant to seizure-induced toxins and amyloid beta peptides. This suggests that tau affects neuronal excitability via another mechanisms. Indeed, it has been suggested that alteration in brain oscillatory pattern could be one of these mechanisms (Morris et al., 2011b). Hippocampal theta waves (5–11 Hz) representing spatial cognition and memory formation (Itskov et al., 2008) have been shown to slow down. Moreover, gamma brain-circuit synchronization (30-80 Hz) has been observed to be altered, probably as a consequence of a reduced interneuron communication. This suggests that tau deficiency might alter interneuron function in the brain (Cantero et al., 2011).

Plaque-associated dystrophies

Dystrophic neurites are hallmarks of Alzheimer`s Disease, already recognized by Alois Alzheimer because of its positive silver staining on histological sections (Alzheimer, 1907). Dystrophic neurites were characterized by globular type of swellings and tortuous neuronal processes that are associated with extracellular amyloid β (A β) plaques.

Dystrophic formations develop at the very earliest time point of amyloid plaque deposition (Gowrishankar et al., 2015). Dystrophies are filled with distinct lysosomes type with low levels of Cathepsin B, D, and L (luminal proteases); which indicates that the maturation of lysosomes while being carried to the soma is affected.

Evidence from transgenic mice demonstrates that most dystrophic neurites are axons (Phinney et al., 1999; Tsai et al., 2004; Spires et al., 2005). The dystrophic neurites are highly enriched with BACE1 (Zhao et al., 2007), VGLUT1, phosphorylated-tau protein but also positive for GAP-43 (presynaptic/axonal growth or plasticity protein).

In vivo and *in vitro* studies demonstrated that neuritic abnormalities develop in the vicinity of amyloid plaques and eventually result in disruption and breakage of neuronal branches. This phenomenon severely disturbs the neuronal connectivity and may contribute to the pathogenesis of dementia (Tsai et al., 2004; Blazquez-Llorca et al., 2017).

Besides, abnormally high expression of BACE1 in dystrophic neurites supports the idea that APP cleavage and A β overproduction is increased in dystrophic neurites (Stokin et al., 2005; Radde et al., 2006; Gouras et al., 2010). A β has been considered to affect axonal transport, which results in axonal swellings and even more A β production. At the same time, the more axonal transport is deficient, the more A β and dystrophic neurites are produced due to increased coincidence of APP and BACE in the same compartments. Eventually, this leads to a positive feedback loop of altered axonal transport together with enhanced A β production as well as worsened oxidative stress and autophagy (Fiala, 2007).

Previously, it has been shown that kinesin-I and specifically the kinesin-light chain takes an important part in the axonal transport of APP (Kamal et al., 2000). Axonal damage or blockage by the release of kinesin-1 from moving vesicles might result in increased APP cleavage due to slow spontaneous rate in axons, which allows higher number of cleavage process. The release of the C-terminal APP fragment with the kinesin-1-binding region might lead to an interruption of anterograde transport as well as the retrograde transport of vesicles (Kamal et al., 2001).

Morphological studies

In human cases, morphological appearances and compositions of dystrophic neurites vary with the pathological stage of Alzheimer's Disease. In AD patients, dystrophic axons were found abundantly in the hippocampal fiber systems originating from the subiculum, CA1, and the entorhinal cortex (Su et al., 1993). In the last stage of AD, several subtypes of dystrophies can be recognized with their complement of specific cytoskeletal proteins,

such as abnormally phosphorylated tau isoforms and synaptic markers (Dickson et al., 1999). Another type of dystrophic neurites in human AD tissue is of swollen, globular morphology. Here dystrophic axons are filled with synaptophysin, chromogranin A and APP (Adams and Munoz, 1993; Guevara et al., 2004). Many proteins are involved in amyloidogenic and neuropathological pathways, such as GAP-43, ubiquitin, ubiquilin, prion protein, cytochrome C, C9 or f72, reticulon-3, and BACE1 have been implicated in dystrophic neurite formation (Zhan et al., 1995; Satoh et al., 2013).

Studies in non-demented controls versus plaque-associated dystrophic neurites in mild or severe AD showed that approximately half of the A β plaques in control group contained neurofilament (NF) positive dystrophic neurites, whereas this ratio was three-fourths in AD patients. In addition to neurofilament-positive dystrophic neurites, the paired helical filament (PHF) as well as tau-positive dystrophic neurites can be detected at A β plaques in the control group, but very rarely; whereas half of the A β plaques in AD were positive for PHF and tau (Su et al., 1998).

Morphologically, most common organelles in dystrophies are double-membrane-bound vesicles with densely compacted amorphous or multilamellar autophagosomes, which contain undigested compacted organelle material. Secondly, single or double membrane vesicles with translucent or amorphous electron-dense material observed in dystrophies reveal the presence of auto-phagosomes with partially digested material and/or the mature degradative forms of autophagolysosomes (AVs). In parallel, LC3-II, a marker of autophagic lipidation, has been found in dystrophies, and synaptosomal & microsomal fractions. This suggests impairment in autophagy mechanism in neuritic dystrophies in AD models. Similarly, degradation and maintenance mechanism for multiple components has dramatically not only increased, but also impaired in AD tissue. The PS1 mutation in AD has been suggested to be the reason for this abnormality, due to its role in autolysosome acidification and maturation (Lee et al., 2010).

Studies on non-AD cases might give clues to the earliest changes related to AD pathology. A subset of non-demented cases shows signs of pathological aging such as widespread neocortical amyloid plaques, but no signs of 'classical' neurofibrillary pathology or overt nerve cell degeneration. Such cases are thought to represent Braak stage III, in other words, a preclinical stage of AD, and contain NF triplet protein and α -internexin-labeled

dystrophic neurites. In contrast, dystrophic neurites in AD cases include NF triplet protein, α -internexin-labeled and also hyperphosphorylated-tau-labelled dystrophic neurites (Dickson et al., 1999). Therefore, it was hypothesized that a NFs and internexin containing dystrophic neurites may be the earliest plaque-associated neuritic pathology to appear, while they appear in both in aging and in AD. The accumulation of phosphorylated-tau occurs at a later time point during AD progression (Dickson et al., 1999; Woodhouse et al., 2009). Therefore, dystrophic neurites observed in in Tg2576 and TgCRND8 AD mouse models exhibited pathology that represents the pathology of aged humans rather than AD, due to presence of NF triplet protein, α -internexin-labeled ring like dystrophic neurite (Woodhouse et al., 2009).

Dystrophic neurites surrounding amyloid plaques remain connected to neuronal bodies over a relatively long period of time. Then retrograde signals from the axonal terminals might be propagated back to the cell body and cause cytoskeletal alterations and neurofibrillary tangle formations. Indeed, it was shown that some dystrophic neurites could be still followed over the period of 168 days in AD mice models (Blazquez-Llorca et al., 2017). Thus, this raises the question as to how dystrophic neurites affect the rest of cellular compartments and why some axons (a minority) seem to be more susceptible than others form the dystrophic pathology.

Neurofilaments in axons might be the explanation why some axons are more susceptible to the dystrophic pathology. It was demonstrated in AD patients' tissue and two other AD transgenic mouse models (APP/PS1 and Tg2576) that neurofilament-positive axons were more susceptible to build dystrophies compared with calretinin positive axons. While the density of Calretinin positive neurite density was significantly reduced at the edge of the plaques, the loss of density of neurofilament positive neurites was significant at the edge, core, and periphery of plaques in all sample groups. Besides, the number of NF+, but not CR+, dystrophic neurites (DN) was significantly correlated to A β plaque size (Mitew et al., 2013)

Numerous other proteins are upregulated in AD patient brains, which can be classified as antioxidant, apoptosis-related, heat-shock, energy metabolism, protein metabolism, signal transduction, structural and synaptosomal and transport proteins (Fountoulakis and Kossida, 2006). Tau protein, dynein heavy chain, GFAP, cathepsin B and D *and* many

more membrane trafficking and cell-adhesion proteins were found enriched in amyloid plaques isolated by laser capture microdissection as compared with non-plaque areas in AD brain tissues (Kornau et al., 1995).

In vivo multiphoton imaging studies have already shown that neuritic dystrophies develop after plaque formation (Calignon et al., 2008) and grow in size as the size of plaques increases (Sanchez-Varo et al., 2012). Over a 72-hour period, neuritic dystrophies appeared as very stable structures (Brendza et al., 2005). Previous studies suggested that dystrophic neurites were absent in areas distant from A β plaques, or before the formation of plaques. Ultra-structural morphometric analysis revealed that 64% of dystrophic neurites in sections are in the range of 10-50 μm^2 , 20% are in the range of 50-100 μm^2 and 5% over 100 μm^2 range, while non-dystrophic neurites are 1.5 μm^2 in size in 4.5-months-old APPxPS1 mice (Sanchez-Varo et al., 2012).

A study from our group on two different AD mouse models (dE9xGFP-M and APP-PS1xGFP-M) showed that axonal dystrophies are very plastic structures that do not simply grow in volume over times, but rather fluctuate in size. The axonal dystrophies can also disappear if located at the end of the axon and if the parental axon remains intact. However, still new dystrophies can appear on the same axon weeks later again. If an axon is disrupted at the dystrophic point, re-growth of long axonal segments has been observed, especially in the APPxPS1 mouse model, but not in dE9xGFP-M mouse model (Blazquez-Llorca et al., 2017). A big advantage of this previous study was that individual dystrophies could be followed over a long period of time and volume dynamics could be related to the changes in amyloid plaque size.

BACE1 (β -site APP cleaving enzyme) protein

BACE1 (β -site APP cleaving enzyme) is a protease belonging to type 1 transmembrane protein group with two aspartate residues with the luminal site. It forms dimers or trimers to function (Yan et al., 1999; Liebsch et al., 2017). *BACE1* mRNA expression levels are highest in the brain and specifically in neurons rather than in glial cells (Vassar, 2004). Strongest expression is found in regions like the neocortex and the hippocampus (Fukumoto et al., 2002).

In AD cases, high level of BACE1 accumulation was observed around A β plaques within axonal dystrophies together with its substrate APP (Zhao et al., 2007; Kandalepas et al., 2013). Here it might promote the production of certain APP-cleavage products such as A β 42 (Sadleir et al., 2015, 2016).

BACE1 is degraded within cells through the following pathways: trafficking between the trans-Golgi network and then to the plasma membrane where BACE1 can be internalized into endosomes, and finally degraded in lysosome (Huse et al., 2000). A di-leucine-based signal is located on the carboxyl terminus of BACE1; which takes a role in sorting of BACE1 from transmembrane proteins to endosomes and lysosomes (Sandoval and Bakke, 1994; Koh et al., 2005).

Knocking out the *BACE1* gene revealed that loss of BACE1 abolishes A β production completely in AD mouse models (Roberds et al., 2001). However, loss of one allele *BACE1* (*BACE1*^{+/-}) lowers A β production only 20% in the cerebrum (McConlogue et al., 2007; Laird et al., 2008); which suggests that the other allele of BACE1 is necessary for A β production and partial loss of one copy can be compensated by another copy.

BACE1 is synthesized in the endoplasmic reticulum as an immature precursor protein (pro-BACE1) with a size of 60 kDa. The maturation of BACE1 occurs by its transportation to Golgi apparatus and by modification of all three oligosaccharide side chains of the protein and by removing the pro-peptide domain by furin proteolysis (Huse et al., 2000). The maturation of BACE1 increases its activity, compared with immature BACE1. In addition, an acidic environment is necessary for its highest activity such as Golgi apparatus, trans-Golgi network (TGN), and endosomes (Kalvodova et al., 2005; Vassar et al., 2014). Mature BACE1 is highly stable which means that it is transported between the cell surface, the endosomal system, and the trans-Golgi network (TGN) multiple times before degradation (Huse et al., 2000).

The role of BACE1 in dystrophies at plaques

The analysis on postmortem brain and CSF of AD patients proved that not only BACE1 activity (Tyler et al., 2002; Yang et al., 2003), but also, protein levels highly increased in the cortex of AD patients (specially temporal neocortex, and frontal neocortex) and hippocampus (Fukumoto et al., 2002; Holsinger et al., 2002; Li and Südhof, 2004) .

Increased BACE1 is strictly located to neurotic dystrophies associated with amyloid plaques (Zhao et al., 2007; Kandalepas et al., 2013). This supports the idea that BACE1 cleaves APP and generate A β at neuritic dystrophies. However, the underlying mechanisms of how APP and BACE accumulates in the same compartment have remained unclear. Dystrophic sites are not specific for the accumulation of BACE1, but also for tubulin and kinesin which indicates an impaired anterograde and retrograde trafficking (Gowrishankar et al., 2015). This relationship has already been shown by a previous study: Inhibition of lysosomal hydrolases cause an accumulation of BACE1 in late endosome/lysosomes (Koh et al., 2005). In another study revealed that the inhibition of lysosomal proteases disrupts the axonal transport of degradative organelles such as autolysosomes, late endosomes, and lysosomes, which lead to their accumulation within dystrophic axonal swellings (Lee et al., 2011). These results suggest that increased BACE1 protein level in AD patients might be due to decreased degradation or impaired lysosomal activity. Peri-plaque dystrophies replete with multi-lamellar vesicles resembling autophagic intermediates and inactive pro-cathepsin D, indicating reduced and impaired lysosomal function (Sadleir et al., 2016).

The Alzheimer mouse model – APPPS1

Radde et al., 2006 generated the APPPS1 (B6-Tg(Thy1-APP^{swe}; Thy1-PS1 L166P) mice which is expressing human APP with the Swedish double mutation (KM670/671NL) and a PSEN1 mutation at L166P under the control of a Thy1 promoter. The APP transgene is overexpressed approximately 3-fold in this mouse. Phenotypic characteristic observed in this AD mouse line is shown in **Figure 5**.

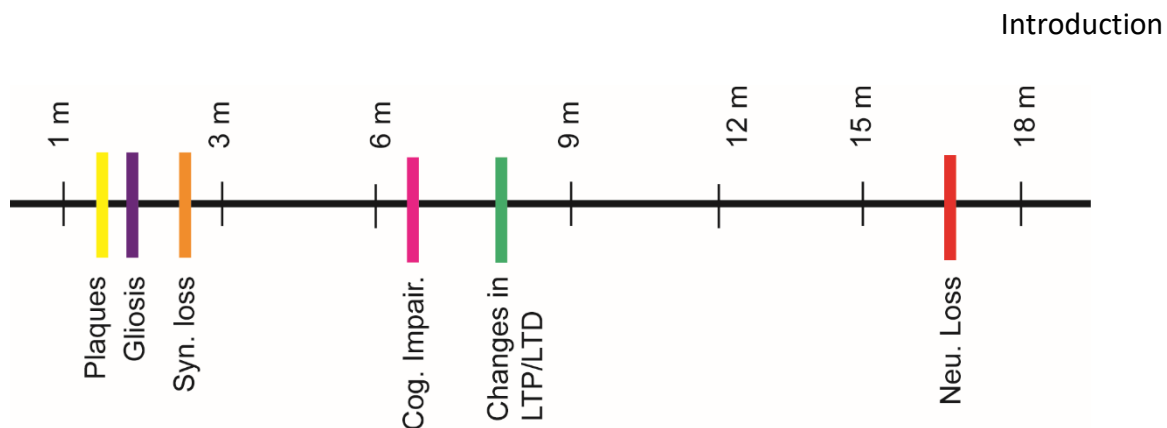


Figure 5. Timeline of APPS1 mouse phenotypic characteristics. While plaques development starts at 2 months of age, cognitive impairment is observed after 6 months of age.

A β 42/A β 40 level decreases with the beginning of the amyloid plaque deposition (Radde et al., 2006; Maia et al., 2013). Amyloid plaque deposition begins around six weeks of age in the neocortex, in the hippocampus about three to four months, then in the striatum, thalamus, and brainstem at four to five months. Phosphorylated tau is observed around amyloid plaque, whereas no fibrillary tau protein can be detected. CSF tau level increases with age. A 5-fold-increase in tau levels has been observed by 18-months of age (Maia et al., 2013).

Behavioural deficits are not profoundly in this mouse line. Radde et al., 2006 reported an impairment in the food-rewarded four-arm spatial maze at eight months of age, Serneels et al., 2009 observed deficits in the Morris Water maze at seven months of age which correlates with impairments in LTP in hippocampal CA1 (Gengler et al., 2010).

There is no severe neuronal loss in this line. Only at 17 months, there is very little neuron loss in the granule cell layer of the dentate gyrus (Serneels et al., 2009).

The VGLUT1^{Venus} mouse line

VGLUT1^{Venus} mouse line was generated by Herzog et al., 2011. Here, a Venus tag was inserted to VGlut1 in the genome. VGLUT1^{Venus} expression is high in the neocortex, hippocampus, cerebellum, olfactory bulb as shown below. It has been shown that the Venus tag does not interrupt the functionality of the VGLUT1 transporter and the trafficking and the dynamics of presynaptic glutamatergic synaptic vesicles. VGLUT1^{Venus}

KI mouse construct and the expression of VGLUT1 tagged with Venus in a mouse brain are shown in **Figure 6**.

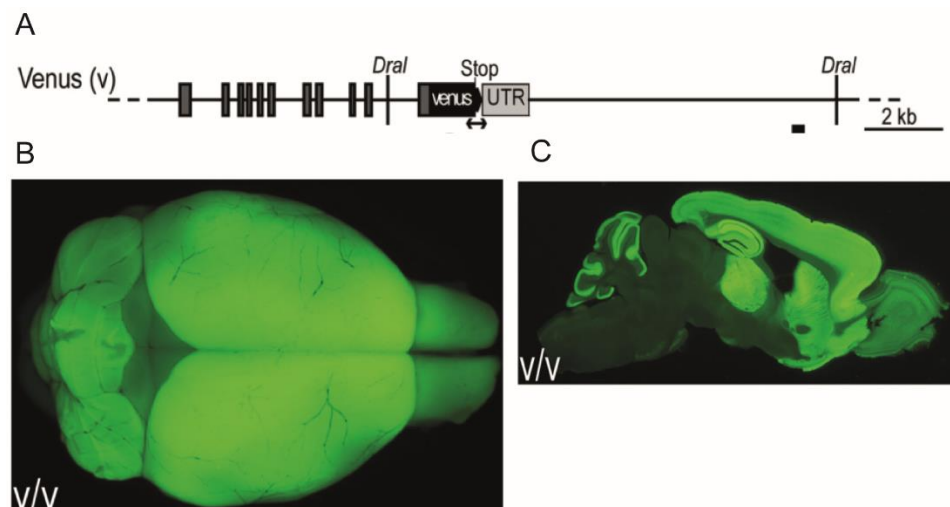


Figure 6. VGLUT1^{Venus} mouse line. (A) VGLUT1^{Venus} KI mouse construct. (B) Overview of direct VGLUT1^{Venus} fluorescence in a paraformaldehyde-fixed mouse brain and within a sagittal section. Image is used with license details and the terms and conditions provided by Copyright Clearance Center (Herzog et al., 2011) (License # 11692504; Jan 12, 2018).

MATERIALS AND METHODS

Transgenic and mutant mice

All protocols and procedures involving animals were approved and conducted in accordance with the regulations of the Ludwig-Maximilian University and the Government of Upper Bavaria (Az. 55.2-1-54-2532-62-12). Heterozygous APPPS1 mice co-express a human APP with the Swedish mutation (KM670/671NL) and mutated PS1 (L166P) under the pan-neuron-specific Thy1-promoter (Radde et al., 2006). APPPS1 mice were crossbred with Tau knock-out mice (Dawson et al., 2001) and homozygous VGLUT1^{Venus} knock-in mice that express the Vesicular Glutamate Transporter 1 (VGLUT1), fused to the fluorescent protein Venus under the endogenous VGLUT1 promoter (Herzog et al., 2011). APPPS1 littermates crossed with homozygous VGLUT1^{Venus} mice served as controls. Mice of both sexes were group housed under pathogen-free conditions until surgery, after which they were single-housed.

DNA extraction for genotyping:

A small section of the tail was removed from each mouse for genotyping. First, the DNA was extracted following instructions from the Invisorb[®] DNA Tissue HTS 96 Kit/C (Strattec molecular, Berlin, Germany). Samples were prepared according to the manufacturer's protocols.

Genotyping protocol with PCR protocol:

The PCR solution consisted of 12,5 µl OneTaq Hot Start QuickLoad (M0488S, New England Biolabs, Massachusetts, USA), 0,5 µl of each forward primer, 0.5 µl of each reverse primer (Sigma-Aldrich, Missouri, USA), 0,5 µl template DNA and 10 µl distilled water.

Table 2. Primer list

Line	Name	Sequence (5'-3')	Length (bp)
APPPS1	IMR 42	CTA GGC CAC AGA ATT GAA AGA TCT	24
	IMR 43	GTA GGT GGA AAT TCT AGC ATC ATC C	25
	IMR 1644	AAT AGA GAA CGG CAG GA	17
	IMR 1645	GCC ATG AGG GCA CTA AT	17

VGlut1^{Venus}	Venus 9420	CTG GCT GGC AGT GAC GAA AG	20
	Venus 9421	CGC TCA GGC TAG AGG TGT ATG GA	23
	Venus 9423	CTT CAA GAT CCG CCA CAA CAT CG	23
Tau	IMR 7415	GCC AGA GGC CAC TTG TGT AG	20
	IMR 7824	AAT GGA AGA CCA TGC TGG AG	20
	IMR 7825	ATT CAA CCC CCT CGA ATT TT	20

The following PCR programs (6321000515, Mastercycler pro, Eppendorf, Hamburg, Germany) were used depending on the purpose.

Table 3. PCR programs

Line	Step	Temp. (°C)	Time	Repeat
APPPS1	1	94	3 min	x 1
	2	94	30 sec	
	3	54	1 min	x 27
	4	68	40 sec	
	5	68	5 min	x 1
	6	10	unlimited	
VGlut1^{Venus}	1	94	3min	1x
	2	94	30sec	
	3	60	1min	27x
	4	68	30 min	
	5	68	2min	1x
	6	10	unlimited	
Tau	1	94	3 min	x 1
	2	94	30 sec	
	3	61	1 min	x 30
	4	68	25 sec	
	5	68	5 min	x 1
	6	10	unlimited	

Plasma and brain homogenization and extraction (western-blot)**A β level determinations in the young mice cohort**

Blood was collected via cardiac puncture into EDTA tubes (BD micro trainer tubes with K2EDTA #365974) on wet ice and was centrifuged at 1500g for 15 min at 4 °C. Plasma was obtained from the supernatant and was frozen at -80 °C. Brains were isolated, quick-frozen on dry ice and stored at -80 °C. Frozen murine forebrains were homogenized in 9 volumes of ice-cold Tris-buffered saline (pH 7.4) containing Complete protease inhibitor cocktail (Roche Diagnostics, Penzberg, Germany) using a Sonifier 450 (Branson) and stored in aliquots at -80 °C. Triton X-100 (Sigma Aldrich, Missouri, USA) soluble A β was extracted by mixing 50 μ l 2% Triton X-100 with 50 μ l brain homogenate, incubating for 15 min on ice with vortexing, followed by ultracentrifugation at 100k x g for 15 min. The clear supernatant was diluted to a final forebrain dilution of 1:100 and used for analysis.

Protein extraction methods**Two-phase protein extraction (for membrane-bound and non-membrane bound fractions)**

Left and right cerebral hemispheres were harvested, followed by liquid nitrogen snap-freezing and stored at -80°C. Brain tissues were lysed using DEA buffer (50 mM NaCl, 0.2% diethylamine, pH = 10) freshly supplemented with protease inhibitors (P8340, Sigma-Aldrich, Missouri, USA). Then, the tissue was homogenized with syringes with 27 G needle (Terumo, Tokio, Japan) and centrifuged (5415R, Mastercycler pro, Eppendorf, Hamburg, Germany) at 5,000 g for 10 min at 4°C. The supernatant (S1) and pellet part (P1) of the homogenates were separated. The pellet (P1) is resuspended in RIPA buffer (20 mM Tris-HCl, pH = 7.5, 150 mM NaCl, 1 mM EDTA, 1 mM EGTA, 1% NP-40, 0.5% sodium deoxycholate, 0.05% Triton X-100) buffer for 30 min, at 4°C. The supernatant (S1) was centrifuged at 130,000 g for 30 min at 4°C and the supernatant (S2) and pellet (P2) were collected. The pellet (P2) part from ultra-centrifugation was resuspended in RIPA buffer. The pellet from the first centrifugation (P1) and the pellet from the ultra-centrifugation (P2) were together ultra-centrifuged again at 130,000 g for 60 min at 4°C to acquire the membrane protein fractions.

Protein concentrations were measured using the BCA (B9643, Sigma Aldrich, Missouri, USA) method. Equal amounts of protein were mixed with Laemmli sample buffer (8% SDS, 40% Glycerol, 0.025% Bromophenol blue, 10% β -Mercaptoethanol, 125 mM Tris pH 6.8).

Four-step protein extraction (for soluble, membrane-bound, intracellular, extracellular non-soluble fractions)

Brain tissues were homogenized in TBS and protease inhibitor pH 7.6 (100 μ l TBS / 10 mg tissue) with 25 g syringe needle. The homogenized tissue was incubated on ice for 30 min. and vortexed every 5 min. After the incubation, the homogenate was centrifuged with 100.000 g for 45 min at 4° C. The supernatant was collected as soluble fraction. The pellet was resuspended in 1 % Triton x-100 in TBS, then incubated on ice for 30 min and vortexed every 5 min. The homogenate was centrifuged with 100.000 for 45 at 4° C. The supernatant was collected as membrane-bound fraction. The pellet was resuspended in 2% SDS in water, incubated on ice for 30 min and vortexed every 5 min. Later on, the homogenate was centrifuged with 100.000 g for 45 min at 4° C. The supernatant was collected as intracellular fraction. The pellet was resuspended in 70% formic acid and centrifuged with 100.000 g for 45 min at 4° C. The supernatant was collected as extracellular non-soluble fractions.

Protein Immunoblotting

The proteins were electrophoresed in Tris-glycine gels with Tris-buffer (25 mM Tris, 190 mM glycine and 0.1% SDS) and transferred onto polyvinylidene difluoride membranes (PVDF, Millipore, Massachusetts, USA). Proteins with low weight are separated with Schagger-gel and with anode buffer (200 mM, pH 8,9) and cathode buffer (0,1 M Tris, 0,1 M Tricine, 0,1% SDS). Otherwise, 8-9% Tris-glycine gels were used to separate the proteins.

The PVDF membranes were blocked in 6% dry-skimmed milk (Thermo Fischer Scientific, Massachusetts, USA) in 0.1% Tween-20 (A4974,0500 Applichem Panreac) in PBS 1X for 30 min at room temperature.

Table 4. Primary antibody list

Antibodies / Dyes	Origin	Company name	Product number	Dilution (WB)	Dilution (IHC)
ALEXAs	goat	Molecular Probes			1/500
APP (Y188)	mouse	Millipore	MAB348	1/1000	1/500
BACE1	rabbit	Cell Signalling	D10E5	1/1000	1/100
CALNEXIN	mouse	Enzo Life Sciences	ADI-SPA-860	1/1000	
Cathepsin	mouse	abcam	ab58802	1/1000	
GAPDH	rabbit	Cell signaling	D16H11	Jan 00	
GSK-3 β	mouse	BD Science	610202	1/1000	
IBA1	rabbit	Wako	019-19741		1/500
LAMP1	rat	abcam	ab25245		1/500
LAMP1	rat	Millipore	MABC39	1/1000	
MAP LC 3 β	goat	Santa Cruz	sc16755	1/500	
Metoxy-X04		Tocris	4920		4-10 μ g/ml
Neurofilament-H	mouse	Biologend	801701	1/1000	1/500
Neurotrace @ 435/455		Molecular Probe	N21479		1/100
Presenilin-1	mouse	Covance	SIG-39194	1/1000	
Tau	rabbit	Invitrogen	PA5-27287	1/1000	1/500

A β quantifications

Six-weeks and 8-months old APPPS1xVGLUT^{venus} and TauKO x APPPS1 x VGLUT^{venus} mice were sacrificed to collect blood and brain samples. A β 40 and 42 levels were determined in the cortex and plasma using the electrochemiluminescence immunoassay kits based on 6E10 from Meso Scale Discovery (Rockville, MD, USA) in either singlet or triplet format. Samples and standards were prepared according to the manufacturer's protocols.

Cranial window surgery

A cranial window was implanted over the right cortical hemisphere as previously reported (Fuhrmann et al., 2007; Holtmaat et al., 2009) and shown in figure 7. In brief, the mice were anesthetized with an intraperitoneal injection of ketamine/xylazine (130/10 mg/kg body weight; WDT/Bayer Health Care). Additionally, dexamethasone (20 μ L at 4 mg/ml; Sigma) was intraperitoneally administered immediately before surgery (Holtmaat et al., 2009) to prevent the development of cerebral edema. Eye cream (Bepanthen, Bayer,

Leverkusen, Germany) is put on the eyes in order to prevent them from drying. The mouse was placed in a mouse holder. (A) The minimum amount of skin was removed in the surgery area, (B) which is cleaned from hair with vacuum suction. (C) Periosteum over the skull was removed gently by a scalpel (Swann Morton, Sheffield, England). (D) In order to make the dental cement adhere better, the skull surface was roughened and (E) location for the cranial window was marked (coordinates of craniotomy: Bregma +1.5 to -3.5 mm, 4 mm lateral from midline). (F) With a smaller dental drill (cat. # 0297, Integra Miltex, NY, USA, cat. # A719003, Schick-dental, Schemmerhofen, Germany) the skull for the window was thinned. (G) The area for a cranial window was removed. (H) In order to prevent the open tissue from drying and bleeding, gel foam (cat. # 0315-08, Pfizer, NY, USA) sucked PBS 1X (14190-094, Life Technologies, California, USA) was placed over the area. (I) Imaging area was shown before window implantation. The 4 mm-diameter glass window (round glasses, Menzel-Glaser, VWR, Pennsylvania, USA) was implanted over the open region and stabilized with cement with glue (Cyano fast and retarder, 152261, 152262, Hagen Werken, Duisburg, Germany). (J) The metal bar is also attached to fix the mouse head during imaging.

After the surgery, mice received subcutaneous analgesic treatment with carprophen (7.5 mg/kg body weight; Rimadyl; Pfizer, New York, USA) and antibiotic treatment with cefotaxime (5 mg/kg body weight; Pharmore, Ohio, USA). Until mouse wakes up, the body temperature is kept at 37 °C.

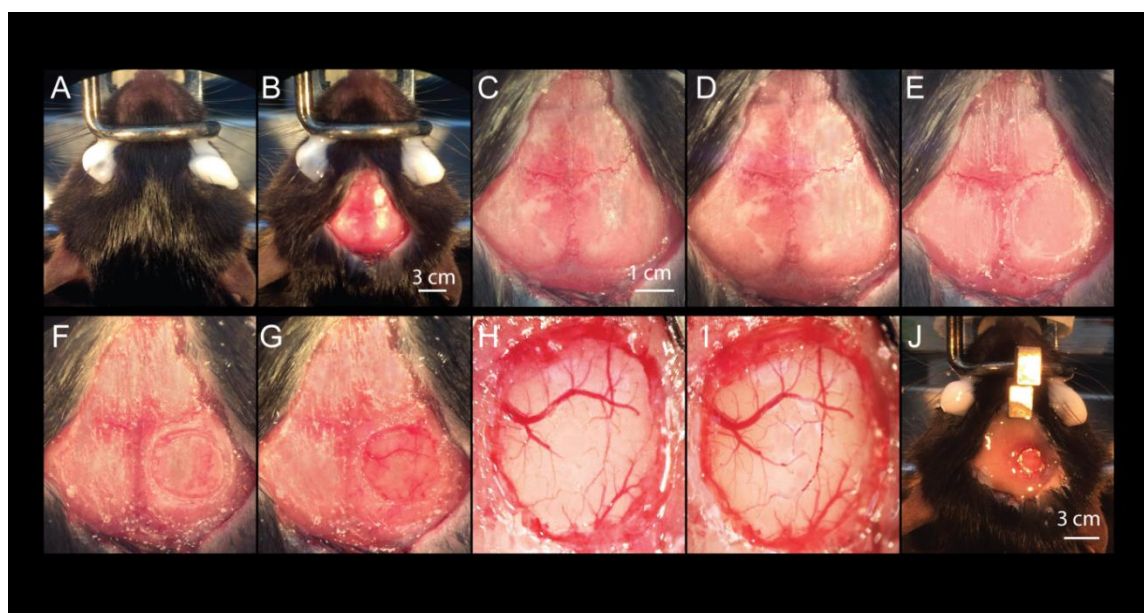


Figure 7. Cranial window operation. (A) The mouse is anesthetized and placed in a mouse holder. The eyes are protected with cream against dryness. The region of operation is disinfected with alcohol. **(B)** A triangle shaped skin piece is cut out. The region is cleaned with PBS 1X. **(C)** Periosteum over the skull is removed gently by a scalpel. **(D)** For strong adherence of the glue, the skull is roughened. **(E)** The area of the window is indicated. **(F)** The skull for the window is thinned. **(G)** The piece of skull is removed. **(H)** Open brain region is cleaned regularly with PBS and bleeding is stopped with gel foam. **(I)** Imaging area before window implantation. **(F)** The window and mouse holder are placed and stabilized by dental cement and glue.

Chronic two-photon *in vivo* imaging

In vivo two-photon imaging was started after a recovery period of 3-4 weeks. For amyloid staining, Methoxy-X04 (4920, Tocris, Bristol, UK) was intraperitoneally injected in the consecutive weeks 0.012 mg with a concentration of 0.15 mg/ml. Throughout the imaging sessions, mice were anesthetized with isoflurane 1% (B06A16A, 1ml/ml, CP Pharma) in 95% O₂, 5% CO₂ (Forene®, Abbott, Illinois, USA), placed on a heating pad to keep body temperature at 37 °C (Fine Science Tools GmbH) and fixed to a custom-made holder using the glued metal bar. *In vivo* two-photon imaging was performed on an LSM 7 MP (Carl Zeiss, Oberkochen, Germany) equipped with standard photomultiplier detectors and a 20X water-immersion objective (W Plan-Apochromat 20x/1.0 DIC, 1.0 NA, Carl Zeiss, Oberkochen, Germany). A region of interest away from big blood vessels to reduce the drift and movement was defined and imaged with weekly intervals (**Figure 8**). To resolve the presynaptic boutons a high-resolution 3D stack was obtained from the VGLUT1^{Venus} fluorescence in cortical layer I at a resolution of 0.10 x 0.10 x 0.4 μm³ and dimensions of 283 x 283 x 60 μm³. VGLUT1^{Venus} was excited at 915 nm and emission was collected from 470 to 550 nm. The imaging session was followed by a larger but less resolved 3D stack was obtained from the Methoxy-X04 fluorescence at a resolution of 0.33 x 0.33 x 0.4 μm³ and dimensions of 425 x 425 x 200 μm³. Methoxy-X04 was excited at 750 nm by a Ti: Sa laser (Mai Tai DeepSee, Spectra-Physics, California, USA) and emission was collected below 485 nm. In subsequent imaging sessions, the previously imaged volumes were identified using the unique blood vessel pattern and coordinates, enabling precise alignment of the same imaged volumes. The laser intensity was adjusted to keep the emitted fluorescence stable at different depths in the microscope control software.

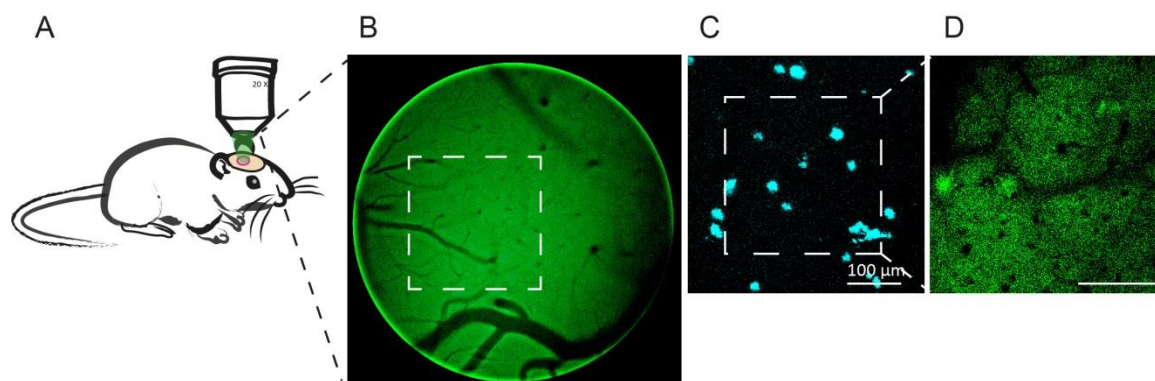


Figure 8. Steps to be followed by the imaging protocol. A) The mouse was placed under the microscope with light anaesthesia to reduce the movement during the experiment B) An overview image was taken as a guide to find the same region for the following imaging sessions. C) Max-intensity projections of imaged plaques with a zoom of 1x and 424 μm x 424 μm x 200 μm in size. D) VGLUT1 image of the previous area with a zoom of 1.5X and 283 μm x 283 μm x 60 μm in size.

Analysis of 3D microscopy image data sets

The analysis was performed by Dr. Finn Peters following a protocol described previously (Peters et al., 2018).

All data stacks obtained by *in vivo* two-photon microscopy were deconvolved using AutoQuant (AutoQuantX3, Media Cybernetics, Rockville, USA). For quantification amyloid plaques as well as BACE1 positive dystrophies, the 3D data stacks of fluorescence intensity were analyzed using custom-written MatLab (Mathworks, Massachusetts, USA) software. Initially, local background subtraction was performed to diminish intensity variations among different stacks. Subsequently, a percentile-based intensity threshold was applied, and a connected component analysis was used to identify contiguous clusters of voxels. This standard analysis was slightly modified for each of the biological readouts with the detailed analysis described below.

To define **BACE1 positive dystrophies** the 50th percentile of immunofluorescence signal was used as a threshold for each image stack. The connected component analysis was applied to identify clusters of contiguous voxels and clusters smaller than 1 μm^3 were excluded.

Amyloid plaques were identified applying the 90th percentile on the Methoxy-X04 fluorescence intensity data. Since amyloid burden typically constitutes 1 to 2 % of brain

volume in the imaged region of APPPS1 mice, this threshold is intendedly set to a very low level. It allows obtaining the total size of amyloid plaques as opposed to thresholding operations such as using local contrast or half-width intensity that rather detect the dense plaque core. Subsequently, individual amyloid plaques were tracked over time. For this purpose, the image data from consecutive time points were loaded as time series in Imaris (Version 7.7.2, Bitplane). Plaque volumes were extracted by 3D-surface-rendering and were semi-automatically tracked over time using the surface tracking module of Imaris. To identify nucleation events, plaques were tracked back to the first time point of appearance and were only assessed when present for at least 3 weeks to warrant unambiguous distinction from background signal. Therefore, quantification of plaque density and formation only include values up to 8 weeks post-treatment even though imaging was performed up to 10 weeks. Correct tracking was manually checked for each amyloid plaque. For reliable determination of the actual size of each amyloid plaque, the largest extension in XY was determined and the radius was calculated as $radius = \sqrt{area/\pi}$ assuming a spherical shape of plaques (Hefendehl et al., 2011). The radii of individual plaques were fitted with a monophasic association function, and the radial growth rate at each time point was obtained by calculating the first derivative of the best fit. All plaques contacting the image border were excluded from the analysis. The distribution of presynaptic boutons, presynaptic dystrophies and BACE1 positive dystrophies was analysed with regards to proximity to the closest amyloid plaque. For this purpose, a quasi euclidean 3D distance transformation was performed to identify the distance of every voxel to the closest plaque border. Distance was calculated at 1 μm resolution from the outer border of plaques into surrounding tissue as well as toward the inside of each plaque. Voxels inside plaques were assigned negative distance from plaque border. To quantify the pathological impact of each plaque separately, the 3D volume was divided into sectors with all voxels closest to a particular plaque constituting the sector of that plaque.

For the correlation of plaque formation rate with plaque distance, the distance to the closest already existing plaque was determined for each formation event at the respective time point of formation. For the analysis, all plaques formed after treatment onset were pooled and closest plaque distance was binned into 20 μm segments. For the frequency

distribution of minimal inter-plaque distance, the distance to the closest plaque was determined for all plaques at week 10, and inter-plaque distance was binned in 20 μm segments.

Statistical Analysis

For statistical analysis, GraphPad Prism 5 (GraphPad Software, California, USA) was used. Data were tested for normal distribution using D'Agostino-Pearson omnibus K2 test and Kolmogorov-Smirnov test. Inter-group comparisons were performed using two-tailed unpaired Student's *t*-test. In the longitudinal measurements, variables were compared across groups using two-way ANOVA (TWA) and *p* values refer to the test of interaction unless specified otherwise. All results are presented as mean \pm SEM unless specified otherwise.

***In vivo* fluorescence recovery after photo-bleaching (FRAP)**

In vivo, FRAP experiments were performed with 6-6.5-months-old mice that were imaged chronically and the protocol followed was similar to the one described by Herzog et al., 2011. The animals were ventilated with a gas mixture of isoflurane (1%), O₂ (95%) and CO₂ (5%) (Forene®, Abbott) and anesthetized with ketamine (0.02% in NaCl). The body temperature was kept at 37 °C with a heating pad (Fine Science Tools GmbH). *In vivo* two-photon imaging was performed on an LSM 7 MP (Carls Zeiss) equipped with standard photomultiplier detectors and a 20x water-immersion objective (W Plan-Apochromat 20x/1.0 DIC, 1.0 NA, Carl Zeiss). Each mouse was reimaged twice with a week interval. Layer I synapses in somatosensory cortex were imaged through the cranial window. 10-12 sub-regions were selected in the center of the images and bleached with 10 – 15 % laser power with an iteration of 50. To resolve the presynaptic boutons a high-resolution 3D stack was obtained from the VGLUT1^{Venus} fluorescence in cortical layer I at a resolution of 0.14 x 0.14 x 0.4 μm^3 and dimensions of 70.71 x 70.71 x 10 μm^3 for first acquisition (6 times 30 seconds) dimensions of 70.71 x 70.71 x 30 μm^3 , for later acquisitions. VGLUT^{Venus} was excited at 915 nm and emission was collected from 470 to 550 nm. Six stacks with 10 μm^2 as z-depth were recorded every 30 s, to assess fast component of the recovery. Two minutes after the acquisition was completed, six stacks with 30 μm^2 as z-depth t every 5

min, 3 stacks with the same z-depth every 7 min and 10 min were recorded to assess slow component of the recovery (**Figure 9.A**).

Analysis of *in vivo* FRAP experiments

Images obtained from the same region over time were aligned with the Imaris software (7.7.2, Bitplane, Belfast, United Kingdom).

The region of interest (ROI) was selected manually on the bleached regions. In addition to that, at least two non-bleached and two background regions were selected for normalization. Average intensities were measured in a small stack of three layers (1.2 μm) and over the time. Normalization (**Figure 9**) was performed as described before (Herzog et al., 2011).

The background intensity was subtracted from the intensity of the ROIs. Normalization was done in reference to the first intensity value before bleaching. The normalized intensities were divided by the normalized time profile of control ROIs for correcting ongoing bleaching. The final signal can thus be written as follows: $S = \frac{(I_{bl}-B)/\langle I_{bl} \rangle}{(I_{ctr}-B)/\langle I_{ctr} \rangle}$ where I_{bl} is the intensity value of the bleached ROI at that specific time and $\langle I_{bl} \rangle$ its average before bleaching. B is the intensity value of the background. I_{ctr} represents the intensity value of an unbleached ROI and is calculated as the average over a few control (unbleached) ROIs. $\langle I_{ctr} \rangle$ is the average of the intensity value of an unbleached ROI before bleaching. Synapses with 80% initial bleaching were discarded. Traces from single synapses were fitted with a double exponential function (nonlinear regression, least square fit) to reduce the noise due to experimental artefacts (mouse movement, low signal-to-noise ratio), which was preferred to suppress high- frequency variations (single aberrant points) without suppressing the fast component of recovery. Then, the average of all fitted curves was fitted with a double exponential function.

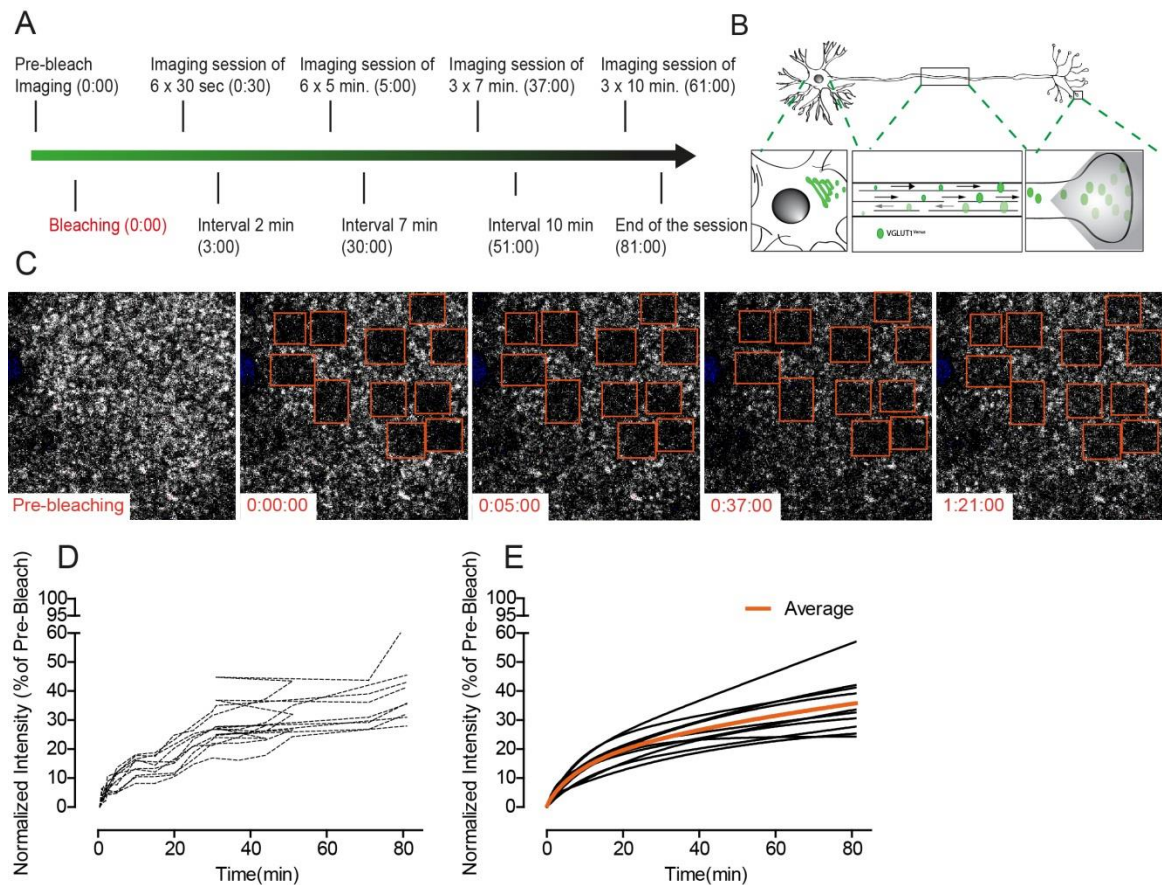


Figure 9. FRAP experiments. (A) Timeline of the fluorescence recovery after the photo-bleaching imaging experiment. (B) Illustration of the cellular localization of VGLU1Venus in neurons. (C) Example images from FRAP experiment. Individual ROIs being followed were indicated with orange colour squares. (D) Individual ROIs fluorescence recovery without nonlinear regression normalization is shown. (E) Fluorescence recovery from individual ROIs after non-linear regression normalization.

Perfusion

Deeply anesthetized mice (130/10 mg/kg b.w. ketamine/xylazine i.p. WDT/Bayer HealthCare) were perfused (cat # 70067811, MA, USA) phosphate-buffered saline (PBS) followed by a fixation with 4% formalin (Carl Roth, Karlsruhe, Germany) for 20 min at 250 mmHg. Mouse brains were dissected and post-fixed in 4% formalin for 24 h.

Immunohistochemistry

Fixed brains were cut into coronal 50 μ m thick sections on a vibratome (VT1000S, Leica, Wetzlar, Germany). Brain slices were permeabilized overnight with 2% Triton X-100 (9002-93-1, Sigma Aldrich, Missouri, USA) – PBS 1X at RT and blocked with 10% serum (Sigma-Aldrich, Missouri, USA) in 0.3% Triton X-100 in PBS 1X. (Zhao et al., 2007) Primary

antibodies were incubated in 0.3 % Triton X-100 for 2 days at 4 °C. Sections were washed in PBS and incubated with the secondary antibody coupled to Alexa with an affinity for different species (1/500, Invitrogen, California, USA) two overnights at 4 °C. To detect amyloid fibrils slices were incubated for 15 min with 10 µg/mL Methoxy-X04 (4920, Tocris, Bristol, UK) in 50% ethanol (2275.5000, Chemsalute) and washed three times with 50% ethanol at RT. Sections were finally washed for 3 times 10 min with PBS before being transferred on a glass slide (polysines slide, J2800AMNZ, Thermo Scientific, Massachusetts, USA) and mounted with glass coverslips (ECN631-1571, 24x24 mm, VWR, Pennsylvania, USA) and fluorescence conserving mounting medium (S3023, Dako, Agilent Pathology Solutions, Santa Clara, United States).

Confocal imaging of dystrophies

Images were acquired with an LSM 780 confocal microscopy (Carls Zeiss, Oberkochen, Germany) equipped with a 40x/1.4 oil immersion objective. For each mouse brain, 3-dimensional 16-bit data stacks of 1024 x 1024 pixels were acquired with 32 µm pinhole size, in the somatosensory cortex at a lateral resolution of 0.1 µm/pixel and an axial resolution of 0.2 µm/pixel. For volumetric analysis, a whole plaque was imaged from top to bottom. 10 plaques regardless of their size from each hemisphere and both hemispheres from each mouse were imaged.

Confocal imaging of mossy-fiber terminals

Images were acquired with an LSM 780 confocal microscopy (Carls Zeiss, Oberkochen, Germany) equipped with a 40x/1.4 oil immersion objective. Mid-section of the hippocampus was acquired with the lateral resolution of 0.346 x 0.346 µm with a size of 1024 x 1024, 16-bit data image. 10 region of interest (ROIs) were chosen in the whole imaged and normalized with the background on the ImageJ program.

Confocal imaging of plaque burden

Images were acquired with an LSM 780 confocal microscope (Carls Zeiss, Oberkochen, Germany) equipped with a 20X objective. Whole slice images were taken with the tile-scan and Z-stack mode. Each tile has lateral 0.761 µm/ pixel and axial 0.8 µm/ pixel resolution with a 32 µm pinhole.

RESULTS

Tau expression is important for plaque growth and the formation of new plaques

In order to investigate the function of the tau protein throughout the progression of amyloid plaque pathology, we performed chronic *in vivo* imaging in an AD mouse model crossed on Tau^{-/-} background (APPPS1 x VGlut1^{Venus} and Tau^{-/-} x APPPS1 x VGlut1^{Venus}). Chronic *in vivo* imaging allowed us to follow individual plaques for a period of 3-months with weekly intervals. As shown in **Figure 10.A**, dynamics of plaque growth could be traced for every existing plaque in somatosensory cortex. Moreover, new appearing plaques in the imaging region could be identified. In each mouse, approximately 67 individual plaques were tracked at consecutive imaging time points **Figure 10.A**, and changes in size were quantified over time. In APPPS1 x VGlut1^{Venus} mice, β amyloid burden [%] increased linearly over the imaging period at a rate of $0.45 \pm 0.05\%$ brain volume occupied by fibrillar A β per week. Tau deletion significantly slowed down β amyloid deposition by 15% **Figure 10.B** (Repeated measure (RM) Two-way ANOVA Interaction_{genotype x age} $F_{[12, 120]} = 3.3$, $p < 0.001$).

β amyloid deposition can occur either by accretion of soluble A β to the surface of existing plaques or via *de novo* plaque formation. In Tau^{-/-} x APPPS1 x VGlut1^{Venus}, the formation rate of plaques was reduced significantly **Figure 10.C** (RM Two-way ANOVA Interaction_{genotype x age} $F_{[12, 143]} = 3.5$, $p < 0.001$). Surprisingly, mean formation rate was similar up to 4.5 months of age between APPPS1 x VGlut1^{Venus} and Tau^{-/-} x APPPS1 x VGlut1^{Venus} and started to decrease in Tau^{-/-} x APPPS1 x VGlut1^{Venus} at compared to in the second week of BACE1 inhibitor treatment and reached a mean reduction by 14fold between five to six months of age. In six months old Tau^{-/-} x APPPS1 mice, the total plaque density was reduced by 13% compared to tau expressing mice **Figure 10.D** (RM Two-way ANOVA Interaction_{genotype x age} $F_{[12, 156]} = 5.24$, $p < 0.0001$).

Growth of individual plaques was quantified as incremental increase of plaque radii per week. Over the imaging period, plaque growth slightly decreased with time in both cohorts **Figure 10.E** (RM Two-way ANOVA-Genotype $F_{[1, 12]} = 6.3$, $p < 0.05$).

Thus, the imaging period relates to the transition phase of A β deposition (Burgold et al., 2014), when the plaque surface available for further A β accretion, starts to exceed the available levels of soluble A β (Yan et al., 2009; Burgold et al., 2011, 2014; Bittner et al., 2012). Apart from the age-dependent decline, the tau knockout cohort had reduced plaque growth rates by approximately 13% **Figure 10**.

We also witnessed that once the plaques were born, none disappeared or shrunk (Hefendehl et al., 2011; Peters et al., 2018). The results indicate that the presence of tau protein is needed for sustaining growth of plaques from the beginning as well as for sustaining plaque formation after 4 months of age. In addition, lack of tau in APPS1 mouse line decreases plaque burden and density in somatosensory region.

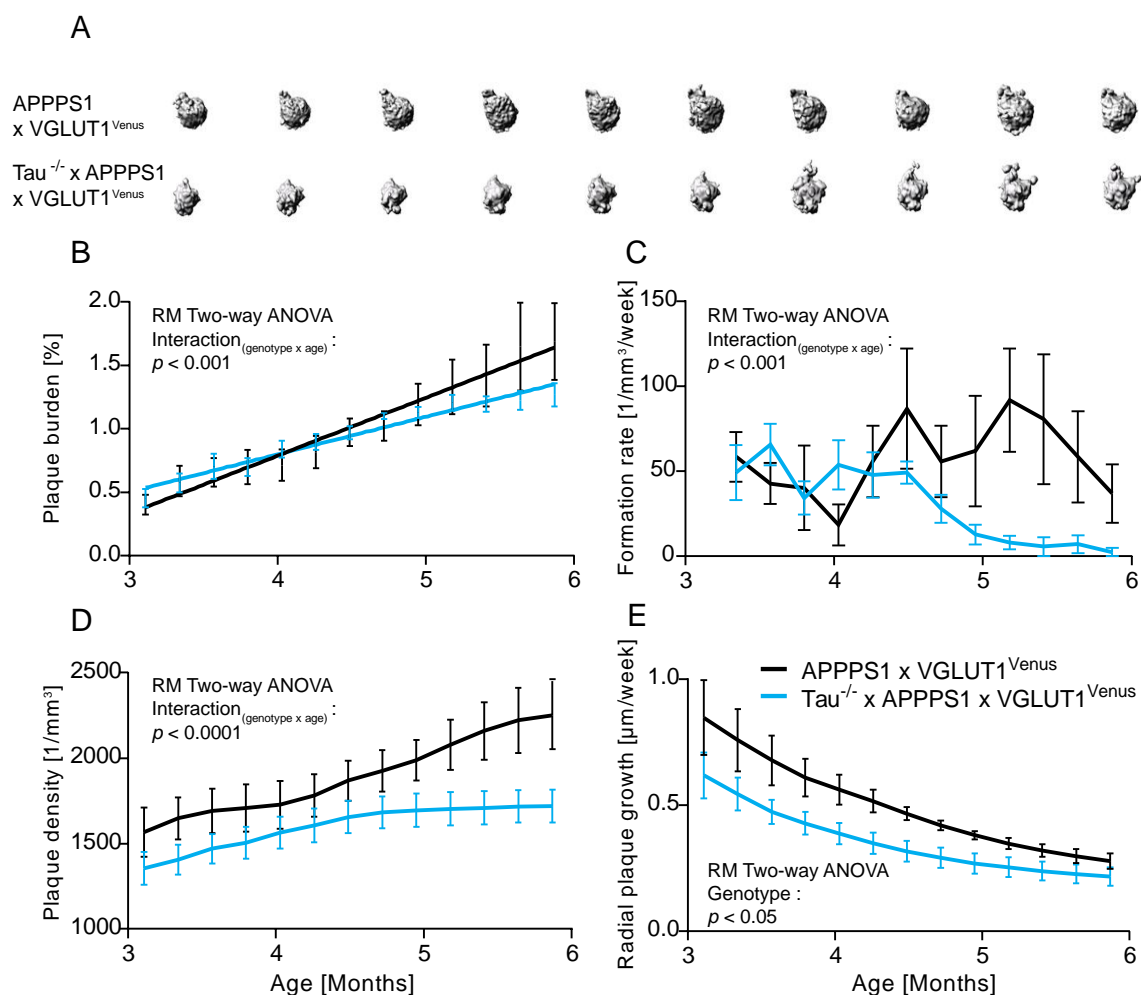


Figure 10. Decreased plaque formation and growth in the absence of Tau in an AD mouse model. (A) An illustrative image of an example plaque from each cohort illustrating the different growth rates of plaques in the two cohorts. **(B)** Integrated volume fraction of all A β plaques (Repeated measure (RM) Two-way ANOVA

Interaction_{genotype x age} $F_{[12, 120]} = 3.3, p < 0.001$). Lines show linear regressions of the data (F-Test, $p < 0.05$). (C) Mean rate of formed plaques (RM Two-way ANOVA Interaction_{genotype x age} $F_{[12, 143]} = 3.5, p < 0.001$). (D) Kinetics of mean plaque density (RM Two-way ANOVA Interaction_{genotype x age} $F_{[12, 156]} = 5.24, p < 0.0001$). (E) Kinetics of mean plaque growth rates (RM Two-way ANOVA-Genotype $F_{[1, 12]} = 6.3, p < 0.05$). Data presented as mean \pm SEM; $n = 7-9$ (mean plaque number analyzed per mouse = 67).

Plaques are less compact in tau deficient APPPS1 mice

If deletion of tau reduces the local production of A β close to plaques, the density of A β fibrils within plaques should be reduced. Methoxy-X04 staining provides a relative measure of A β fibril density and typically is low in the periphery of plaques and increases toward their centre **Figure 11.B**. In APPPS1 mice, the Methoxy-X04 intensity sharply increases from the border toward the centre of plaques and the maximum intensity increases with plaque size. In Tau^{-/-} x APPPS1 mice, Methoxy-X04 intensity increased significantly less toward the plaque centre, comparing plaques of similar size **Figure 11.B** (Two-way ANOVA Interaction_{genotype x distance} $F_{[42, 344]} = 1.0, p > 0.05$ (for plaque size of 0-4 μm); $F_{[44, 405]} = 11.0, p < 0.0001$ (for plaque size of 4-8 μm); $F_{[48, 441]} = 3.5, p < 0.0001$ (for plaque size of 8-12 μm); $F_{[50, 459]} = 8.7, p < 0.0001$ (for plaque size of 12-16 μm); $F_{[50, 459]} = 1.7, p < 0.05$ (for plaque size of 16-20 μm); $F_{[52, 477]} = 3.5, p < 0.0001$ (for plaque size of 20-24 μm).

We addressed whether the reduced A β deposition might be a result of an overall reduced A β production in the brain of Tau^{-/-} x APPPS1 mice. For this, soluble A β 40 and A β 42 levels were determined via ELISA in 2 months old mice, i.e. before onset of A β deposition in APPPS1 mice. Tau deletion did not significantly change the levels of soluble A β 40 and A β 42 in the forebrain **Figure 11.C** ($p = 0.9, 0.8$ (A β 40, 42) > 0.05 , $n=5-7$, t-test, Mann-Whitney).

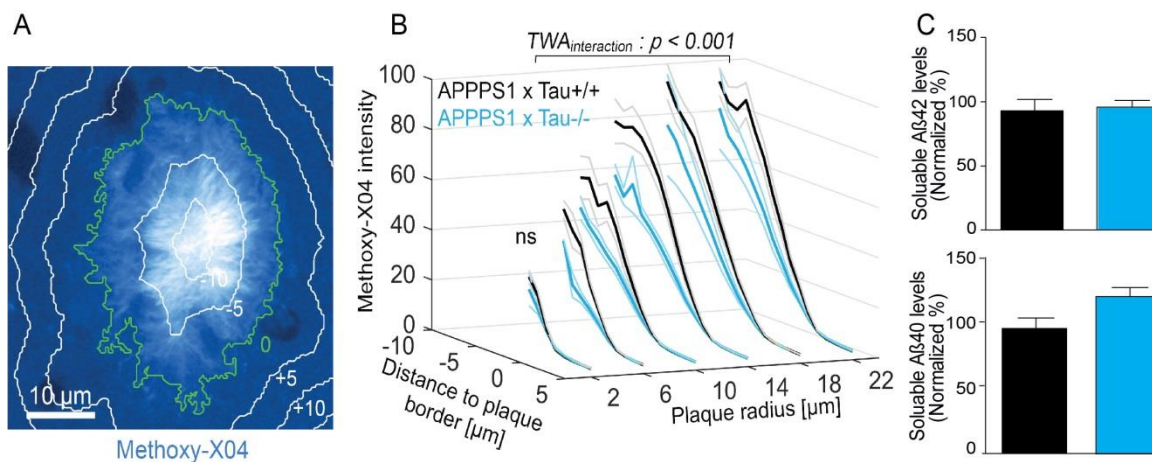


Figure 11. Methoxy-X04 stained plaques show lower intensity profiles from the plaque border toward their center in $\text{Tau}^{-/-}$ x APPPS1 x mice. (A) A representative image of an example plaque. (B) Integrated volume fraction of all $\text{A}\beta$ plaques (for each plaque radius Two-way ANOVA Interaction_{genotype x distance}, except 2 μm plaque radius, $p < 0.01$). Data presented as mean \pm SEM; $n = 7-9$ mice (mean plaque number analyzed per mouse = 118-124). (C) In the forebrain of 2 months old mice the levels of $\text{A}\beta_{40}$ and $\text{A}\beta_{42}$ were not different between genotypes. ($p = 0.9, 0.8$ ($\text{A}\beta_{40}, 42$), $n=5-7$, t-test, Mann-Whitney).

Tau expression contributes to the formation of new plaques in close proximity of pre-existing plaques

It was shown previously; plaque formation is enhanced within 40 μm vicinity of pre-existing plaques (Peters et al., 2018) (**Figure 12.A**). In order to investigate the distribution of plaque formation in comparison to the distance to pre-existing plaques, all the plaques within the imaged area were studied during the entire imaging period. In APPPS1, significantly more satellite plaques were formed within the radius of 10 μm around pre-existing plaques compared to $\text{Tau}^{-/-}$ x APPPS1 (**Figure 12.B**) (Two-way ANOVA Interaction_{genotype x distance} $F[4, 70] = 2.7$, $p < 0.05$, $n=7, 6$ (APPPS1, $\text{Tau}^{-/-}$ x APPPS1 respectively). Plaque formation was approximately 3-fold higher in 10 μm distance to the pre-existing plaque than the one in 30 μm distance in APPPS1. This shows clearly, that the expression of tau contributes to formation of new plaques in close proximity of pre-existing plaques.

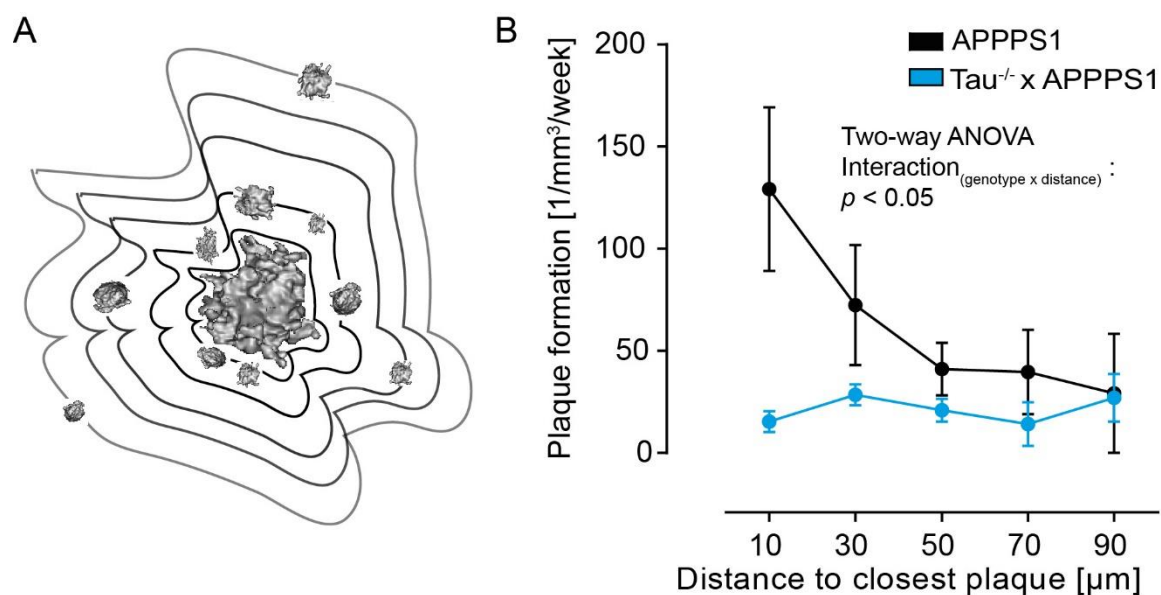


Figure 12. Decreased formation of new plaques in close proximity to pre-existing plaques in TauKO x APPS1. (A) Illustrative image for plaque formation relative to the distance between plaques. Lines around the plaques define distance from the plaque to the border of the big plaque in the center of the image. More plaques were present close to the plaque border of the big plaque in the center. (B) Plaque formation rate relative to the distance to the side of the formation of a new plaque in APPS1 compared to Tau^{-/-} x APPS1. Plaques formed significantly more common within a 10 μm radius (Two-way ANOVA Interaction_{genotype x distance} $F_{[4, 70]} = 2.7$, $p < 0.05$, $n=7, 6$ (APPS1, Tau^{-/-} x APPS1 respectively).

Lack of Tau decreases BACE1 volume fraction around plaques

In previous experiment, we observed a reduction in the plaque formation rate and a reduction in plaque growth when APPS1 mice are lacking Tau. It has been suggested that local Aβ production could be caused by increased BACE1 accumulation in axonal dystrophies surrounding plaques (Sadleir et al., 2016). In the APPS1 mouse model, there are no plaques without associated dystrophies; however, the relationship between BACE1 containing dystrophies and plaques had not been elucidated.

Approximately 10 individual plaques for each hemisphere and two hemispheres for each mouse were tracked using high resolution, volumetric stack imaging. Custom-written MATLAB cluster analysis was applied for automated morphological segmentation in order to quantify the fraction of BACE1 positive structures and to estimate how BACE1 fraction relates to the distance of nearby plaques. Similar BACE1 accumulation with distance to the plaque was categorized for plaques with different sizes (between 4 -24 μm in radius)

in the old-cohort of APPPS1 and $\text{Tau}^{-/-}$ x APPPS1 mice (**Figure 13-A**). Accumulation of BACE1 at the border of plaques increased dramatically in APPPS1 with the increase in plaque size, while this increase was not present in $\text{Tau}^{-/-}$ x APPPS1. The fraction of BACE1 positive volume declined as the distance to the plaque increased (**Figure 13-B-C**). Independent of the plaque size, BACE1 accumulation was mostly detected up to 5 μm away from the border of the plaque in both cohorts. This demonstrates that the corona of BACE1 accumulation does not correlate with the plaque size.

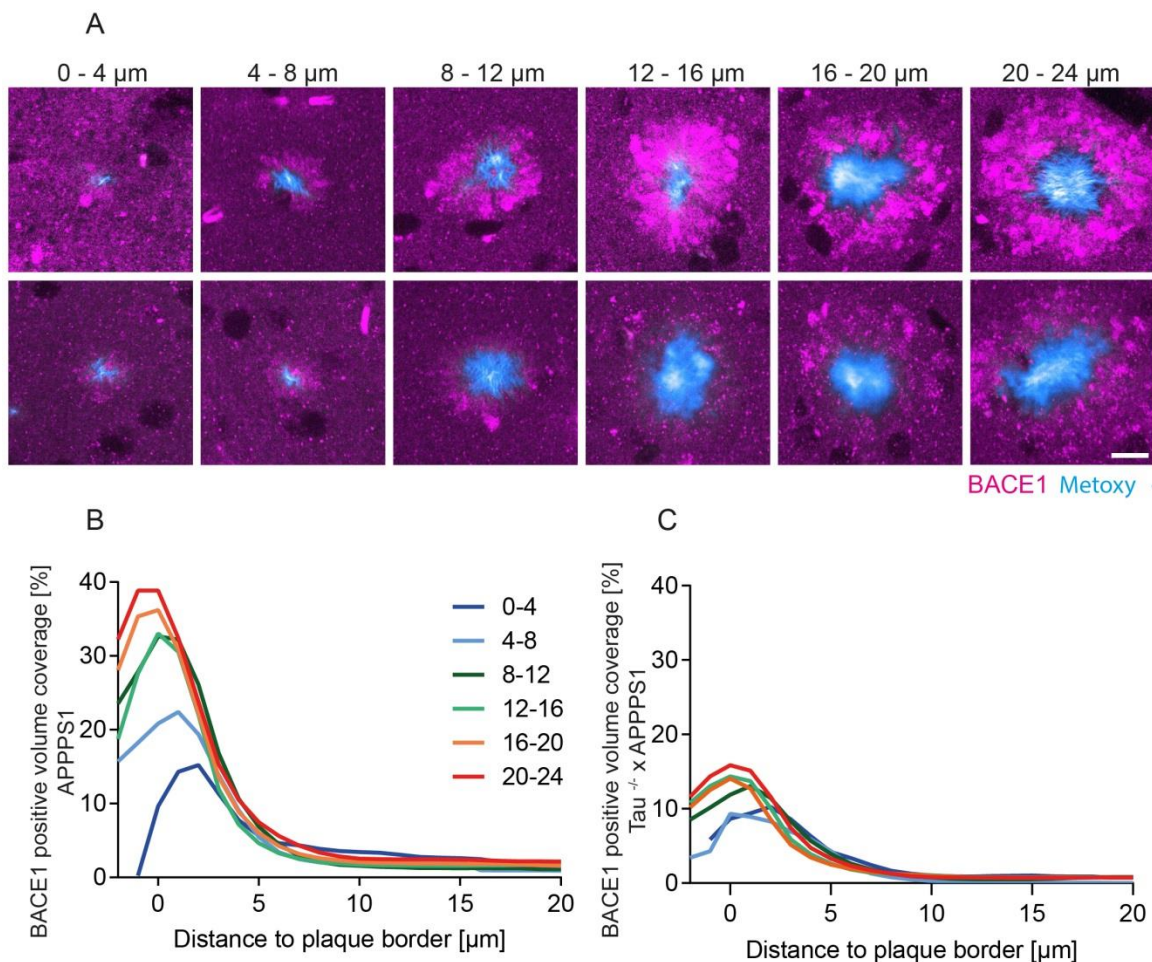


Figure 13. BACE1 positive volume around plaques in the absence of Tau in APPPS1. (A) Representative images of BACE1 accumulation at plaques categorized for different sizes of plaques in APPPS1 and $\text{Tau}^{-/-}$ x APPPS1 mice of the old-cohort. **(B)** BACE1 positive volume fraction for APPPS1 changes according to the distance to the plaque. The highest fraction of BACE1 was observed at the plaque border and increased with the size of plaques. **(C)** BACE1 positive volume fraction in $\text{Tau}^{-/-}$ x APPPS1 mice. Highest BACE1 staining was observed at the plaque border and did not increase with the size of plaques to the extent observed in APPPS1. $n=4-5$, a number of plaques per mouse = 10. Plaque border is indicated as 0 on x-axis.

The decrease in BACE1 volume fraction around plaques was observed in Tau^{-/-} x APPPS1 mice

Since BACE1 accumulation is characteristic of dystrophies (Gowrishankar S. et. al. 2015), we examined BACE1 accumulation around the plaques not only in the old-cohort (8 months) (**Figure 14.A-B**) of APPPS1 and Tau^{-/-} x APPPS1 mice.

Secondly, the percentage of volumetric BACE1 fraction was considerably less especially at the plaques whose radius was 6 μm or more in Tau^{-/-} x APPPS1 mice (**Figure 14.B**) (Two-way ANOVA Genotype $F_{[1, 52]} = 40.6$, $p < 0.0001$, $n=5, 6$ (APPPS1, Tau^{-/-} x APPPS1 respectively)).

We concluded that absence of Tau in APPPS1 mice decreases BACE1 accumulation at the plaque border in an age-dependent fashion (**Figure 15**). While plaques with different sizes from both genotypes affect BACE1 accumulation at most within 5 μm distances from the plaque borders.

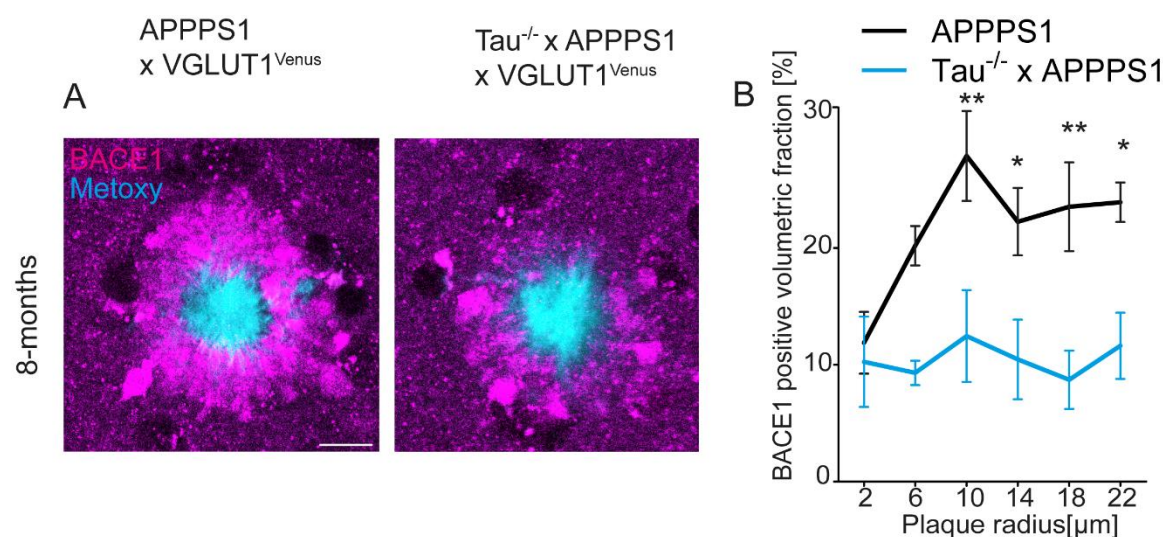


Figure 14. Decreased BACE1 positive volume fraction at the plaque border was observed only in the old-cohort of Tau^{-/-} x APPPS1 mice. (A) Example images of BACE1 and Methoxy-X04 staining in APPPS1 x VGLUT1^{Venus} and Tau^{-/-} x APPPS1 x VGLUT1^{Venus} brain tissue sections. (B) BACE1 volumetric quantification around plaques in the 8-months old cohort. BACE1 volumetric fraction is significantly higher in APPPS1 x VGLUT1^{Venus} (Two-way ANOVA Genotype $F_{[1, 52]} = 40.6$, $p < 0.0001$, $n=5, 6$ (APPPS1, Tau^{-/-} x APPPS1 respectively)). Plaque radius bin = 4 μm. The scale bars indicate 10 μm.

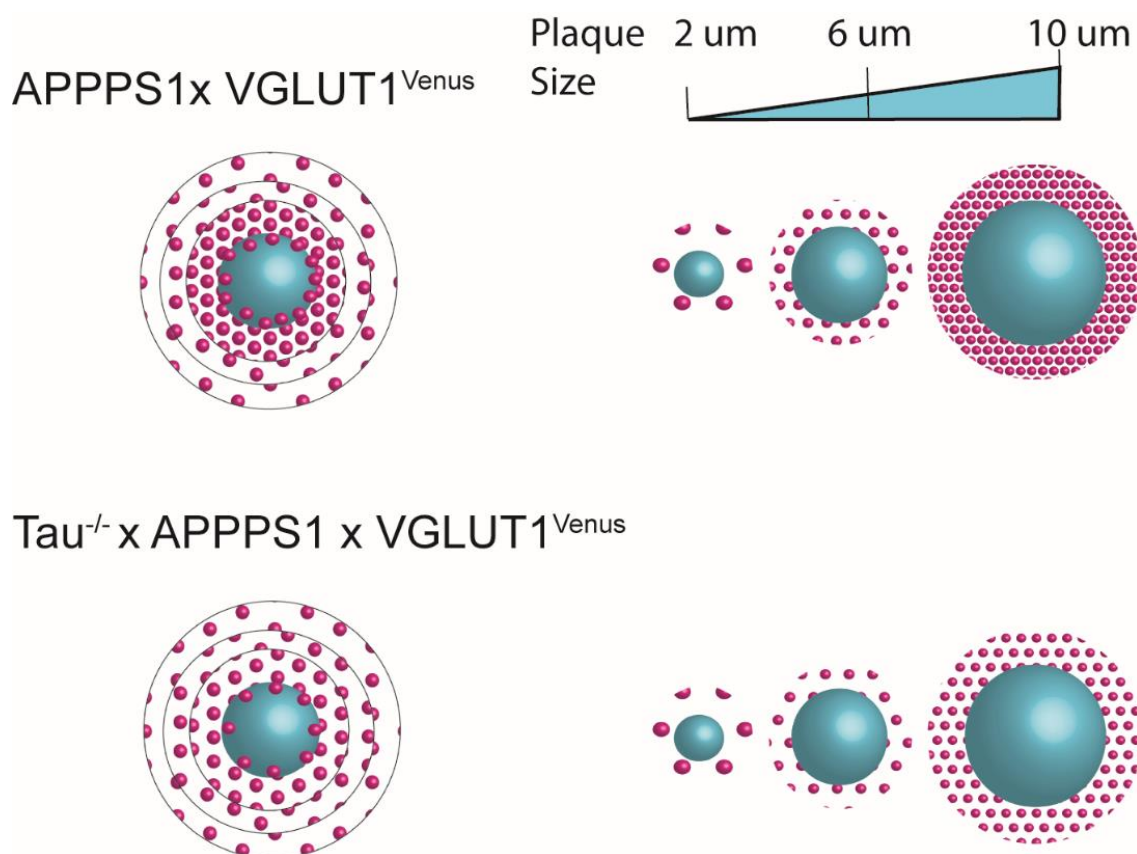


Figure 15. Illustration the accumulation of BACE around plaques. Although BACE1 positive volume is significantly altered, the effect of plaques is detected mostly in the 5 μ m vicinity.

Tau expression modulates APP-positive accumulations in peri-plaque dystrophies

In addition to BACE1, LAMP1 (lysosomal marker), VGLUT1 (pre-synaptic marker) and APP (amyloid-precursor protein) are aberrantly localized in peri-plaque dystrophic neurites (Cataldo et al., 1991; Nixon et al., 2005; Kandalepas et al., 2013; Sadleir et al., 2016). Lysosomes accumulating at amyloid plaques have been shown to have a low luminal protease content and are unable to degrade proteinaceous cargos (Gowrishankar et al., 2015) To assess whether the absence of Tau has a beneficial impact on other proteins localized in dystrophies, the volume fraction and profiles of APP and LAMP1 were quantified in APP^{PS1} x VGLut1^{Venus} and $\tau^{-/-}$ x APP^{PS1} x VGLut1^{Venus}. This analysis was important not only to understand the possible beneficial impact of the lack of tau in dystrophies, but also to shed light on mechanisms triggering the accumulation of different proteins in peri-plaque dystrophies.

APP positive volume fraction was significantly reduced in $Tau^{-/-}$ x APPPS1 x VGLU1^{Venus} at plaque radius of 10 and 18 μ m (**Figure 16.B**) (Two-way ANOVA Genotype $F_{[1, 18]}=24.0$, $p < 0.0001$, $n=4, 3$ (APPPS1, $Tau^{-/-}$ x APPPS1 respectively)). Unlike APP, LAMP1 accumulation at plaques was not significantly different between APPPS1 x VGLut1^{Venus} and $Tau^{-/-}$ x APPPS1 x VGLut1^{Venus} in old-cohort (8-months) (**Figure 16.D**) (Two-way ANOVA – all factors $p > 0.05$).

APP and BACE1 accumulated less around plaques in $Tau^{-/-}$ x APPPS1 x VGLut1^{Venus} in the old cohort (8-months) compared with APPPS1 x VGLut1^{Venus} (**Figure 15-16**) while lysosomal membrane marker, LAMP1, did not differ in $Tau^{-/-}$ x APPPS1 x VGLut1^{Venus} in the old-cohort in term of its volumetric percentage and the dystrophic corona radius. This discrepancy between LAMP1, APP and BACE1 protein accumulations at plaques might suggest that APP and BACE1 are regulated by a distinct mechanism around plaques different to LAMP1.

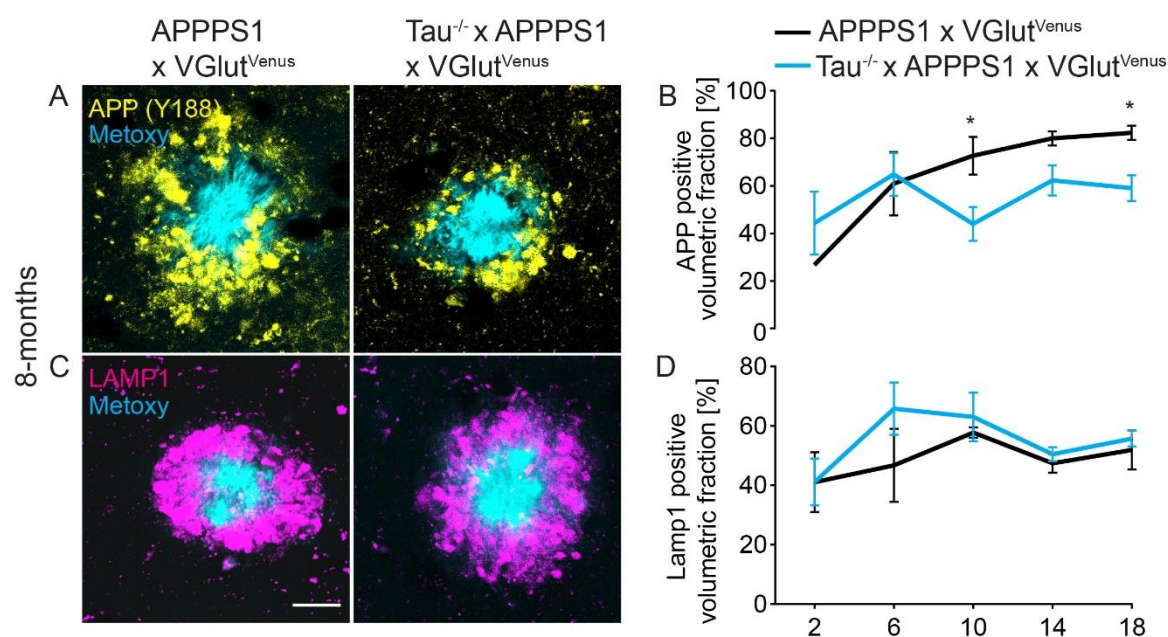


Figure 16. Decreased APP, but not LAMP1 accumulation at the plaque border in $Tau^{-/-}$ x APPPS1x VGLut1^{Venus} at 8 months of age. (A) A representative image from APP and Methoxy-X04 stained 8 months old APPPS1 x VGLUT1^{Venus} and $Tau^{-/-}$ x APPPS1x VGLut1^{Venus} brain tissue sections. (B) APP-positive volumetric quantification around plaques for the old cohort (Two-way ANOVA Genotype $F_{[1, 18]}=24.0$, $p < 0.0001$, $n=4, 3$ (APPPS1, $Tau^{-/-}$ x APPPS1 respectively)). (C) Representative images from LAMP1 and Methoxy-X04 from 8 months old APPPS1 x VGLut1^{Venus} and $Tau^{-/-}$ x APPPS1 x VGLut1^{Venus} mice. (D) LAMP1-positive volumetric quantification around plaques for the old cohort (Two-way ANOVA – all factors $p > 0.05$). Plaque radius bin = 4 μ m. The scale bars indicate 10 μ m.

Pre-synaptic transportation of VGLUT1 is not affected by absence of Tau

In the previous experiment we showed that APP and BACE1 protein expression at plaques is changed if Tau is lacking. The Tau protein is a microtubule-associated cytoskeleton protein associated with anterograde axonal transport (Mandelkow, 2003). Its absence might affect trafficking of presynaptic proteins involved in APP cleavage and hence, might affect plaque growth and formation (Groemer et al., 2011). Therefore, we investigated the anterograde transport of VGlut1^{Venus} (**Figure 17**) using fluorescence recovery (FRAP) (Ishikawa-Ankerhold et al., 2012), a technique to study protein mobility within cells. The principle behind our experiment is that initially, genetically fluorescently tagged VGlut1 proteins are bleached. The fluorescent signal recovers due to transportation of VGlut1^{Venus} into the region of interest. The same presynaptic terminals were monitored for 81 minutes and the fluorescence recovery was measured between four different genotypes: VKIN x VGlut1^{Venus}, Tau^{-/-} x VGlut1^{Venus}, APPPS1 x VGlut1^{Venus} and Tau^{-/-} x APPPS1 xVGlut1^{Venus}.

The normalized intensity recovery curves of Tau^{-/-} x VGlut1^{Venus} and Tau^{-/-} x APPPS1 x VGlut1^{Venus} were overlapping (**Figure 17.B**) (least-square non-linear regression). The recovery period was studied in more comprehensive manner in order to understand whether all the components of the recovery period had similar properties. First of all, the difference between the mobile fraction, which was defined as the amount of recovery at the end of experiment, was insignificant between the groups (One-way ANOVA, $p = 0.06 > 0.05$, $n=4, 5$) which suggests that the population variation (recovering and non-recovering terminals) at the bleached areas was similar (**Figure 17.C**).

Intensity recovery curve consists of two phases, a fast and a slow-recovery phase. The fast recovery phase is defined as a phase where proteins are available within the readily-releasable pool to fuse and takes place within the range of minutes. The slow-recovery phase is defined as the phase of vesicles transportation along the axon. The half-life of these phases is defined as the time needed for signal to recovery to 50%. The half-life of the fast (One-way ANOVA, $p = 0.2 > 0.05$, $n=4, 5$; (**Figure 17.D**) and slow-recovery (One-way ANOVA, $p = 0.52 > 0.05$, $n=4, 5$) (**Figure 17.E**) was not different between the groups,

which indicates that there was no difference in fusion and axonal transportation mechanism in the AD mouse model APPPS1 x VGlut1^{Venus}, Tau^{-/-} x APPPS1 x VGlut1^{Venus}, VGlut1^{Venus} and Tau^{-/-} x VGlut1^{Venus}. The percentage of fast-recovery within the imaging time was not considerably changed between the group (One-way ANOVA, $p = 0.7 > 0.05$, $n=4,5$), which means that the percentage of the readily releasable vesicle pools between the groups was similar (**Figure 17.F**).

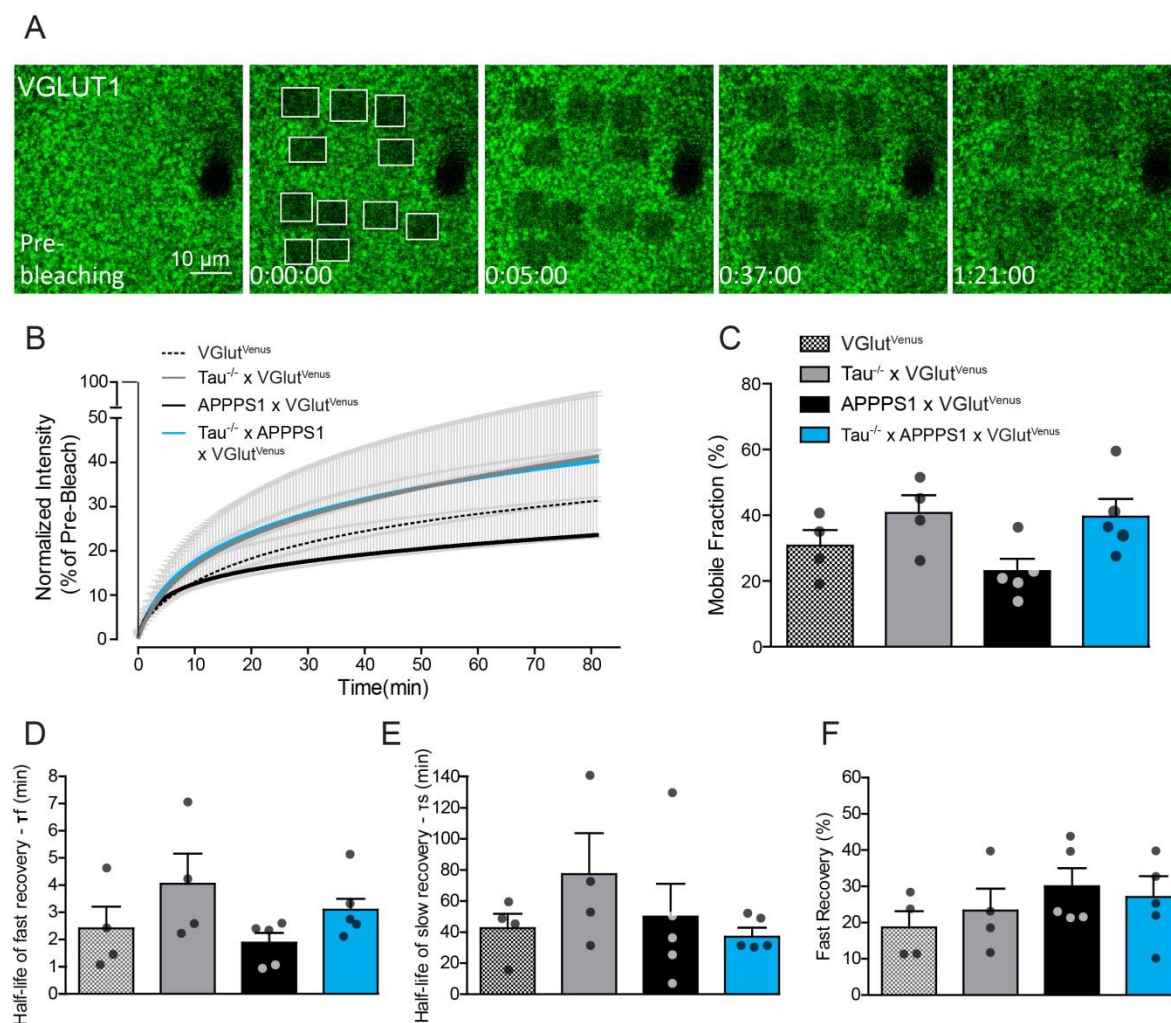


Figure 17. No change in the axonal transport of VGlut1 positive synaptic vesicles between mouse lines. (A) Representative images of an APPPS1 mouse during a FRAP experiment at different time points. (B) Normalized intensity curves for VGlut1^{Venus}, Tau^{-/-} x VGlut1^{Venus}, APPPS1 x VGlut1^{Venus} and Tau^{-/-} x APPPS1 x VGlut1^{Venus}. (C) Mobile fraction of bleach recovery which corresponds to the percentage of normalized intensity at the last imaging time point. No significant difference between the genotypes (One-way ANOVA, $p = 0.06 > 0.05$). (D) Half-life of fast recovery. No significant difference in the comparison of the genotypes (One-way ANOVA, $p = 0.2 > 0.05$). (E) Half-life of slow recovery. No significant difference in the comparison of the genotypes (One-way ANOVA, $p = 0.52 > 0.05$). (F) Percentage of fast recovery. No significant difference in the

comparison of the genotypes (One-way ANOVA, $p = 0.7 > 0.05$, $n=4$ (for $\text{Tau}^{-/-}$ x $\text{VGlut1}^{\text{Venus}}$ and $\text{VGlut1}^{\text{Venus}}$) and $n=5$ (for APPPS1 x $\text{VGlut1}^{\text{Venus}}$ and $\text{Tau}^{-/-}$ x APPPS1 x $\text{VGlut1}^{\text{Venus}}$). Number of mean ROIs per mouse = 10. Scale bar: 10 μm .

Tau deficiency does not affect the expression of APP, BACE and LAMP1 in pre-synaptic terminals

Proteins might have different anterograde transportation rate, according to their function (Maday et al., 2014). Therefore, the comparison of anterograde transport between different proteins by bleaching $\text{VGlut1}^{\text{Venus}}$ might not be valid for proteins involved in the disease, such as BACE1 (Buggia-Prévoit et al., 2014; Hung and Coleman, 2016; Ye et al., 2017), LAMP1 (Harada et al., 1998; Hendricks et al., 2010) and APP (Kamal et al., 2000). We hypothesized that in case of presynaptic axonal transport deficit, BACE1, VGlut1 , LAMP1 and APP might be reduced in expression at would be expressed less in the presynaptic terminals. In order to investigate if any change in the presynaptic expression of BACE1, VGlut1 , LAMP1 and APP (dystrophy-related proteins) does occur if tau is lacking, we compared the expression intensity of these proteins at mossy-fiber terminals, terminals that are known to express these proteins to high amounts (**Figure 18.A**).

The localization of BACE1, LAMP1, APP and VGlut1 was not changed in $\text{Tau}^{-/-}$ x APPPS1 x $\text{VGlut1}^{\text{Venus}}$ compared with APPPS1 x $\text{VGlut1}^{\text{Venus}}$ in the old-cohort ($p > 0.05$, $n=4$, Mann-Whitney, t-test) (**Figure 18.B**). This might suggest that the anterograde transport of BACE1, LAMP1, and APP is not altered in VGlut1 in $\text{Tau}^{-/-}$ x APPPS1 x $\text{VGlut1}^{\text{Venus}}$ compared to APPPS1 x $\text{VGlut1}^{\text{Venus}}$.

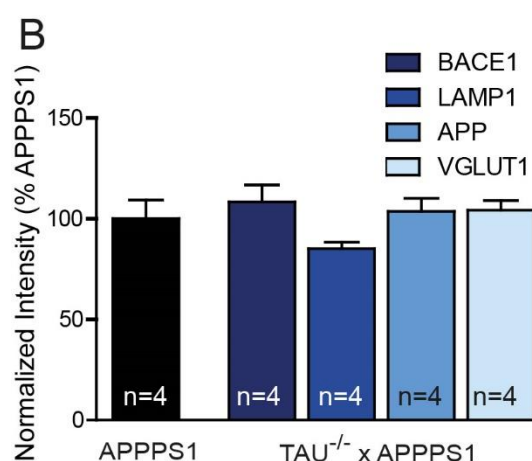
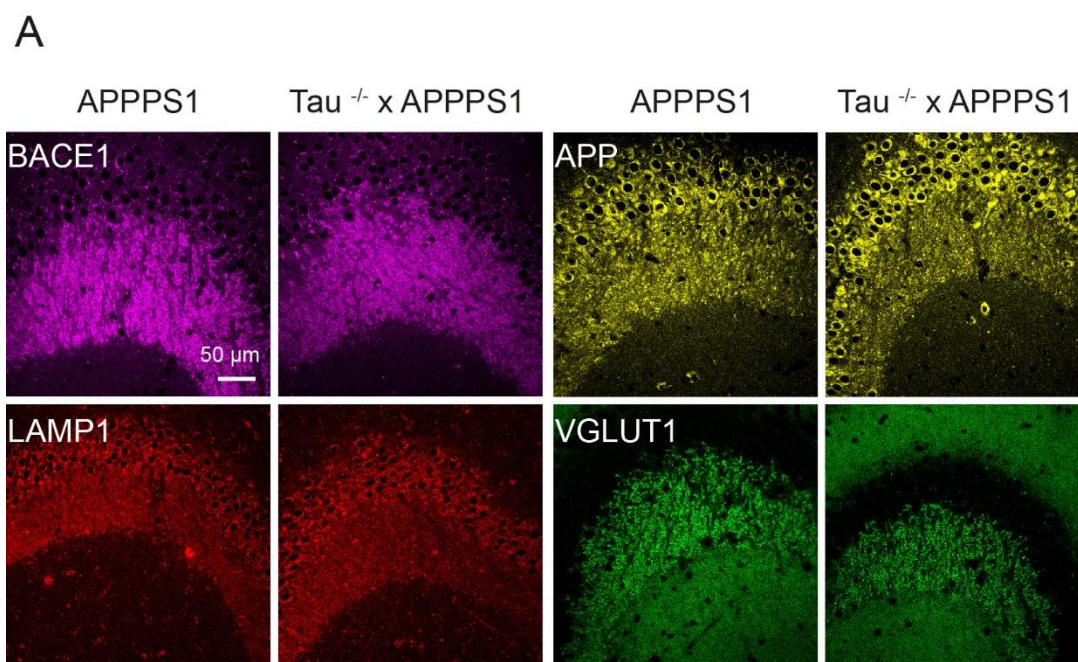


Figure 18. The expression of APP, BACE, VGLUT1 and LAMP1 is not altered in hippocampal pre-synaptic terminals of Tau^{-/-} x APPPS1 mice. (A) Representative images of mossy-fiber terminals stained with BACE1, LAMP1, APP and VGLUT1 antibodies in 8-months old APPPS1 mice. (B) Comparison of the normalized expression of BACE1, LAMP1, APP and VGLut1 at mossy fiber terminals between APPPS1 and Tau^{-/-} x APPPS1 at 8 months of age. No significant difference was observed ($p > 0.05$, Mann-Whitney, t=test). Data presented as mean \pm SEM; n=4. The scale bar indicates 50 μ m.

The anterograde transport of VGLUT1 within axonal dystrophies is not altered by lack of tau

The reduced BACE1 and APP accumulation in dystrophies around plaques and the decreased plaque growth and formation in Tau^{-/-} x APPPS1 x VGLut1^{Venus} mice might be due to a change in anterograde axonal transport only within dystrophies, while the anterograde transport is generally not altered. Since dystrophies are unique in terms of

the content and concentration of proteins that accumulate, anterograde transport deficit might explain the reduced BACE1 and LAMP1 protein accumulation in dystrophies at plaques. In order to investigate if there is any localized anterograde transport alteration, we performed fluorescence recovery after photo bleaching experiments in the dystrophies, as in **Figure 17**. We compared the fluorescence recovery for a period of 81 minutes in the areas without dystrophies versus areas containing dystrophies (**Figure 19.A-B**) using FRAP. The normalized intensity of the recovery did not vary significantly between dystrophic areas in $\text{Tau}^{-/-} \times \text{APP}^{\text{PS1}} \times \text{VGlut1}^{\text{Venus}}$ and non-dystrophic areas in $\text{Tau}^{-/-} \times \text{APP}^{\text{PS1}} \times \text{VGlut1}^{\text{Venus}}$. The percentage of a mobile fraction, also indicated by the last time point of the normalized intensity at 81 min, was not significantly different ($p = 0.1 > 0.05$, $n=5$, Mann-Whitney, t-test) (**Figure 19.C**). The percentage of fast recovery ($p = 0.7 > 0.05$, $n=4$, Mann-Whitney, t-test) (**Figure 19.D**) half-life of fast ($p = 0.8 > 0.05$, $n=4$, Mann-Whitney, t-test) (**Figure 19.E**) and slow recovery ($p = 0.59 > 0.05$, $n=4$ (non-dystrophy), $n=5$ (dystrophy), Mann-Whitney, t-test) (**Figure 19.F**) were comparable between the groups.

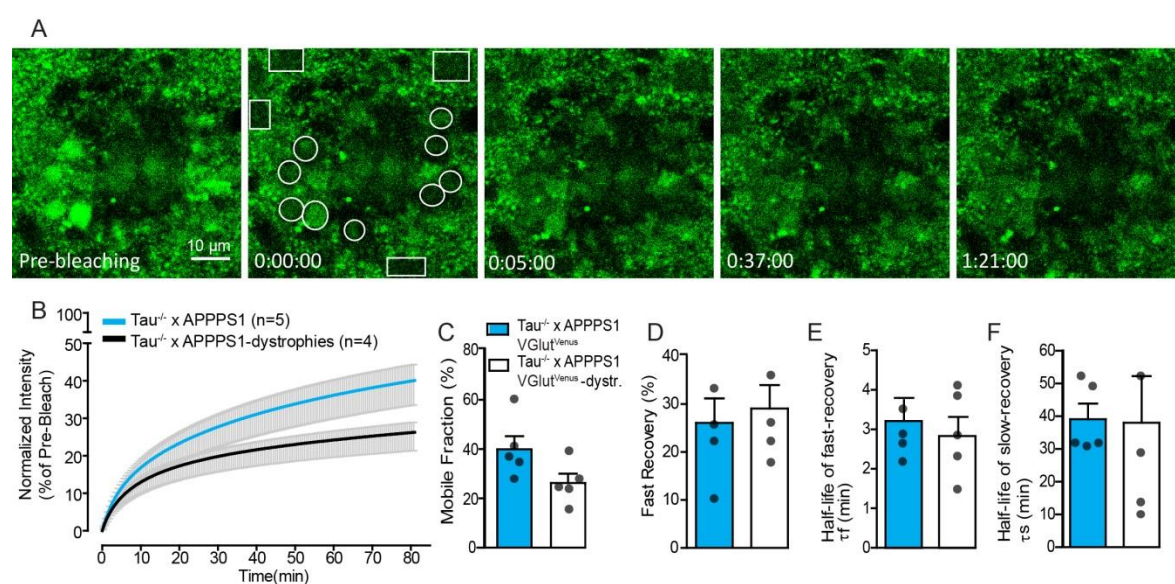


Figure 19. No change in axonal transport of $\text{VGlut1}^{\text{Venus}}$ within dystrophies in APP^{PS1} mice lacking tau. (A) Representative images of $\text{Tau}^{-/-} \times \text{APP}^{\text{PS1}}$ during FRAP experiment at different time points. (B) Normalized recovery curves for $\text{Tau}^{-/-} \times \text{VGlut1}^{\text{Venus}}$ at non-dystrophies and $\text{Tau}^{-/-} \times \text{VGlut1}^{\text{Venus}}$ at dystrophies. (C) Mobile fraction, which corresponds to the percentage of normalized intensity at the last imaging time point. No significant difference between dystrophic areas in $\text{Tau}^{-/-} \times \text{APP}^{\text{PS1}} \times \text{VGlut1}^{\text{Venus}}$ and non-dystrophic areas in $\text{Tau}^{-/-} \times \text{APP}^{\text{PS1}} \times \text{VGlut1}^{\text{Venus}}$ ($p = 0.1 > 0.05$, $n=5$, Mann-Whitney, t-test). (D) Percentage of fast recovery. No significant difference between the

conditions ($p = 0.7 > 0.05$, $n=4$, Mann-Whitney, t-test). (E) Half-life of fast recovery. No significant difference between the genotypes ($p = 0.8 > 0.05$, $n=4$, Mann-Whitney, t-test). (F) Half-life of slow recovery. No significant difference between the conditions ($p = 0.59 > 0.05$, $n=4$, Mann-Whitney, t-test). Data is averaged within each mouse and then within each group \pm SEM; $n=4-5$. A number of mean ROIs per mouse = 8-10.

Microglia activation at plaques is independent of the presence of tau

Microglia are immune cells of central nervous system (CNS) and responsible for scavenging A β peptides, damaged neurons and synapses as well as infectious agents (Gehrmann et al., 1995). In order to understand whether the decrease in plaque growth and formation in Tau^{-/-} x APPPS1 are might be a consequence of differences in microglia activation, which affects plaque growth; we measured the microglia volume fraction at the plaque border for different plaque sizes based on IBA1 stainings to label microglia (**Figure 20.A-C**). In addition, we analysed the volumetric profile of microglia according to the distance to the plaques which shows the volume taken by microglia at different distances to the plaque (**Figure 20.B-D**). APPPS1 x VGlut1^{Venus} and Tau^{-/-} x APPPS1 x VGlut1^{Venus} did not display differences in the IBA1 positive volume fraction of plaques of different size (**Figure 20.B**) ($p > 0.05$, $n=4$, Mann-Whitney, t-test). Moreover, the distribution of IBA1 positive structures in relation to the distance to the plaque borders exhibited a similar tendency in both genotypes (**Figure 20.D**) (RM Two-way ANOVA all factors $p = 0.7 > 0.05$, $n=4$). These experiments suggest that molecular alterations observed in Tau^{-/-} x APPPS1 x VGlut1^{Venus} compared with APPPS1 x VGlut1^{Venus} do most likely not depend on the changes in reactive microglia abundance and activity.

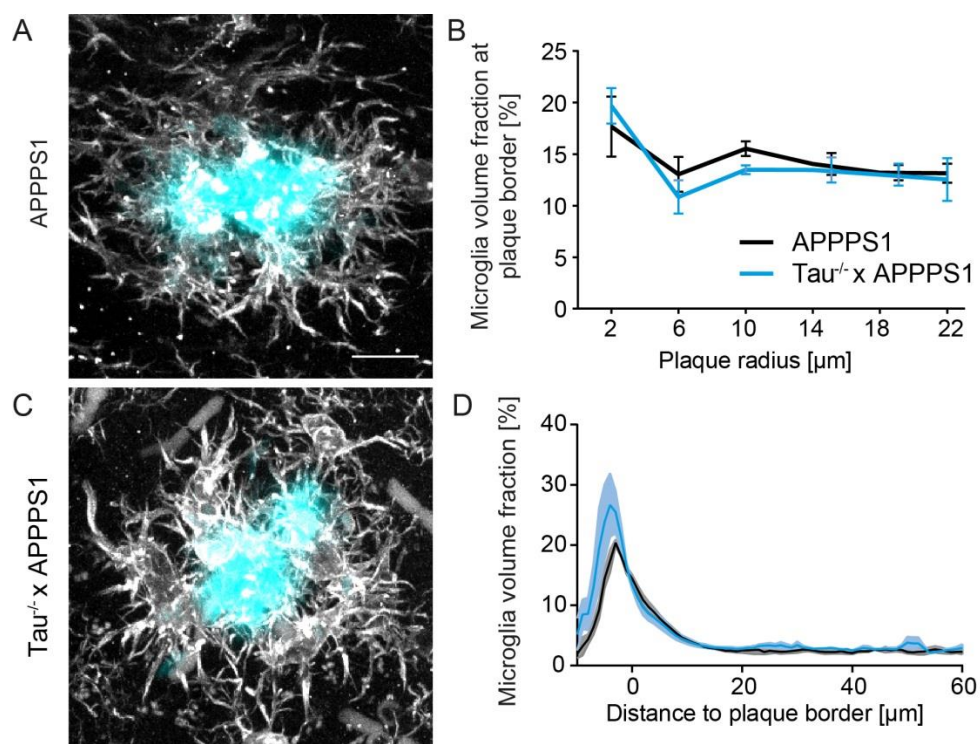


Figure 20. Lack of tau did not alter microglia activation at the plaque borders. (A) Representative images of IBA1 staining in APPPS1 x VGlut1^{Venus} and Tau^{-/-} x APPPS1 x VGlut1^{Venus}. (B) The microglia volume fraction was comparable between genotypes and between plaque radius ($p > 0.05$, $n=4$, t-test, Mann-Whitney (test was performed between genotypes per plaque radius)) (C) Microglia volume fraction changes with the distance to the plaque border. However, change in microglia volume fraction was not significantly different between the mouse lines (RM Two-way ANOVA all factors $p > 0.05$, $n=4$).

BACE1 protein levels are significantly reduced in the whole brains of Tau^{-/-} x APPPS1

Previously we saw that certain proteins are reduced in dystrophic areas around plaques. In order to examine if these proteins are reduced in the entire brain, we quantified BACE1, LAMP1, APP levels by western-blot analysis. BACE1 protein levels were significantly reduced in Tau^{-/-} x APPPS1 x VGlut1^{Venus} (Figure 21.A-B) ($p = 0.03 < 0.05$, $n=5, 7$, t-test, Mann-Whitney). Additionally, we analysed the protein levels of APP in whole brain lysates. The results indicate that the amount of APP, whose expression was transgenically regulated (due to APP mutation in APPPS1 mice) and decreased in the dystrophies according to immunostaining, was unaffected (Figure 21.A-B) ($p > 0.05$, $n=5, 7$, t-test, Mann-Whitney). This result suggests that reduction in protein level at neurotic dystrophies is not due to a change in translation or transcription but due to changes in

protein degradation or distribution. We also analyzed other dystrophic markers such as LAMP1, LC3 and Cathepsin B, all of which were not altered in expression in whole brain lysates ($p > 0.05$, $n=5, 7$, t-test, Mann-Whitney)

All these experiments suggest that BACE1 and APP are distributed in a tau dependent manner within neurotic dystrophies very different to other proteins accumulating at neuritic dystrophies like LAMP1.

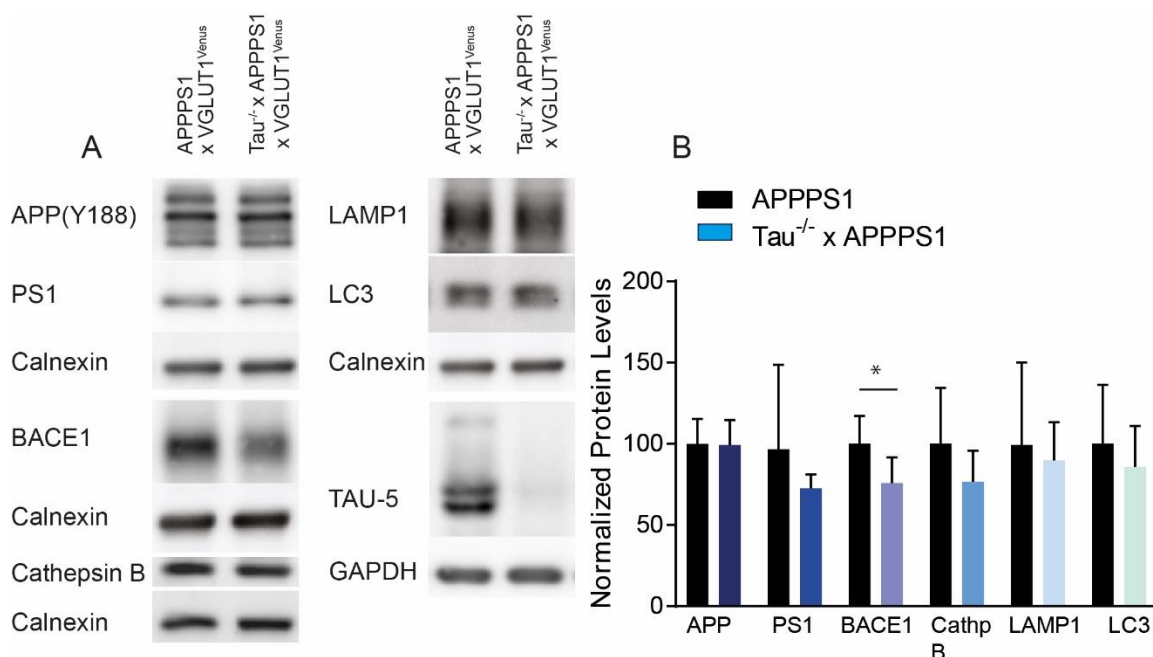


Figure 21. BACE1 protein levels are significantly reduced in whole brain lysates of Tau^{-/-} x APPPS1 mice. (A) Representative bands from whole brain protein lysates. (B) Protein levels were normalized to a housekeeping protein (Calnexin for membrane-bound fraction and GAPDH for soluble) and compared. BACE1 protein level was significantly reduced in Tau^{-/-} x APPPS1 ($p = 0.03 < 0.05$, $n=5, 7$, t-test, Mann-Whitney). Data presented as the mean of each mouse in the groups \pm SEM.

DISCUSSION

Alzheimer`s disease is an extremely complex neurodegenerative disease. Therefore, understanding the disease and pathology require multi-functional studies and broad collaborations within the scientific community. In this section, we will explain briefly our contribution in understanding the disease in comparison to previous studies. Additionally, we argue about possible follow-up studies and speculate about the mechanisms that underlie the observations in our mouse model. For ease of reading, the discussion is organized in a topic specific fashion. First of all, the physiology of compensatory mechanisms in different TauKO mouse models is discussed. Then, the role of endosomal/lysosomal proteins in subcellular trafficking of specifically APP and BACE1 is stated. Lastly, the way how changes in the regulation of endo/lysosomes trafficking and maturation might affect the disease pathology is argued.

A growing body of genetic and biochemical evidence indicates a strong relation between amyloid beta and tau in the pathogenesis of AD. Here, we demonstrate with high temporal and spatial resolution imaging that the protein tau is not needed for the initiation of plaque growth and the formation of axonal dystrophies. Rather, tau seems to be a contributing factor in AD pathology. In other words, plaques are formed and grow still despite the lack of tau, but at a reduced rate. The absence of tau mostly affects the growth of amyloid plaques and the content of dystrophies at plaques. We observed that the effect of tau on plaque growth and formation is much more prominent at the cohort of older animals compared to younger ones. Additionally, BACE1 and APP protein abundance, which are two well-known markers for dystrophies in AD, are substantially reduced within dystrophies. Thus, therapeutics for a general reduction of tau protein may slow down the formation of the highly characteristic axonal dystrophies at plaques and the formation of new plaques in close proximity of existing neuritic plaques.

In AD patients, pathological depositions, namely plaques and neurofibrillary tangles show a discrepancy from one individual to another, which applies to AD mouse models as well (for review Nelson et al., 2009). Even within one AD mouse line, variation is high between genders and individuals (Wang et al., 2003), which makes identification of true positive

changes in plaque load challenging. However, by tracking the changes in individual plaques and normalizing them for plaque growth we attempt to overcome this issue.

One of the most important advantages of *in vivo* two-photon imaging is the allowance to follow chronic individual plaque changes. Therefore, age-dependent changes can be monitored and interfered with at a given time. We witnessed a more pronounced effect of tau in aged mice. This could be due to an accumulated effect of the lack of tau over time. In other words, long-term absence of tau might be needed to observe changes in plaque dynamics instead of short-term lack of tau. Alternatively, is the effect of tau depletion more important if there are more axonal dystrophies at plaques, which is the case if the animals are older. In order to study the short-term absence of tau on plaques and dystrophies, conditional knockout animals are required. By this way, the effect of the lack of tau only after a certain age might be able to be studied.

Previous studies showed that partial reduction of BACE1 improves amyloid neuropathology and reduce A β levels (Laird et al., 2005; Kimura et al., 2010; Rabe et al., 2011; Sadleir et al., 2016). Those studies compared BACE1 homozygous and heterozygous knockout mice crossed with APP^{swe}PS1 Δ E9 which exhibited a 50% A β burden in younger, but not older mice (Laird et al., 2005). Another study indicated that a 50% BACE1 reduction in 5XFAD/BACE1^{+/-} mice decreased A β 42 plaque levels only in females to 40% and did not affect the A β 42 plaque level in males (Sadleir et al., 2015). Rabe et al., 2011 showed that 50% decrease in BACE1 enzyme activity resulted in 20% reduction in A β levels in an animal model with the Swedish mutation (APP23 mice) and 16% for non-mutated APP mice. In light of these studies, a slight reduction in BACE1 protein level in Tau^{-/-} x APPPS1 as observed in our study might not dramatically diminish A β levels in the whole brain. This result might explain why A β 40/42 levels in soluble and fibrillar fractions did not drastically differ in our study between TauKOxAPPPS1 and APPPS1, even in the old cohort.

Previously, we showed that BACE1 inhibition in AD mice significantly reduces plaque formation, although do not have significant effects on presynaptic dystrophies. In those studies, we show that absence of tau significantly reduces accumulation of disease-associated proteins in presynaptic dystrophies which most likely cause a reduction in plaque growth. All in all, these results suggest that these two approaches namely BACE1

inhibition and endogenous Tau reduction complement each other in terms of actions. While BACE1 is acting mainly on plaque formation, absence of tau affects plaque growth and the density of presynaptic dystrophies. Thus, the results support the notion that combinatorial effect of BACE1 inhibition and lack of tau might effectively prevent the progression of disease pathology.

In our study, BACE1 localization in axonal dystrophies at plaques was shown to be affected by tau expression. This specific reduction of BACE1 in axonal dystrophies could be related with a change in the axonal transportation of BACE1. Therefore, axonal transportation of another pathology-related presynaptic protein, VGLUT1, was investigated. Although a significant change was not observed, it does not rule out the possibility that the axonal transportation of BACE1 protein is affected. As shown in the dystrophies surrounding amyloid plaques, the BACE1 fraction, but not VGLUT1 fraction, was reduced, indicating that intra-axonal accumulation of BACE1 is not simply the consequence of an altered transport of a presynaptic protein. Thus, more studies are needed to validate if BACE1 axonal trafficking might be regulated by the tau protein.

Electrophysiological experiments in hippocampal slices showed similar NMDA/AMPA receptor currents, synaptic transmission and synaptic plasticity between wild-type and tau knockout mice (Roberson et al., 2011; Shipton et al., 2011). However, Tau knockout mice in Alzheimer's disease are more resistant to seizure-induced toxins and amyloid beta peptides, which suggest that tau takes part in neuronal excitability or via multiple other mechanisms (Roberson et al., 2007; Ittner et al., 2010; Roberson et al., 2011). Thus, it was suggested that alterations in brain oscillatory patterns could be one of the mechanisms (Morris et al., 2011b). Hippocampal theta waves (5–11 Hz) representing spatial cognition and memory formation (Itskov et al., 2008) and levels of gamma brain-circuit synchronization (30-80 Hz). The later represents communication between interneurons (Sohal et al., 2009) which have been shown to be slowed down. This suggests that tau deficiency in AD mouse models might alter maturation of interneurons by disturbing long-range gamma synchronization in the brain (Cantero et al., 2011). Finally, crossing TauKO mice with amyloid β -forming AD mouse lines rescued AD-related memory deficits and improved survival (Roberson et al., 2007; Ittner et al., 2010).

Although lack of tau does not affect axonal transport in physiologic condition, the combination of tau and A β in AD cases may alter axonal transport (Vossel et al., 2010). A β oligomers disrupt axonal transport of cargoes with involvement of following factors: mediating through N-methyl-D-aspartate receptor signalling (Decker et al., 2010), activation of glycogen synthase kinase 3 β (Rui et al., 2006; Decker et al., 2010), casein kinase 2 (Pigino et al., 2009), and actin polymerization (Hiruma et al., 2003). Why tau is necessary for the impairment of axonal transport in the presence of A β is uncertain. However, tau might interact directly or indirectly with any of these pathways or contribute to the impairment by competing with motor proteins for microtubule access (Dixit et al., 2008).

Possible compensatory mechanisms

Although tau is expressed abundantly in neurons, complete tau knockout does not cause a severe phenotype. The lack of a severe phenotype of tau deficiency can be explained by compensatory mechanisms taking place by other microtubule associated proteins. Although exact compensatory mechanism is not known, possible changes that might take place in the absence of tau are argued in the following paragraphs.

There are four different tau knockout mouse lines available (Ke et al., 2012). However, there are controversies in behavioral results between these models. In summary, hyperactivity, muscle weakness, reduced motor coordination, locomotion (Ikegami et al., 2000; Roberson et al., 2007) and spatial memory deficits (Ma et al., 2014) in older mice were reported in TauKO mice lines, but no gross physical abnormalities and neurophysiological defects. This might be explained by confounding factors like diet (Ma et al., 2014), genetic background (Lei et al., 2014) and environment (Zou et al., 2016).

The lack of obvious behavioral impairments in tau deficient mice might be due to compensation by other MAPs. It was reported that MAP1A expression increases under the lack of tau, even though MAP1A is a constituent of cross-bridge structures between MTs that are longer than ~ 20 nm (Sato-Yoshitake et al., 1989). Although the microtubule-associated protein 1A (MAP1B, MAP1.2, MAP1X or MAP5) and tau are the prime members of neuronal MAPs (Cleveland et al., 1977; Bloom et al., 1985; Noble et al., 1989), Tau has a specific average velocity during axonal transport, characteristic interaction with

microtubules and a single kinetic pool (Mercken et al., 1995). Transfection studies have revealed that tau induces elongation of processes of non-neuronal cells through the formation of MT bundles (Kanai et al., 1989; Chen et al., 1992). However, axonal transport defects were not observed in tau knockout mice, as seen in Figure 16; Tau^{-/-} exhibited a slight tendency for faster axonal transport. In compliance with the previous findings the axonal transport characteristic of tau is relatively slow (Mercken et al., 1995) due to its repetitive association and disassociation from microtubules while MAP1A migrates with 0.8-1 mm/d, which might explain the tendency for faster axonal transport observed in TauKO mice during FRAP experiments. In addition, the entire tau population behaves like a single kinetic pool that is moving with 0.2-0.4 mm/d while MAP1A has two pools; the stationary pool is forming approximately one-third, and the kinetic pool (with the speed of 0.8-1 mm/d) is forming two-third of the total pool. Dynamic interaction of tau with microtubules is explained by “kiss and hop” mechanism (Yuan et al., 2008; Janning et al., 2014). According to this hypothesis, tau dwells on a single microtubule for ~ 40 ms before it hops to the next one, while MAPs interaction with microtubules are less dynamic and more retained. Because of the “kiss and hop” mechanism, the microtubule-binding region of tau interact with other proteins localized in different cellular compartments like actin filaments and protein phosphatase 2A (Janning et al., 2014). Tau does not interfere with the function of axonal transportation related proteins such as kinesin, which has an average velocity of ~1 μm/s (Kaether et al., 2000) while Tau moves much slower (Yuan et al., 2008; Janning et al., 2014). Therefore, pathological shifts in dwell time of tau on microtubules may result in the dynamic disequilibrium of tau with MTs.

The biggest groups of tau-interacting proteins according to their localization are membrane-bound proteins which can be more specifically categorized as mitochondrial (40.4%), plasma membrane (25.5%) and vesicle membrane proteins (21.3%) (Liu et al., 2016). However, tau in disease condition might influence not only its sub-cellular localization but also its binding partners and its function. As in the case of AD patients, colocalization of pathogenic Tau with both pre- and post-synaptic markers is enriched in synaptosomes (Fein et al., 2008; Sokolow et al., 2015). Because of higher subcellular localization of pathogenic tau in synapses, it might interfere with presynaptic functions such as synaptic vesicle mobility and vesicle release rate by its binding to synaptic vesicles

via its N-terminal domain and via the F-actin network (Zhou et al., 2017; McInnes et al., 2018). These data imply that pathogenic mechanisms of non-aggregated Tau in neurons induce early synaptic deficits preceding synapse and neuronal loss in AD.

Postsynaptically, pathogenic tau might act via glutamate receptor (NMDAR and AMPAR) trafficking and organization (Hoover et al., 2010; Ittner et al., 2010; Suzuki and Kimura, 2017). Moreover it has been shown that pathogenic tau localize Fyn kinase to postsynaptic terminals. The Fyn-mediated interaction between NMDAR and PSD-95 has been proposed to be necessary for A β toxicity in certain AD mouse models like the APP23 (Ittner et al., 2010). Therefore, postsynaptic accumulation of tau might affect localization of other postsynaptic dementia-related proteins on dendritic spines (Ittner et al., 2009).

The role of endosomal/lysosomal proteins in subcellular trafficking of disease associated proteins

In this section, the relation between regulation of endosomes and lysosomes and disease-associated proteins is discussed: more precisely, the regulation of APP by LRP1, SorLA, CD2AP and the regulation of BACE1 by BIN1, reticulon/Nogo and Snapin. In general, these proteins are responsible for sorting APP or BACE1 into endosomes or lysosomes. Any dysfunction during sorting might increase the chance of APP and BACE1 encounters, or changes the subcellular location in which encounters take place. Therefore, the production and subcellular localisation of A β might be altered by irregular sorting.

APP is a type-I transmembrane protein with a large extracellular and luminal moiety and a short cytoplasmic domain which can be proteolytically cleaved at many positions (Eggert et al., 2018b). Although the respective enzymes reside in diverse subcellular sites, intracellular APP trafficking was suggested as a main mechanism regulating the access of APP to its secretases (Sannerud and Annaert, 2009; Haass et al., 2012; Zhang and Song, 2013). Altered subcellular trafficking of APP is thought to directly influence the amount of A β generated (Eggert et al., 2018b). Thus, the mechanisms underlying intracellular APP transport are critical not only to understand AD pathogenesis, but also to target the disease with pharmacological interventions.

The intracellular itinerary of APP has been studied in undifferentiated cells (Eggert et al., 2018b). The APP is posttranslationally modified in the ER. Afterwards APP enters the

secretory pathway. Then it is translocated through the Golgi apparatus, which consecutively localizes APP to the plasma membrane (Caporaso et al., 1994; Guo et al., 2012; Haass et al., 2012). From there on, APP is either processed or internalized. APP endocytosis happens mainly via cholesterol dependent, clathrin-coated vesicles into early endosomes; this implicates an overlap of clathrin and cholesterol dependent endocytosis. After internalization of APP, it might follow three different pathways. Firstly, APP might go for recycling (Guo et al., 2012; Haass et al., 2012) or it can be transported retrogradely from endosomes back to the TGN in a retromer-mediated pathway (Willnow and Andersen, 2013) or APP is degraded through fusion of late endosomes with lysosomes (Cole et al., 1992; Haass et al., 1992).

Intracellular sorting, targeting, and internalization of transmembrane proteins are facilitated by usually short sequences of amino acids on cytoplasmic domains which are recognized by cytosolic adaptor proteins. A number of type-I transmembrane proteins have been verified to modulate the intracellular itinerary of APP, its proteolytic processing and/or clearance of A β . Remarkably, specific intracellular targeting events can occur independently of the intracellular domain of APP, such as anterograde axonal transport (King and Scott Turner, 2004; Eggert et al., 2018b).

SorLA is a type-1 transmembrane protein involved in intracellular transport of APP (Jacobsen et al., 1996; Yamazaki et al., 1996). It binds to APP directly and redirects it into the Golgi, which results in reduced processing of A β (Andersen et al., 2006). SorLA is considered as a risk factor for late and early onset AD (Andersen et al., 2016). In AD patients, expression levels of SorLA are significantly reduced. In parallel, SorLA knockout mice models possess increased A β levels; additionally, overexpression of SorLA in neurons decreases A β levels (Andersen et al., 2005). Thus, SorLA is considered as a negative regulator of APP by increasing retrogrades sorting of APP from endosomal compartments to the trans-Golgi network. Besides, it was shown that this redirection of APP by SorLA was significantly reduced after dimerization of APP (Eggert et al., 2018b, 2018a). Taken together, our results suggest that SorLA might play a role in trafficking of APP to dystrophies.

Another disease-associated protein, namely BACE1, can be regulated by many factors. One of them are the reticulon/Nogo proteins (He et al., 2004; Murayama et al., 2006) which retain BACE1 in the ER, where the environment is suboptimal for BACE1 activity for cleaving APP (Shi et al., 2014). The reticulon family of proteins has four members: RTN1, RTN2, RTN3 and RTN4 (also known as Nogo) (Yan et al., 2006; Yang and Strittmatter, 2007). An increase in the expression of any reticulon protein, specifically RTN3, substantially reduces the production of A β by reducing cell surface localized BACE1. On the contrary, lowering the expression of RTN3 by RNA interference increases the secretion of A β as well as expression of BACE1 (Shi et al., 2009; Araki et al., 2013), suggesting that reticulon proteins are negative modulators of BACE1. In the context of dystrophic neurites, RTN3 is enriched in dystrophic neurites around plaques in AD brain. Additionally, neuritic abnormalities can be caused by overexpression of RTN3 (Hu et al., 2007).

Snapin provides another mechanistic insight into the complex regulation of BACE1. Snapin is a dynein motor adaptor for late endosomes and mediates retrograde transport of late endosomes and BACE1 in neurons (Cai et al., 2010). Deletion of snapin and disruption of Snapin-dynein coupling causes reduction in BACE1 transport to lysosomes and increases BACE1 accumulation in late endosomes and multivesicular bodies whose acidic environment is optimal for β -secretase activity (Huse et al., 2000) and therefore, increases APP processing (Ginsberg et al., 2010b; Ye and Cai, 2014). Late endosomes containing BACE1 and A β 42 are clustered in distal processes and presynaptic terminals (Takahashi et al., 2002; Takahashi, 2004). In fact, overexpression of Snapin enhances BACE1 turnover and therefore reduces APP cleavage by BACE1 (Ye and Cai, 2014) and removes BACE1 from presynaptic terminals to the soma (Ye et al., 2017).

BIN1 is another factor for regulating BACE1 endosomal trafficking (Miyagawa et al., 2016; Ubelmann et al., 2017). Reduction of BIN1 levels controls A β generation in axons by trapping BACE1 in tubules of early endosomes; as a result, BACE1 cannot be sorted for degradation in dendrites. On the contrary, the reduction of CD2AP levels controls A β generation by trapping APP at the membrane of early endosomes. Thus, reduction of both BIN1 and CD2AP increases A β generation by bringing BACE1 and APP in the same early endosomes. The reduction of BIN1 increases the possibility of an APP and BACE1 encounter in axons. On the other hand, the reduction of CD2AP enhances their encounter

in dendrites (Ubelmann et al., 2017). This results in an A β accumulation in different subcellular locations. All regulating factors might play a role in reduction of A β generation by affecting volumetric BACE1 fraction in dystrophies of the Tau^{-/-} x APPPS1 mouse.

Endocytosis of APP and BACE into early endosomes is necessary for A β generation, which is restricted by segregating APP and BACE1 into separate compartments (Grbovic et al., 2003; Cirrito et al., 2008). During early endosome maturation, APP is sorted into lysosomes (Morel et al., 2013) whereas BACE1 trafficked back to the plasma membrane (Buggia-Prévot et al., 2013; Morel et al., 2013). In case of dysregulation of either mechanism, A β generation is alleviated. A recent study showed that Bin1 and CD2AP take a role in polarisation of the A β generation in neurons (Ubelmann et al., 2017). As mentioned before, Bin1 depletion increases the chance of APP and BACE1 meeting in axons, whereas CD2AP increase this chance in dendrites. Different localisation of A β generation may probably influence the local A β toxicity as well as the overall disease progression. As shown in the result section, reduction plaque growth as well as a reduced BACE1 and APP accumulation in axonal dystrophies In TauKO x APPPS1 which led us to believe that local A β generation at the plaques might be reduced. However, measurements by using ELISA did not indicate changes in A β levels. This discrepancy could be explained by the possibility that A β production is not affected in non-dystrophic areas in TauKO x APPPS1.

Impairment in maturation of endosomes

In the previous section it was discussed how the site of A β generation and production might be affected if the localisation of APP or BACE1 in endosomes/lysosomes is altered. However, A β generation may also be affected by an intrinsic regulation of lysosomes. Any changes in endosome to lysosome maturation, incomplete degradation of proteins in lysosomes or suboptimal lysosomal environment may prolong APP and BACE1 interaction. Therefore, A β generation would be indirectly affected. In this section, regulating factors for functional lysosomes in disease context, mainly lysosomal proteolysis, proton or cholesterol regulation are discussed.

Under normal conditions, the route of membrane components for hydrolysis goes through late endosomes, then lysosomes, where these components are hydrolyzed with

hydrolytic enzymes. Previous evidence supports the notion that deficiencies in retrograde transport of late endosomes, a lack of activity from hydrolases or dysfunction in cholesterol efflux might cause impairment of the maturation of endosomes. This might cause the formation of axonal dystrophies (Cataldo et al., 2000, 2004; Grbovic et al., 2003; Maxfield and Tabas, 2005; Ginsberg et al., 2010a; Lee et al., 2011). Increased cholesterol levels play a role in maturation and enlargement of endosomes. Although a precise mechanism is not known, changes in lipid composition or cholesterol content in endosomes might alter endocytic sorting. As a late endosome luminal protein, NPC1 binds cholesterol and carries cholesterol out of late endosomes (Friedland et al., 2003). Failure in NPC1/2 will result in imbalanced cholesterol levels in endosomes and lysosomes (Cossec et al., 2010b). In the disease context, both the NPC1 mRNA and protein expression are upregulated specially in the brain regions which are severely affected in AD such as the hippocampus and the frontal cortex (Kågedal et al., 2010). Moreover, the deletion of NPC1 in an APPPS1 mouse model increases the co-localization of APP, BACE1 and PS1 within enlarged early, or recycling endosomes, by decreasing APP recycling to the cell surface (Malnar et al., 2010, 2012; Maulik et al., 2015) as well as an A β accumulation (Borbon and Erickson, 2011). Besides, the inhibition of NPC1/2 alters the localization of PS1 in early/late endosomes (Runz et al., 2002; Burns et al., 2003). Collectively, these results show that NPC1/2 is involved in cholesterol regulation in AD and potentially acting upstream in the A β production pathway. The reduction in amyloid plaque growth and APP accumulation at the plaques in the TauKO x APPPS1 mouse model in our study might be related with changes in the cholesterol and NPC1/2 function.

Cholesterol is required in neurons. Cholesterol import is performed by apolipoprotein E and via lipoprotein receptor-related protein 1 (LRP1) receptors on the surface. In AD, malfunction of cholesterol import was thought to starve neurons of cholesterol. LRP1 is associated with effective clearance of A β from the brain to the periphery across the blood-brain barrier. In addition, LRP1 might be an important candidate for the APP turnover. Indeed, an increase in LRP1 results in APP endocytosis and an increased secretion of A β (Ulery et al., 2000; Cam et al., 2005). LRP1 is transported with a velocity of less than 1 $\mu\text{m/s}$, while APP is transported with a velocity faster than 1 $\mu\text{m/s}$ (Wagner and Pietrzik,

2012; Eggert et al., 2018b). This implies that LRP1 might affect APP transport by leading it into common transport vesicles.

Of particular relevance to AD, cholesterol is a highly specific ligand APP- β CTF. It acts directly on β CTF to deliver lipid rafts and influences its access to other secretases. APP was already suggested as a cellular cholesterol sensor which suppresses cellular cholesterol uptake (Beel et al., 2008, 2010; Barrett et al., 2012). High dietary LDL cholesterol and overexpression of its receptor APOE are associated with high-level β CTF and BACE1 levels and enlargement of RAB5 endosomes (Ji et al., 2006; Cossec et al., 2010a). Lipoprotein receptors mediating glia-derived cholesterol transport within the CNS, and specifically present in end lysosomes, are essential to maintain the cellular homeostasis (Mauch et al., 2001). The patho-molecular background of AD resembles the lysosomal storage disorders, such as the AD risk factor APOE4 (Fu et al., 2012; Colacurcio et al., 2018), and implicates that altered cholesterol homeostasis could be a common mechanism.

The selective maturation or transport failure of APP and BACE1 containing autophagic vesicles/lysosomal compartments and axonal accumulation within dystrophic axonal swellings in response to tau expression provides a unique molecular mechanism specific for AD. Several of our observations may be relevant to the molecular mechanism by which tau expression impedes the transport of specifically APP and BACE1 containing organelles. Selective recovery of APP and BACE1 protein accumulation in dystrophies in $\text{Tau}^{-/-}$ x APPPS1 is highly distinguishable from the other accumulated proteins that are still present in dystrophic neurites, and which are not predominantly regulated by tau. Presenilin 1 (PS1) is a catalytic component of γ -secretase complex, which is involved in cleavage of APP and generation of A β peptides (Steiner and Haass, 2000; Selkoe and Wolfe, 2007; De Strooper and Annaert, 2010; Chávez-Gutiérrez et al., 2012). In the light of a large body of literature describing PSEN during lysosomal functioning, PSEN1 holoprotein plays a role in γ -secretase-independent roles in wnt signaling (Kang et al., 1999), ER Ca^{2+} regulation (Tu et al., 2006; Shilling et al., 2014) and in lysosomal function and autophagy (Wilson et al., 2004; Lee et al., 2010; Coen et al., 2012; Wolfe et al., 2013). Intracellular organelles maintain an optimal pH suited for their biochemical functions by action of a primary electrogenic proton pump (Wolfe et al., 2013). Vacuolar-type ATPase (v-ATPase)

maintains lysosomal pH, which regulates targeting and maturation of lysosomes as well as modulation of lysosomal Ca^{2+} levels (Lee et al., 2010; Mindell, 2012). PSEN1 loss-of-function facilitates incomplete glycosylation of the V0a1 subunit, which causes V0a1 subunit being rapidly degraded by the endoplasmic reticulum, which results in a deficiency in proton pumping activity of the lysosomal lumen (Lee et al., 2010, 2015). Of importance, PS1 takes an active role in PI3K/Akt activation. Thus, it also regulates phosphorylation / inactivation of glycogen synthase kinase-3 (GSK-3) which suppresses phosphorylation of tau (Baki et al., 2004). Therefore, a strong reduction of APP and BACE1 at the plaques in $\text{Tau}^{-/-}$ x APPPS1 could be explained by the relationship between PS1 and tau. Consistent with this, hAPP x TauKO mouse line fail to exhibit changes in plaque growth and formation (Roberson et al., 2007). APP metabolites including, notably, the transmembrane C-terminal fragments (Siman et al., 1993; Boland et al., 2010), are known to disturb endosomal trafficking and size (Jiang et al. 2010). In the light of these findings, the increase in APP-CTF levels may underlie an additional pathogenic consequence of lysosomal dysfunction relevant to AD (Jiang et al., 2010)

CONCLUSION

According to amyloid hypothesis, $\text{A}\beta$ peptides are considered as the main reason for the development of AD related pathology such as the formation of neurofibrillary tangles and neuronal death. However, tau does not act pathologically because of $\text{A}\beta$, but tau also contributes to that pathology in AD. Our data indicate that Tau is involved in the cascade that leads to accumulation of BACE1 and APP in peri-plaque dystrophies and thereby exacerbates $\text{A}\beta$ deposition. Thereby, we posit a novel connection between tau and $\text{A}\beta$, suggesting of positive feed forward mechanism. In conclusion, tau contributes to the kinetics of plaque formation and the development of dystrophic neurites in AD. Although THE precise mechanism how tau is involved in the pathology is not known yet, we speculate that tau in combination with endosome/lysosome regulatory proteins might alter localization of APP and BACE1 and subsequently the generation of $\text{A}\beta$ peptides.

CONTRIBUTIONS

Finn Peters wrote the MatLab scripts and performed automated analysis on *in vivo* imaging and immunostainings data. Stefan Lichtenthaler, Martina Pigoni and supervised biochemical experiments (western-blot) and donated antibodies.

KEYWORDS

Alzheimer's disease; β -amyloid plaque; tau; two-photon *in vivo* microscopy; presynaptic dystrophies; plaque formation; plaque growth.

ACCEPTED PAPERS

BACE1 inhibition more effectively suppresses initiation than progression of β -amyloid pathology

Authors

Finn Peters^{1,2}, Hazal Salihoglu¹, Eva Rodrigues¹, Etienne Herzog^{5,6}, Tanja Blume^{1,2}, Severin Filser^{1,2}, Mario Dorostkar^{1,3}, Derya R. Shimshek⁷, Nils Brose⁴, Ulf Neumann⁷, Jochen Herms^{1,2,3*}

Affiliations

¹ German Center for Neurodegenerative Diseases (DZNE), Munich, Germany.

² Munich Cluster of Systems Neurology (SyNergy), Munich, Germany.

³ Center for Neuropathology and Prion Research, Ludwig-Maximilians University, Munich, Germany.

⁴ Department of Molecular Neurobiology, Max Planck Institute of Experimental Medicine – Göttingen, Germany.

⁵ Université Bordeaux, IINS, UMR 5297, F-33000 Bordeaux, France.

⁶ CNRS, IINS, UMR 5297, F-33000 Bordeaux, France.

⁷ Neuroscience, Novartis Institutes for BioMedical Research (NIBR), – Basel, Switzerland.

*To whom correspondence should be addressed: Jochen Herms, DZNE, Feodor-Lynen Str. 17, 81377 Munich, Germany; Tel: +49 89 4400 46427; FAX: +49 89 4400 46429; jochen.herms@med.uni-muenchen.de.

Acknowledgments

We thank Mathias Jucker for providing the APPPS1 mouse model and Nadine Lachner, Sarah Hanselka, and Eric Griesinger for their excellent technical support and animal care. We like to give special thanks to Dr. Carmelo Sgobio and Dr. Steffen Burgold for scientific support and advice on the manuscript.

Funding

This work was funded by the Munich Cluster for Systems Neurology SyNergy (EXC1010) and by the ITN Extrabrain (606950).

Conflict of interest

D.R.S. and U.N. are full-time employees of Novartis Pharma AG, Basel Switzerland. The remaining authors declare no conflict of interest.

Author contributions

F.P., H.S., E.R., and T.B. performed the measurements. F.P. analyzed and quantified the data. E.H. and N.B. provided the VGLUT1^{Venus} mouse model. D.R.S. and U.N. provided the BACE1 inhibitor NB-360 and performed measurements of soluble A β . F.P., S.F., U.N. and J.H. interpreted the data. F.P., S.F., M.D., U.N. and J.H. contributed to the conception and design of the study. F.P., S.F., U.N. and J.H. wrote the manuscript. F.P., E.H., T.B., S.F., N.B., U.N. and J.H. provided critical revisions. All authors approved the final manuscript.

Abstract

BACE1 is the rate-limiting protease in the production of synaptotoxic β -amyloid (A β) species and hence one of the prime drug targets for potential therapy of Alzheimer's disease (AD). However, so far pharmacological BACE1 inhibition failed to rescue the cognitive decline in mild-to-moderate AD patients, which indicates that treatment at symptomatic stage might be too late. In the current study, chronic *in vivo* two-photon microscopy was performed in a transgenic AD model to monitor the impact of pharmacological BACE1 inhibition on early β -amyloid pathology. The longitudinal approach allowed to assess the kinetics of individual plaques and associated presynaptic pathology, before and throughout treatment. BACE1 inhibition could not halt but slow down progressive β -amyloid deposition and associated synaptic pathology. Notably, the data revealed that the initial process of plaque formation, rather than the subsequent phase of gradual plaque growth, is most sensitive to BACE1 inhibition. This finding of particular susceptibility of plaque formation has profound implications to achieve optimal therapeutic efficacy for the prospective treatment of AD.

Keywords

Alzheimer's disease; β -amyloid plaque; two-photon *in vivo* microscopy; BACE1 inhibitor treatment; presynaptic dystrophies; plaque formation.

CURRICULUM VITAE

Würzstrasse 1, 81371, Munich Germany
 +49 176 45854094 | hazalsalihoglu@gmail.com



Work Experience

- 2013-2018** **DZNE - Ludwig - Maximilian University** – Munich, Germany
Ph.D. Student in Neuroscience supervised by Prof. Dr. Jochen Herms
 The role of tau in plaque growth and formation in a transgenic Alzheimer`s mouse model
- 2012** **Bordeaux Université** – Bordeaux, France
Research assistant - 8-month internship supervised by Dr. Laurent Groc
 Surface trafficking of NMDAR in mesencephalic primary cell culture
 Nanotechnology
 Quantum-dots
- 2011** **Bordeaux Université** – Bordeaux, France
Research assistant - 6-month internship supervised by Dr. Giovanni Marsicano
 The role of CB1 receptor in mitochondrial respiration and biochemistry
 Western-blots
- 2010** **Gothenburg University** – Gothenburg, Sweden
Research assistant - 4-month internship supervised by Dan Rohme
 Type-1 Diabetes
- 2009** **Johannes Gutenberg University** – Mainz, Germany
Research assistant - 3-months Erasmus summer internship supervised by Prof. Dr. Thomas Hankeln
 Hemoglobin isoforms in *Drosophila melanogaster*
- 2007** **Volunteer work** – Mersin, Turkey
Volunteer for a WWF project supervised by Dr. Hakan Durmus (WWF) –
 Establish protected areas in the Mediterranean and collaborating with governments and local conservation organizations to protect loggerhead nesting beaches in Mersin, Turkey

Education & Qualifications

- 2013-current** **Ludwig-Maximilian University** – Munich, Germany
Ph.D. Student in Neuroscience
- 2011-2013** **Bordeaux Université** – Bordeaux, France
Master of Science
Accepted to NEURASMUS master program with full scholarship (only 15 students all around the world)
Double diploma
- 2011-2013** **Vrije University** – Amsterdam, Netherlands
Master of Science
Accepted to very exclusive NEURASMUS master program with full scholarship (only 15 students all around the world)
Double diploma
- 2006-2011** **Bogazici University** – Istanbul, Turkey
Bachelor of Science: Molecular Biology and Genetics
Entered with an excellent success at the National University Entrance Exam (in 0.24% rank among 1,678 383 participants)
TUBITAK (Turkish National Science Institute) Academic Achievement Scholarship
Graduated with honors (GPA: 3.16)
- 2010** **Gothenburg University** – Gothenburg, Sweden
Bachelor of Science: Erasmus Exchange
Coursework in molecular biology
- 2009** **Johannes Gutenberg University** – Mainz, Germany
Bachelor of Science: Erasmus Summer Internship
- 2006** **Istanbul Ataturk Science High School** – Istanbul, Turkey
High School Diploma: Science
Accepted with and excellent success in the national exam (ranked 916th among 614 164 participants)

Languages

Turkish (mother tongue)
English (fluent)
German (upper-intermediate)

REFERENCES

- Adams LA, Munoz DG (1993) Differential incorporation of processes derived from different classes of neurons into senile plaques in Alzheimer's disease. *Acta Neuropathol* 86:365–370.
- Alzheimer A (1907) Über eine eigenartige Erkrankung der Hirnrinde. *Allg Zeitschrift für Psychiatrie und Psych Medizin* 64:146–148.
- Amos LA (2014) Why do brains need tau (MAPT)? *FEBS J* 281:iv–v.
- Andersen OM, Reiche J, Schmidt V, Gotthardt M, Spoelgen R, Behlke J, von Arnim CAF, Breiderhoff T, Jansen P, Wu X, Bales KR, Cappai R, Masters CL, Gliemann J, Mufson EJ, Hyman BT, Paul SM, Nykjaer A, Willnow TE (2005) Neuronal sorting protein-related receptor sorLA/LR11 regulates processing of the amyloid precursor protein. *Proc Natl Acad Sci* 102:13461–13466.
- Andersen OM, Rudolph IM, Willnow TE (2016) Risk factor SORL1: from genetic association to functional validation in Alzheimer's disease. *Acta Neuropathol* 132:653–665.
- Andersen OM, Schmidt V, Spoelgen R, Gliemann J, Behlke J, Galatis D, McKinstry WJ, Parker MW, Masters CL, Hyman BT, Cappai R, Willnow TE (2006) Molecular dissection of the interaction between amyloid precursor protein and its neuronal trafficking receptor SorLA/LR11. *Biochemistry* 45:2618–2628.
- Araki W, Oda A, Motoki K, Hattori K, Itoh M, Yuasa S, Konishi Y, Shin R-W, Tamaoka A, Ogino K (2013) Reduction of β -amyloid accumulation by reticulon 3 in transgenic mice. *Curr Alzheimer Res* 10:135–142.
- Arendt T, Brückner MK, Mosch B, Lösche A (2010) Selective cell death of hyperploid neurons in Alzheimer's disease. *Am J Pathol* 177:15–20.
- Armstrong R. (1999) Do β -amyloid (A β) deposits in patients with Alzheimer's disease and Down's syndrome grow according to the log-normal model? *Neurosci Lett* 261:97–100.
- Arriagada P V, Growdon JH, Hedley-Whyte ET, Hyman BT (1992) Neurofibrillary tangles but not senile plaques parallel duration and severity of Alzheimer's disease. *Neurology* 42:631–631.
- Avila J, Jiménez JS, Sayas CL, Bolós M, Zabala JC, Rivas G, Hernández F (2016) Tau Structures. *Front Aging Neurosci* 8:1–10.
- Avila J, Wandosell F, Hernández F (2010) Role of glycogen synthase kinase-3 in Alzheimer's disease pathogenesis and glycogen synthase kinase-3 inhibitors. *Expert Rev Neurother* 10:703–710.
- Baker M, Litvan I, Houlden H, Adamson J, Dickson D, Perez-Tur J, Hardy J, Lynch T, Bigio E, Hutton M (1999) Association of an extended haplotype in the tau gene with progressive supranuclear palsy. *Hum Mol Genet* 8:711–715.
- Baki L, Shioi J, Wen P, Shao Z, Schwarzman A, Gama-Sosa M, Neve R, Robakis NK (2004) PS1 activates PI3K thus inhibiting GSK-3 activity and tau overphosphorylation: Effects of FAD mutations. *EMBO J* 23:2586–2596.
- Bakota L, Brandt R (2016) Tau biology and tau-directed therapies for Alzheimer's disease. *Drugs* 76:301–313.
- Barrett PJ, Song Y, Van Horn WD, Hustedt EJ, Schafer JM, Hadziselimovic A, Beel AJ, Sanders CR (2012) The amyloid precursor protein has a flexible transmembrane domain and binds cholesterol. *Science* (80-) 336:1168–1171.
- Beel AJ, Mobley CK, Hak JK, Tian F, Hadziselimovic A, Jap B, Prestegard JH, Sanders CR (2008)

- Structural studies of the transmembrane C-terminal domain of the amyloid precursor protein (APP): Does APP function as a cholesterol sensor? *Biochemistry* 47:9428–9446.
- Beel AJ, Sakakura M, Barrett PJ, Sanders CR (2010) Direct binding of cholesterol to the amyloid precursor protein: An important interaction in lipid-Alzheimer's disease relationships? *Biochim Biophys Acta - Mol Cell Biol Lipids* 1801:975–982.
- Benilova I, Karran E, De Strooper B (2012) The toxic A β oligomer and Alzheimer's disease: an emperor in need of clothes. *Nat Neurosci* 15:349–357.
- Bittner T, Burgold S, Dorostkar MM, Fuhrmann M, Wegenast-Braun BM, Schmidt B, Kretzschmar H, Herms J (2012) Amyloid plaque formation precedes dendritic spine loss. *Acta Neuropathol* 124:797–807.
- Blazquez-Llorca L, Valero-Freitag S, Rodrigues EF, Merchán-Pérez Á, Rodríguez JR, Dorostkar MM, DeFelipe J, Herms J (2017) High plasticity of axonal pathology in Alzheimer's disease mouse models. *Acta Neuropathol Commun* 5:14.
- Blennow K, Vanmechelen E, Hampel H (2001) CSF total tau, A β 42 and phosphorylated tau protein as biomarkers for Alzheimer's disease. *Mol Neurobiol* 24:087–098.
- Borbon IA, Erickson RP (2011) Interactions of Npc1 and amyloid accumulation/deposition in the APP/PS1 mouse model of Alzheimer's. *J Appl Genet* 52:213–218.
- Braak H, Braak E (1991) Neuropathological staging of Alzheimer-related changes. *Acta Neuropathol* 82:239–259.
- Braak H, Braak E (1997) Frequency of stages of Alzheimer-related lesions in different age categories. *Neurobiol Aging* 18:351–357.
- Brandt R, Léger J, Lee G (1995) Interaction of tau with the neural plasma membrane mediated by tau's amino-terminal projection domain. *J Cell Biol* 131:1327–1340.
- Brendza RP, Bacskai BJ, Cirrito JR, Simmons KA, Skoch JM, Klunk WE, Mathis CA, Bales KR, Paul SM, Hyman BT, Holtzman DM (2005) Anti-Abeta antibody treatment promotes the rapid recovery of amyloid-associated neuritic dystrophy in PDAPP transgenic mice. *J Clin Invest* 115:428–433.
- Brettschneider J, Del Tredici K, Lee VM-Y, Trojanowski JQ (2015) Spreading of pathology in neurodegenerative diseases: a focus on human studies. *Nat Rev Neurosci* 16:109–120.
- Brion J, Passareiro H, Nunez J, Flament-Durand J (1985) Immunological detection of tau protein in the lesions of the neurofibrillary degeneration of Alzheimer's disease. *Arch Biol* 95:229–235.
- Buggia-Prévot V, Fernandez CG, Riordan S, Vetrivel KS, Roseman J, Waters J, Bindokas VP, Vassar R, Thinakaran G (2014) Axonal BACE1 dynamics and targeting in hippocampal neurons: a role for Rab11 GTPase. *Mol Neurodegener* 9:1.
- Buggia-Prévot V, Fernandez CG, Udayar V, Vetrivel KS, Elie A, Roseman J, Sasse VA, Lefkow M, Meckler X, Bhattacharyya S, George M, Kar S, Bindokas VP, Parent AT, Rajendran L, Band H, Vassar R, Thinakaran G (2013) A function for EHD family proteins in unidirectional retrograde dendritic transport of BACE1 and Alzheimer's disease A β production. *Cell Rep* 5:1552–1563.
- Burgold S, Bittner T, Dorostkar MM, Kieser D, Fuhrmann M, Mitteregger G, Kretzschmar H, Schmidt B, Herms J (2011) In vivo multiphoton imaging reveals gradual growth of newborn amyloid plaques over weeks. *Acta Neuropathol* 121:327–335.
- Burgold S, Filser S, Dorostkar MM, Schmidt B, Herms J (2014) In vivo imaging reveals sigmoidal growth kinetic of β -amyloid plaques. *Acta Neuropathol Commun* 2:30.

- Burns M, Gaynor K, Olm V, Mercken M, LaFrancois J, Wang L, Mathews PM, Noble W, Matsuoka Y, Duff K (2003) Presenilin redistribution associated with aberrant cholesterol transport enhances beta-amyloid production in vivo. *J Neurosci* 23:5645–5649.
- Bussi re T, Bard F, Barbour R, Grajeda H, Guido T, Khan K, Schenk D, Games D, Seubert P, Buttini M (2004) Morphological characterization of Thioflavin-S-positive amyloid plaques in transgenic Alzheimer mice and effect of passive A β immunotherapy on their clearance. *Am J Pathol* 165:987–995.
- Caceres A, Kosik K, S. (1990) Inhibition of neurite polarity by tau antisense oligonucleotides in primary cerebellar neurons. *Nature* 343:461–463.
- Cai Q, Lu L, Tian JH, Zhu YB, Qiao H, Sheng ZH (2010) Snapin-regulated late endosomal transport is critical for efficient autophagy-lysosomal function in neurons. *Neuron* 68:73–86.
- Calignon A De, Rozkalne A, Koenigsknecht-talboo J, Holtzman DM (2008) Rapid appearance and local toxicity of amyloid- β plaques in a mouse model of Alzheimer’s disease. *Nature* 451:720–724.
- Cam JA, Zerbinatti C V, Li Y, Bu G (2005) Rapid endocytosis of the low density lipoprotein receptor-related protein modulates cell surface distribution and processing of the beta-amyloid precursor protein. *J Biol Chem* 280:15464–15470.
- Cantero JL, Moreno-Lopez B, Portillo F, Rubio A, Hita-Ya nez E, Avila J (2011) Role of tau protein on neocortical and hippocampal oscillatory patterns. *Hippocampus* 21:827–834.
- Caporaso G, Takei K, Gandy S, Matteoli M, Mundigl O, Greengard P, de Camilli P (1994) Morphologic and biochemical analysis of the intracellular trafficking of the Alzheimer beta/A4 amyloid precursor protein. *J Neurosci* 14:3122–38.
- Cataldo AM, Paskevich PA, Kominami E, Nixon RA (1991) Lysosomal hydrolases of different classes are abnormally distributed in brains of patients with Alzheimer disease. *Proc Natl Acad Sci U S A* 88:10998–11002.
- Cataldo AM, Petanceska S, Terio NB, Peterhoff CM, Durham R, Mercken M, Mehta PD, Buxbaum J, Haroutunian V, Nixon RA (2004) A β localization in abnormal endosomes: Association with earliest A β elevations in AD and Down syndrome. *Neurobiol Aging* 25:1263–1272.
- Cataldo AM, Peterhoff CM, Troncoso JC, Gomez-Isla T, Hyman BT, Nixon RA (2000) Endocytic pathway abnormalities precede amyloid β deposition in sporadic Alzheimer’s disease and down syndrome: Differential effects of APOE genotype and presenilin mutations. *Am J Pathol* 157:277–286.
- Ch vez-Guti rrez L, Bammens L, Benilova I, Vandersteen A, Benurwar M, Borgers M, Lismont S, Zhou L, Van Cleynenbreugel S, Esselmann H, Wiltfang J, Serneels L, Karran E, Gijzen H, Schymkowitz J, Rousseau F, Broersen K, De Strooper B (2012) The mechanism of γ -Secretase dysfunction in familial Alzheimer disease. *EMBO J* 31:2261–2274.
- Chen J, Kanai Y, Cowan NJ, Hirokawa N (1992) Projection domains of MAP2 and tau determine spacings between microtubules in dendrites and axons. *Nature* 360:674–677.
- Cirrito JR, Kang J-E, Lee J, Stewart FR, Verges DK, Silverio LM, Bu G, Mennerick S, Holtzman DM (2008) Endocytosis is required for synaptic activity-dependent release of amyloid-beta in vivo. *Neuron* 58:42–51.
- Coen K, Flannagan RS, Baron S, Carraro-Lacroix LR, Wang D, Vermeire W, Michiels C, Munck S, Baert V, Sugita S, Wuytack F, Hiesinger PR, Grinstein S, Annaert W (2012) Lysosomal calcium homeostasis defects, not proton pump defects, cause endo-lysosomal dysfunction in PSEN-deficient cells. *J Cell Biol* 198:23–35.

- Colacurcio DJ, Pensalfini A, Jiang Y, Nixon RA (2018) Dysfunction of autophagy and endosomal-lysosomal pathways: Roles in pathogenesis of Down syndrome and Alzheimer's Disease. *Free Radic Biol Med* 114:40–51.
- Cole GM, Bell L, Truong QB, Saitoh T (1992) An endosomal-lysosomal pathway for degradation of amyloid precursor protein. *Ann N Y Acad Sci* 674:103–117.
- Collingridge GL, Peineau S, Howland JG, Wang YT (2010) Long-term depression in the CNS. *Nat Rev Neurosci* 11:459–473.
- Cossec JC, Marquer C, Panchal M, Lazar AN, Duyckaerts C, Potier MC (2010a) Cholesterol changes in Alzheimer's disease: methods of analysis and impact on the formation of enlarged endosomes. *Biochim Biophys Acta - Mol Cell Biol Lipids* 1801:839–845.
- Cossec JC, Simon A, Marquer C, Moldrich RX, Leterrier C, Rossier J, Duyckaerts C, Lenkei Z, Potier MC (2010b) Clathrin-dependent APP endocytosis and A β secretion are highly sensitive to the level of plasma membrane cholesterol. *Biochim Biophys Acta - Mol Cell Biol Lipids* 1801:846–852.
- Crowe SL, Tsukerman S, Gale K, Jorgensen TJ, Kondratyev AD (2011) Phosphorylation of histone H2A.X as an early marker of neuronal endangerment following seizures in the adult rat brain. *J Neurosci* 31:7648–7656.
- Dawson HN, Cantillana V, Jansen M, Wang H, Vitek MP, Wilcock DM, Lynch JR, Laskowitz DT (2010) Loss of tau elicits axonal degeneration in a mouse model of Alzheimer's disease. *Neuroscience* 169:516–531.
- Dawson HN, Ferreira A, Eyster M V, Ghoshal N, Binder LI, Vitek MP (2001) Inhibition of neuronal maturation in primary hippocampal neurons from tau deficient mice. *J Cell Sci* 114:1179–1187.
- De Strooper B, Annaert W (2010) Novel research horizons for presenilins and γ -secretases in cell biology and disease. *Annu Rev Cell Dev Biol* 26:235–260.
- Decker H, Lo KY, Unger SM, Ferreira ST, Silverman MA (2010) Amyloid-beta peptide oligomers disrupt axonal transport through an NMDA receptor-dependent mechanism that is mediated by Glycogen Synthase Kinase 3 in primary cultured hippocampal neurons. *J Neurosci* 30:9166–9171.
- DeVos SL, Goncharoff DK, Chen G, Kebodeaux CS, Yamada K, Stewart FR, Schuler DR, Maloney SE, Wozniak DF, Rigo F, Bennett CF, Cirrito JR, Holtzman DM, Miller TM (2013) Antisense reduction of tau in adult mice protects against seizures. *J Neurosci* 33:12887–12897.
- Dickson DW, Crystal H, Mattiace LA, Kress Y, Schwagerl A, Ksiezak-Reding H, Davies P, Yen S-H (1989) Diffuse Lewy body disease: light and electron microscopic immunocytochemistry of senile plaques. *Acta Neuropathol* 78:572–584.
- Dickson TC, King CE, McCormack GH, Vickers JC (1999) Neurochemical diversity of dystrophic neurites in the early and late stages of Alzheimer's disease. *Exp Neurol* 156:100–110.
- Dixit R, Ross JL, Goldman YE, Holzbaur ELF (2008) Differential regulation of dynein and kinesin motor proteins by tau. *Science* (80-) 319:1086–1089.
- Drubin DG, Kirschner MW (1986) Tau protein function in living cells. *J Cell Biol* 103:2739–2746.
- Ebneth A, Godemann R, Stamer K, Illenberger S, Trinczek B, Mandelkow E-M, Mandelkow E (2011) Overexpression of tau protein inhibits kinesin-dependent overexpression of vesicles, mitochondria, and endoplasmic trafficking reticulum : for Alzheimer's disease implications. *Cell* 143:777–794.

- Eggert S, Gonzalez AC, Thomas C, Schilling S, Schwarz SM, Tischer C, Adam V, Strecker P, Schmidt V, Willnow TE, Hermey G, Pietrzik CU, Koo EH, Kins S (2018a) Dimerization leads to changes in APP (amyloid precursor protein) trafficking mediated by LRP1 and SorLA. *Cell Mol Life Sci* 75:301–322.
- Eggert S, Thomas C, Kins S, Hermey G (2018b) Trafficking in Alzheimer's disease: modulation of APP transport and processing by the transmembrane proteins LRP1, SorLA, SorCS1c, Sortilin, and Calsyntenin. *Mol Neurobiol* 55:5809–5829.
- Eisenberg D, Jucker M (2012) The amyloid state of proteins in human diseases. *Cell* 148:1188–1203.
- Fein JA, Sokolow S, Miller CA, Vinters H V., Yang F, Cole GM, Gylys KH (2008) Co-localization of amyloid beta and tau pathology in Alzheimer's disease synaptosomes. *Am J Pathol* 172:1683–1692.
- Fiala JC (2007) Mechanisms of amyloid plaque pathogenesis. *Acta Neuropathol* 114:551–571.
- Fountoulakis M, Kossida S (2006) Proteomics-driven progress in neurodegeneration research. *Electrophoresis* 27:1556–1573.
- Friedland N, Liou H-L, Lobel P, Stock AM (2003) Structure of a cholesterol-binding protein deficient in Niemann-Pick type C2 disease. *Proc Natl Acad Sci* 100:2512–2517.
- Fu R, Yanjanin NM, Elrick MJ, Ware C, Lieberman AP, Porter FD (2012) Apolipoprotein E genotype and neurological disease onset in Niemann-Pick disease, type C1. *Am J Med Genet Part A* 158 A:2775–2780.
- Fuhrmann M, Mitteregger G, Kretschmar H, Herms J (2007) Dendritic pathology in prion disease starts at the synaptic spine. *J Neurosci* 27:6224–6233.
- Fujio K, Sato M, Uemura T, Sato T, Sato-Harada R, Harada A (2007) 14-3-3 proteins and protein phosphatases are not reduced in tau-deficient mice. *Neuroreport* 18:1049–1052.
- Fukumoto H, Cheung BS, Hyman BT, Irizarry MC (2002) Beta-secretase protein and activity are increased in the neocortex in Alzheimer disease. *Arch Neurol* 59:1381–1389.
- Fulga T a, Elson-Schwab I, Khurana V, Steinhilb ML, Spires TL, Hyman BT, Feany MB (2007) Abnormal bundling and accumulation of F-actin mediates tau-induced neuronal degeneration in vivo. *Nat Cell Biol* 9:139–148.
- Gauthier-Kemper A, Weissmann C, Golovyashkina N, Sebö-Lemke Z, Drewes G, Gerke V, Heinisch JJ, Brandt R (2011) The frontotemporal dementia mutation R406W blocks tau's interaction with the membrane in an annexin A2-dependent manner. *J Cell Biol* 192:647–661.
- Gehrmann J, Matsumoto Y, Kreutzberg GW (1995) Microglia: Intrinsic immuneffector cell of the brain. *Brain Res Rev* 20:269–287.
- Gengler S, Hamilton A, Hölscher C (2010) Synaptic plasticity in the hippocampus of a APP/PS1 mouse model of Alzheimer's disease is impaired in old but not young mice. Gaetani S, ed. *PLoS One* 5:e9764.
- Gheyara AL, Ponnusamy R, Djukic B, Craft RJ, Ho K, Guo W, Finucane MM, Sanchez PE, Mucke L (2014) Tau reduction prevents disease in a mouse model of Dravet syndrome. *Ann Neurol* 76:443–456.
- Ginsberg SD, Alldred MJ, Counts SE, Cataldo AM, Neve RL, Jiang Y, Wu J, Chao M V., Mufson EJ, Nixon RA, Che S (2010a) Microarray analysis of hippocampal CA1 neurons implicates early endosomal dysfunction during Alzheimer's disease progression. *Biol Psychiatry* 68:885–893.

- Ginsberg SD, Mufson EJ, Counts SE, Wu J, Alldred MJ, Nixon RA, Che S (2010b) Regional selectivity of rab5 and rab7 protein upregulation in mild cognitive impairment and Alzheimer's disease. *J Alzheimer's Dis* 22:631–639.
- Glenner GG, Wong CW (1984) Alzheimer's disease: initial report of the purification and characterization of a novel cerebrovascular amyloid protein. *Biochem Biophys Res Commun* 120:885–890.
- Goedert M (2009) Oskar Fischer and the study of dementia. *Brain* 132:1102–1111.
- Goedert M (2015) NEURODEGENERATION. Alzheimer's and Parkinson's diseases: The prion concept in relation to assembled A β , tau, and α -synuclein. *Science* 349:1255–1259.
- Goedert M, Ghetti B, Spillantini MG (2012) Frontotemporal Dementia: Implications for Understanding Alzheimer Disease. *Cold Spring Harb Perspect Med* 2:a006254–a006254.
- Goedert M, Jakes R (1990) Expression of separate isoforms of human tau protein: correlation with the tau pattern in brain and effects on tubulin polymerization. *EMBO J* 9:4225–4230.
- Goedert M, Spillantini MG, Crowther RA (1992) Cloning of a big tau microtubule-associated protein characteristic of the peripheral nervous system. *Proc Natl Acad Sci U S A* 89:1983–1987.
- Golbe LI, Lazzarini AM, Sychala JR, Johnson WG, Stenroos ES, Mark MH, Sage JI (2001) The tau A0 allele in Parkinson's disease. *Mov Disord* 16:442–447.
- Golde TE, Eckman CB, Younkin SG (2000) Biochemical detection of AL isoforms : implications for pathogenesis , diagnosis , and treatment of Alzheimer ' s disease. 1502:172–187.
- Götz J, Probst A, Spillantini MG, Schäfer T, Jakes R, Bürki K, Goedert M (1995) Somatodendritic localization and hyperphosphorylation of tau protein in transgenic mice expressing the longest human brain tau isoform. *EMBO J* 14:1304–1313.
- Götz J, Streffer JR, David D, Schild A, Hoernli F, Pennanen L, Kurosinski P, Chen F (2004) Transgenic animal models of Alzheimer's disease and related disorders: histopathology, behavior and therapy. *Mol Psychiatry* 9:664–683.
- Gouras GK, Tampellini D, Takahashi RH, Capetillo-Zarate E (2010) Intraneuronal β -amyloid accumulation and synapse pathology in Alzheimer's disease. *Acta Neuropathol* 119:523–541.
- Gowrishankar S, Yuan P, Wu Y, Schrag M, Paradise S, Grutzendler J, De Camilli P, Ferguson SM (2015) Massive accumulation of luminal protease-deficient axonal lysosomes at Alzheimer's disease amyloid plaques. *Proc Natl Acad Sci* 112:E3699–E3708.
- Grbovic OM, Mathews PM, Jiang Y, Schmidt SD, Dinakar R, Summers-Terio NB, Ceresa BP, Nixon RA, Cataldo AM (2003) Rab5-stimulated up-regulation of the endocytic pathway increases intracellular β -cleaved amyloid precursor protein carboxyl-terminal fragment levels and A β production. *J Biol Chem* 278:31261–31268.
- Greene LA, Liu DX, Troy CM, Biswas SC (2007) Cell cycle molecules define a pathway required for neuron death in development and disease. *Biochim Biophys Acta* 1772:392–401.
- Groemer TW, Thiel CS, Holt M, Riedel D, Hua Y, Hüve J, Wilhelm BG, Klingauf J (2011) Amyloid precursor protein is trafficked and secreted via synaptic vesicles Okazawa H, ed. *PLoS One* 6:e18754.
- Guevara J, Dilhuydy H, Espinosa B, Delacourte A, Quirion R, Mena R, Joannette Y, Zenteno E, Robitaille Y (2004) Coexistence of reactive plasticity and neurodegeneration in Alzheimer diseased brains. *Histol Histopathol* 19:1075–1084.

- Guo Q, Li H, Gaddam SSK, Justice NJ, Robertson CS, Zheng H (2012) Amyloid precursor protein revisited: Neuron-specific expression and highly stable nature of soluble derivatives. *J Biol Chem* 287:2437–2445.
- Haass C, Kaether C, Thinakaran G, Sisodia S (2012) Trafficking and proteolytic processing of APP. *Cold Spring Harb Perspect Med* 2:a006270.
- Haass C, Koo EH, Mellon A, Hung AY, Selkoe DJ (1992) Targeting of cell-surface β -amyloid precursor protein to lysosomes: alternative processing into amyloid-bearing fragments. *Nature* 357:500–503.
- Harada A, Oguchi K, Okabe S, Kuno J, Terada S, Ohshima T, Sato-Yoshitake R, Takei Y, Noda T, Hirokawa N (1994) Altered microtubule organization in small-calibre axons of mice lacking tau protein. *Nature* 369:488–491.
- Harada A, Takei Y, Kanai Y, Tanaka Y, Nonaka S, Hirokawa N (1998) Golgi vesiculation and lysosome dispersion in cells lacking cytoplasmic dynein. *J Cell Biol* 141:51–59.
- He W, Lu Y, Qahwash I, Hu X-Y, Chang A, Yan R (2004) Reticulon family members modulate BACE1 activity and amyloid- β peptide generation. *Nat Med* 10:959–965.
- Hefendehl JK, Wegenast-Braun BM, Liebig C, Eicke D, Milford D, Calhoun ME, Kohsaka S, Eichner M, Jucker M (2011) Long-term in vivo imaging of β -amyloid plaque appearance and growth in a mouse model of cerebral β -amyloidosis. *J Neurosci* 31:624–629.
- Hendricks AG, Perlson E, Ross JL, Schroeder HW, Tokito M, Holzbaur ELF (2010) Motor Coordination via a Tug-of-War Mechanism Drives Bidirectional Vesicle Transport. *Curr Biol* 20:697–702.
- Herzog E, Nadrigny F, Silm K, Biesemann C, Helling I, Bersot T, Steffens H, Schwartzmann R, Nagerl U V., El Mestikawy S, Rhee J, Kirchhoff F, Brose N (2011) In vivo imaging of intersynaptic vesicle exchange using VGLUT1Venus knock-in mice. *J Neurosci* 31:15544–15559.
- Hiruma H, Katakura T, Takahashi S, Ichikawa T, Kawakami T (2003) Glutamate and amyloid beta-protein rapidly inhibit fast axonal transport in cultured rat hippocampal neurons by different mechanisms. *J Neurosci* 23:8967–8977.
- Höglinger GU et al. (2011) Identification of common variants influencing risk of the tauopathy progressive supranuclear palsy. In: *Nature Genetics*, pp 699–705.
- Holsinger RMD, McLean CA, Beyreuther K, Masters CL, Evin G (2002) Increased expression of the amyloid precursor β -secretase in Alzheimer's disease. *Ann Neurol* 51:783–786.
- Holth JK, Bomben VC, Reed JG, Inoue T, Younkin L, Younkin SG, Pautler RG, Botas J, Noebels JL (2013) Tau loss attenuates neuronal network hyperexcitability in mouse and *Drosophila* genetic models of epilepsy. *J Neurosci* 33:1651–1659.
- Holtmaat A, Bonhoeffer T, Chow DK, Chuckowree J, De Paola V, Hofer SB, Hübener M, Keck T, Knott G, Lee W-C a, Mostany R, Mrcic-Flogel TD, Nedivi E, Portera-Cailliau C, Svoboda K, Trachtenberg JT, Wilbrecht L (2009) Long-term, high-resolution imaging in the mouse neocortex through a chronic cranial window. *Nat Protoc* 4:1128–1144.
- Holtzman DM, Bales KR, Paul SM, DeMattos RB (2002) A β immunization and anti-A β antibodies: potential therapies for the prevention and treatment of Alzheimer's disease. *Adv Drug Deliv Rev* 54:1603–1613.
- Hoover BR, Reed MN, Su J, Penrod RD, Kotilinek LA, Grant MK, Pitstick R, Carlson GA, Lanier LM, Yuan L-L, Ashe KH, Liao D (2010) Tau mislocalization to dendritic spines mediates synaptic dysfunction independently of neurodegeneration. *Neuron* 68:1067–1081.

- Houlden H et al. (2001) Corticobasal degeneration and progressive supranuclear palsy share a common tau haplotype. *Neurology* 56:1702–1706.
- Hu X, Shi Q, Zhou X, He W, Yi H, Yin X, Gearing M, Levey A, Yan R (2007) Transgenic mice overexpressing reticulon 3 develop neuritic abnormalities. *EMBO J* 26:2755–2767.
- Hung COY, Coleman MP (2016) KIF1A mediates axonal transport of BACE1 and identification of independently moving cargoes in living SCG neurons. *Traffic* 17:1155–1167.
- Huse JT, Pijak DS, Leslie GJ, Lee VM-Y, Doms RW (2000) Maturation and endosomal targeting of β -Site amyloid precursor protein-cleaving enzyme. *J Biol Chem* 275:33729–33737.
- Hwang SC, Jhon D-Y, Bae YS, Kim JH, Rhee SG (1996) Activation of phospholipase C-g by the concerted action of tau proteins and arachidonic acid. *J Biol Chem* 271:18342–18349.
- Ikegami S, Harada A, Hirokawa N (2000) Muscle weakness, hyperactivity, and impairment in fear conditioning in tau-deficient mice. *Neurosci Lett* 279:129–132.
- Ishikawa-Ankerhold HC, Ankerhold R, Drummen GPC (2012) Advanced fluorescence microscopy techniques-FRAP, FLIP, FLAP, FRET and FLIM. *Molecules* 17:4047–4132.
- Itskov V, Pastalkova E, Mizuseki K, Buzsaki G, Harris KD (2008) Theta-mediated dynamics of spatial information in hippocampus. *J Neurosci* 28:5959–5964.
- Ittner LM, Ke YD, Delerue F, Bi M, Gladbach A, van Eersel J, Wölfing H, Chieng BC, Christie MJ, Napier IA, Eckert A, Staufenbiel M, Hardeman E, Götz J (2010) Dendritic function of tau mediates amyloid-beta toxicity in Alzheimer's disease mouse models. *Cell* 142:387–397.
- Ittner LM, Ke YD, Götz J (2009) Phosphorylated Tau interacts with c-Jun N-terminal kinase-interacting protein 1 (JIP1) in Alzheimer disease. *J Biol Chem* 284:20909–20916.
- Jacobsen L, Madsen P, Moestrup SK, Lund AH, Tommerup N, Nykjaer A, Sottrup-Jensen L, Gliemann J, Petersen CM (1996) Molecular characterization of a novel human hybrid-type receptor that binds the alpha2-macroglobulin receptor-associated protein. *J Biol Chem* 271:31379–31383.
- Jahshan A, Esteves-Villanueva JO, Martic-Milne S (2016) Evaluation of ferritin and transferrin binding to tau protein. *J Inorg Biochem* 162:127–134.
- Janning D, Igaev M, Sundermann F, Bruhmann J, Beutel O, Heinisch JJ, Bakota L, Piehler J, Junge W, Brandt R (2014) Single-molecule tracking of tau reveals fast kiss-and-hop interaction with microtubules in living neurons. *Mol Biol Cell* 25:3541–3551.
- Jansen WJ et al. (2015) Prevalence of cerebral amyloid pathology in persons without dementia. *JAMA* 313:1924.
- Jeganathan S, von Bergen M, Brutlach H, Steinhoff H-J, Mandelkow E (2006) Global hairpin folding of Tau in solution. *Biochemistry* 45:2283–2293.
- Ji ZS, Müllendorff K, Cheng IH, Miranda RD, Huang Y, Mahley RW (2006) Reactivity of apolipoprotein E4 and amyloid β peptide: Lysosomal stability and neurodegeneration. *J Biol Chem* 281:2683–2692.
- Jin M, Shepardson N, Yang T, Chen G, Walsh D, Selkoe DJ (2011) Soluble amyloid β -protein dimers isolated from Alzheimer cortex directly induce Tau hyperphosphorylation and neuritic degeneration. *Proc Natl Acad Sci* 108:5819–5824.
- Jucker M, Walker LC (2013) Self-propagation of pathogenic protein aggregates in neurodegenerative diseases. *Nature* 501:45–51.
- Jung D, Filliol D, Mische M, Rendon A (1993) Interaction of brain mitochondria with microtubules

- reconstituted from brain tubulin and MAP2 or TAU. *Cell Motil Cytoskeleton* 24:245–255.
- Kaether C, Skehel P, Dotti CG (2000) Axonal membrane proteins are transported in distinct carriers: a two-color video microscopy study in cultured hippocampal neurons Lippincott-Schwartz J, ed. *Mol Biol Cell* 11:1213–1224.
- Kågedal K, Kim WS, Appelqvist H, Chan S, Cheng D, Agholme L, Barnham K, McCann H, Halliday G, Garner B (2010) Increased expression of the lysosomal cholesterol transporter NPC1 in Alzheimer's disease. *Biochim Biophys Acta - Mol Cell Biol Lipids* 1801:831–838.
- Kahlson MA, Colodner KJ (2015) Glial Tau Pathology in Tauopathies: Functional Consequences. *J Exp Neurosci* 9:43–50.
- Kalvodova L, Kahya N, Schwille P, Eehalt R, Verkade P, Drechsel D, Simons K (2005) Lipids as modulators of proteolytic activity of BACE: Involvement of cholesterol, glycosphingolipids, and anionic phospholipids in vitro. *J Biol Chem* 280:36815–36823.
- Kamal a, Almenar-Queralt a, LeBlanc JF, Roberts E a, Goldstein LS (2001) Kinesin-mediated axonal transport of a membrane compartment containing beta-secretase and presenilin-1 requires APP. *Nature* 414:643–648.
- Kamal A, Stokin GB, Yang Z, Xia C-H, Goldstein LS. (2000) Axonal transport of amyloid precursor protein is mediated by direct binding to the kinesin light chain subunit of Kinesin-I. *Neuron* 28:449–459.
- Kanaan NM, Morfini GA, LaPointe NE, Pigino GF, Patterson KR, Song Y, Andreadis A, Fu Y, Brady ST, Binder LI (2011) Pathogenic forms of tau inhibit kinesin-dependent axonal transport through a mechanism involving activation of axonal phosphotransferases. *J Neurosci* 31:9858–9868.
- Kandalepas PC, Sadleir KR, Eimer WA, Zhao J, Nicholson DA, Vassar R (2013) The Alzheimer's β -secretase BACE1 localizes to normal presynaptic terminals and to dystrophic presynaptic terminals surrounding amyloid plaques. *Acta Neuropathol* 126:329–352.
- Kang DE, Soriano S, Frosch MP, Collins T, Naruse S, Sisodia SS, Leibowitz G, Levine F, Koo EH (1999) Presenilin 1 facilitates the constitutive turnover of beta-catenin: differential activity of Alzheimer's disease-linked PS1 mutants in the beta-catenin-signaling pathway. *J Neurosci* 19:4229–4237.
- Kato S, Gondo T, Hoshii Y, Takahashi M, Yamada M, Ishihara T (1998) Confocal observation of senile plaques in Alzheimer's disease: senile plaque morphology and relationship between senile plaques and astrocytes. *Pathol Int* 48:332–340.
- Kawas C, Gray S, Brookmeyer R, Fozard J, Zonderman A (2000) Age-specific incidence rates of Alzheimer's disease: the Baltimore Longitudinal Study of Aging. *Neurology* 54:2072–2077.
- Ke YD, Suchowerska AK, van der Hoven J, De Silva DM, Wu CW, van Eersel J, Ittner A, Ittner LM (2012) Lessons from tau-deficient mice. *Int J Alzheimers Dis* 2012:873270.
- Kimura R, Devi L, Ohno M (2010) Partial reduction of BACE1 improves synaptic plasticity, recent and remote memories in Alzheimer's disease transgenic mice. *J Neurochem* 113:248–261.
- Kimura T, Whitcomb DJ, Jo J, Regan P, Piers T, Heo S, Brown C, Hashikawa T, Murayama M, Seok H, Sotiropoulos I, Kim E, Collingridge GL, Takashima A, Cho K (2013) Microtubule-associated protein tau is essential for long-term depression in the hippocampus. *Philos Trans R Soc B Biol Sci* 369:20130144–20130144.
- King GD, Scott Turner R (2004) Adaptor protein interactions: modulators of amyloid precursor protein metabolism and Alzheimer's disease risk? *Exp Neurol* 185:208–219.

- King ME, Kan H-M, Baas PW, Erisir A, Glabe CG, Bloom GS (2006) Tau-dependent microtubule disassembly initiated by prefibrillar β -amyloid. *J Cell Biol* 175:541–546.
- Koh YH, von Arnim CAF, Hyman BT, Tanzi RE, Tesco G (2005) BACE is degraded via the lysosomal pathway. *J Biol Chem* 280:32499–32504.
- Komori T (1999) Tau-positive glial inclusions in progressive supranuclear palsy, corticobasal degeneration and Pick's disease. *Brain Pathol* 9:663–679.
- Kornau HC, Schenker LT, Kennedy MB, Seeburg PH (1995) Domain interaction between NMDA receptor subunits and the postsynaptic density protein PSD-95. *Science* 269:1737–1740.
- Lacovich V, Espindola SL, Alloatti M, Pozo Devoto V, Cromberg LE, Čarná ME, Forte G, Gallo J-M, Bruno L, Stokin GB, Avale ME, Falzone TL (2017) Tau Isoforms Imbalance Impairs the Axonal Transport of the Amyloid Precursor Protein in Human Neurons. *J Neurosci* 37:58–69.
- Laird FM, Cai H, Savonenko A V, Farah MH, He K, Melnikova T, Wen H, Chiang H, Xu G, Koliatsos VE, Borchelt DR, Price DL, Lee H, Wong PC (2005) BACE1, a major determinant of selective vulnerability of the brain to amyloid-beta amyloidogenesis, is essential for cognitive, emotional, and synaptic Functions. *J Neurosci* 25:11693–11709.
- Laird FM, Cai H, Savonenko A V, Farah MH, Kaiwen H, Melnikova T, Wen H, Chiang H, Xu G, Koliatsos VE, Borchelt DR, Price DL, Lee H, Wong PC (2008) BACE1, a major determinant of selective vulnerability of the brain to Amyloid- β amyloidogenesis, is essential for cognitive, emotional, and synaptic functions. *J Neurosci* 25:11693–11709.
- Lee G, Newman ST, Gard DL, Band H, Panchamoorthy G (1998) Tau interacts with src-family non-receptor tyrosine kinases. *J Cell Sci* 111 (Pt 2:3167–3177.
- Lee H-G, Casadesus G, Zhu X, Castellani RJ, McShea A, Perry G, Petersen RB, Bajic V, Smith MA (2009) Cell cycle re-entry mediated neurodegeneration and its treatment role in the pathogenesis of Alzheimer's disease. *Neurochem Int* 54:84–88.
- Lee J-H, McBrayer MK, Wolfe DM, Haslett LJ, Kumar A, Sato Y, Lie PPY, Mohan P, Coffey EE, Kompella U, Mitchell CH, Lloyd-Evans E, Nixon RA (2015) Presenilin 1 maintains lysosomal Ca²⁺ homeostasis via TRPML1 by regulating vATPase-mediated lysosome acidification. *Cell Rep* 12:1430–1444.
- Lee J-H, Yu WH, Kumar A, Lee S, Mohan PS, Peterhoff CM, Wolfe DM, Martinez-Vicente M, Massey AC, Sovak G, Uchiyama Y, Westaway D, Cuervo AM, Nixon RA (2010) Lysosomal proteolysis and autophagy require Presenilin 1 and are disrupted by Alzheimer-related PS1 mutations. *Cell* 141:1146–1158.
- Lee S, Sato Y, Nixon RA (2011) Lysosomal proteolysis inhibition selectively disrupts axonal transport of degradative organelles and causes an Alzheimer's-like axonal dystrophy. *J Neurosci* 31:7817–7830.
- Lei P, Ayton S, Finkelstein DI, Spoerri L, Ciccotosto GD, Wright DK, Wong BXW, Adlard PA, Cherny RA, Lam LQ, Roberts BR, Volitakis I, Egan GF, McLean CA, Cappai R, Duce JA, Bush AI (2012) Tau deficiency induces parkinsonism with dementia by impairing APP-mediated iron export. *Nat Med* 18:291–295.
- Lei P, Ayton S, Moon S, Zhang Q, Volitakis I, Finkelstein DI, Bush AI (2014) Motor and cognitive deficits in aged tau knockout mice in two background strains. *Mol Neurodegener* 9:29.
- León-Espinosa G, García E, García-Escudero V, Hernández F, DeFelipe J, Avila J (2013) Changes in tau phosphorylation in hibernating rodents. *J Neurosci Res* 91:954–962.
- Leroy K, Ando K, Laporte V, Dedecker R, Suain V, Authélet M, Héraud C, Pierrot N, Yilmaz Z, Octave

- J-N, Brion J-P (2012) Lack of Tau proteins rescues neuronal cell death and decreases amyloidogenic processing of APP in APP/PS1 mice. *Am J Pathol* 181:1928–1940.
- Li Q, Südhof TC (2004) Cleavage of amyloid-beta precursor protein and amyloid-beta precursor-like protein by BACE 1. *J Biol Chem* 279:10542–10550.
- Liebsch F, Aurousseau MRP, Bethge T, McGuire H, Scolari S, Herrmann A, Blunck R, Bowie D, Multhaup G (2017) Full-length cellular γ -secretase has a trimeric subunit stoichiometry, and its sulfur-rich transmembrane interaction site modulates cytosolic copper compartmentalization. *J Biol Chem* 292:13258–13270.
- Liu C, Götz J (2013) Profiling murine Tau with ON, 1N and 2N isoform-specific antibodies in brain and peripheral organs reveals distinct subcellular localization, with the 1N isoform being enriched in the nucleus Gong C-X, ed. *PLoS One* 8:e84849.
- Liu C, Song X, Nisbet R, Götz J (2016) Co-immunoprecipitation with Tau isoform-specific antibodies reveals distinct protein interactions and highlights a putative role for 2N Tau in disease. *J Biol Chem* 291:8173–8188.
- Ma Q-L, Zuo X, Yang F, Ubeda OJ, Gant DJ, Alaverdyan M, Kioseva NC, Nazari S, Chen PP, Nothias F, Chan P, Teng E, Frautschy SA, Cole GM (2014) Loss of MAP function leads to hippocampal synapse loss and deficits in the Morris Water Maze with aging. *J Neurosci* 34:7124–7136.
- Maday S, Twelvetrees AE, Moughamian AJ, Holzbaur ELF (2014) Axonal transport: cargo-specific mechanisms of motility and regulation. *Neuron* 84:292–309.
- Maia LF, Kaeser SA, Reichwald J, Hruscha M, Martus P, Staufienbiel M, Jucker M (2013) Changes in amyloid- β and Tau in the cerebrospinal fluid of transgenic mice overexpressing Amyloid Precursor Protein. *Sci Transl Med* 5:194re2-194re2.
- Malnar M, Kosicek M, Lisica A, Posavec M, Krolo A, Njavro J, Omerbasic D, Tahirovic S, Hecimovic S (2012) Cholesterol-depletion corrects APP and BACE1 mistrafficking in NPC1-deficient cells. *Biochim Biophys Acta - Mol Basis Dis* 1822:1270–1283.
- Malnar M, Kosicek M, Mitterreiter S, Omerbasic D, Lichtenthaler SF, Goate A, Hecimovic S (2010) Niemann-Pick type C cells show cholesterol dependent decrease of APP expression at the cell surface and its increased processing through the β -secretase pathway. *Biochim Biophys Acta - Mol Basis Dis* 1802:682–691.
- Mandelkow E (2003) Clogging of axons by tau, inhibition of axonal traffic and starvation of synapses. *Neurobiol Aging* 24:1079–1085.
- Masters CL, Bateman R, Blennow K, Rowe CC, Sperling RA, Cummings JL (2015) Alzheimer's disease. *Nat Rev Dis Prim* 1:15056.
- Masters CL, Selkoe DJ (2012) Biochemistry of Amyloid beta -Protein and Amyloid Deposits in Alzheimer Disease. *Cold Spring Harb Perspect Med* 2:a006262–a006262.
- Masters CL, Simms G, Weinman NA, Multhaup G, McDonald BL, Beyreuther K (1985) Amyloid plaque core protein in Alzheimer disease and Down syndrome. *Proc Natl Acad Sci U S A* 82:4245–4249.
- Mauch DH, Nägler K, Schumacher S, Göritz C, Müller EC, Otto A, Pfrieder FW (2001) CNS synaptogenesis promoted by glia-derived cholesterol. *Science* (80-) 294:1354–1357.
- Maulik M, Peake K, Chung J, Wang Y, Vance JE, Kar S (2015) APP overexpression in the absence of NPC1 exacerbates metabolism of amyloidogenic proteins of Alzheimer's disease. *Hum Mol Genet* 24:ddv413.
- Maxfield FR, Tabas I (2005) Role of cholesterol and lipid organization in disease. *Nature* 438:612–

621.

- Maynard CJ, Cappai R, Volitakis I, Cherny RA, Masters CL, Li Q-X, Bush AI (2006) Gender and genetic background effects on brain metal levels in APP transgenic and normal mice: implications for Alzheimer beta-amyloid pathology. *J Inorg Biochem* 100:952–962.
- McConlogue L, Buttini M, Anderson JP, Brigham EF, Chen KS, Freedman SB, Games D, Johnson-Wood K, Lee M, Zeller M, Liu W, Motter R, Sinha S (2007) Partial reduction of BACE1 has dramatic effects on Alzheimer plaque and synaptic pathology in APP transgenic mice. *J Biol Chem* 282:26326–26334.
- McInnes J, Wierda K, Snellinx A, Bounti L, Wang Y-C, Stancu I-C, Apóstolo N, Gevaert K, Dewachter I, Spires-Jones TL, De Strooper B, De Wit J, Zhou L, Verstreken P (2018) Synaptogyrin-3 mediates presynaptic dysfunction induced by Tau. *Neuron* 97:823–835.e8.
- Mercken M, Fischer I, Kosik KS, Nixon RA (1995) Three distinct axonal transport rates for tau, tubulin, and other microtubule-associated proteins: evidence for dynamic interactions of tau with microtubules in vivo. *J Neurosci* 15:8259–8267.
- Miao Y, Chen J, Zhang Q, Sun A (2010) Deletion of *tau* attenuates heat shock-induced injury in cultured cortical neurons. *J Neurosci Res* 88:102–110.
- Mindell JA (2012) Lysosomal acidification mechanisms. *Annu Rev Physiol* 74:69–86.
- Mitew S, Kirkcaldie MTK, Dickson TC, Vickers JC (2013) Neurites containing the neurofilament-triplet proteins are selectively vulnerable to cytoskeletal pathology in Alzheimer’s disease and transgenic mouse models. *Front Neuroanat* 7:30.
- Miyagawa T, Ebinuma I, Morohashi Y, Hori Y, Young Chang M, Hattori H, Maehara T, Yokoshima S, Fukuyama T, Tsuji S, Iwatsubo T, Prendergast GC, Tomita T (2016) BIN1 regulates BACE1 intracellular trafficking and amyloid- β production. *Hum Mol Genet* 25:ddw146.
- Montagna E, Dorostkar MM, Herms J (2017) The Role of APP in Structural Spine Plasticity. *Front Mol Neurosci* 10:136.
- Morel E, Chamoun Z, Lasiecka ZM, Chan RB, Williamson RL, Vetanovetz C, Dall’Armi C, Simoes S, Point Du Jour KS, McCabe BD, Small SA, Di Paolo G (2013) Phosphatidylinositol-3-phosphate regulates sorting and processing of amyloid precursor protein through the endosomal system. *Nat Commun* 4:2250.
- Morris GP, Clark IA, Vissel B (2014) Inconsistencies and controversies surrounding the amyloid hypothesis of Alzheimer’s disease. *Acta Neuropathol Commun* 2:135.
- Morris M, Hamto P, Adame A, Devidze N, Masliah E, Mucke L (2013) Age-appropriate cognition and subtle dopamine-independent motor deficits in aged Tau knockout mice. *Neurobiol Aging* 34:1523–1529.
- Morris M, Koyama A, Masliah E, Mucke L (2011a) Tau reduction does not prevent motor deficits in two mouse models of Parkinson’s disease. *PLoS One* 6:1–7.
- Morris M, Maeda S, Vossel K, Mucke L (2011b) The many faces of tau. *Neuron* 70:410–426.
- Mucke L, Masliah E, Yu GQ, Mallory M, Rockenstein EM, Tatsuno G, Hu K, Kholodenko D, Johnson-Wood K, McConlogue L (2000) High-level neuronal expression of abeta 1-42 in wild-type human amyloid protein precursor transgenic mice: synaptotoxicity without plaque formation. *J Neurosci* 20:4050–4058.
- Murayama KS, Kametani F, Saito S, Kume H, Akiyama H, Araki W (2006) Reticulons RTN3 and RTN4-B/C interact with BACE1 and inhibit its ability to produce amyloid β -protein. *Eur J Neurosci* 24:1237–1244.

- Nelson PT, Braak H, Markesbery WR (2009) Neuropathology and cognitive impairment in Alzheimer disease: A complex but coherent relationship. *J Neuropathol Exp Neurol* 68:1–14.
- Nixon RA, Wegiel J, Kumar A, Yu WH, Peterhoff C, Cataldo A, Cuervo AM (2005) Extensive involvement of autophagy in Alzheimer disease: an immuno-electron microscopy study. *J Neuropathol Exp Neurol* 64:113–122.
- Noetzli M, Eap CB (2013) Pharmacodynamic, pharmacokinetic and pharmacogenetic aspects of drugs used in the treatment of Alzheimer's disease. *Clin Pharmacokinet* 52:225–241.
- Norton S, Matthews FE, Barnes DE, Yaffe K, Brayne C (2014) Potential for primary prevention of Alzheimer's disease: An analysis of population-based data. *Lancet Neurol* 13:788–794.
- Nussbaum JM, Schilling S, Cynis H, Silva A, Swanson E, Wangsanut T, Tayler K, Wiltgen B, Hatami A, Röncke R, Hutter-paier B, Alexandru A, Jagla W, Graubner S, Glabe CG, Demuth H, Bloom GS (2012) Prion-like behavior and Tau-dependent cytotoxicity of Pyroglutamylated β -Amyloid. *Nature* 485:651–655.
- Ossenkoppele R et al. (2015) Prevalence of Amyloid PET Positivity in Dementia Syndromes. *JAMA* 313:1939.
- Peters F, Salihoglu H, Rodrigues E, Herzog E, Blume T, Filser S, Dorostkar M, Shimshek DR, Brose N, Neumann U, Herms J (2018) BACE1 inhibition more effectively suppresses initiation than progression of β -amyloid pathology. *Acta Neuropathol*:1–16.
- Phinney AL, Deller T, Stalder M, Calhoun ME, Frotscher M, Sommer B, Staufenbiel M, Jucker M (1999) Cerebral amyloid induces aberrant axonal sprouting and ectopic terminal formation in Amyloid Precursor Protein transgenic mice. *J Neurosci* 19:8552–8559.
- Pigino G, Morfini G, Atagi Y, Deshpande A, Yu C, Jungbauer L, LaDu M, Busciglio J, Brady S (2009) Disruption of fast axonal transport is a pathogenic mechanism for intraneuronal amyloid beta. *Proc Natl Acad Sci* 106:5907–5912.
- Qi-Takahara Y, Morishima-Kawashima M, Tanimura Y, Dolios G, Hirotsu N, Horikoshi Y, Kametani F, Maeda M, Saido TC, Wang R, Ihara Y (2005) Longer forms of amyloid beta protein: implications for the mechanism of intramembrane cleavage by gamma-secretase. *J Neurosci* 25:436–445.
- Rabe S, Reichwald J, Ammaturo D, de Strooper B, Saftig P, Neumann U, Staufenbiel M (2011) The Swedish APP mutation alters the effect of genetically reduced BACE1 expression on the APP processing. *J Neurochem* 119:231–239.
- Radde R, Bolmont T, Kaeser S a, Coomaraswamy J, Lindau D, Stoltze L, Calhoun ME, Jäggi F, Wolburg H, Gengler S, Haass C, Ghetti B, Czech C, Hölscher C, Mathews PM, Jucker M (2006) A β 42-driven cerebral amyloidosis in transgenic mice reveals early and robust pathology. *EMBO Rep* 7:940–946.
- Rapoport M, Dawson HN, Binder LI, Vitek MP, Ferreira A (2002) Tau is essential to beta -amyloid-induced neurotoxicity. *Proc Natl Acad Sci U S A* 99:6364–6369.
- Roberds SL et al. (2001) BACE knockout mice are healthy despite lacking the primary beta-secretase activity in brain: implications for Alzheimer's disease therapeutics. *Hum Mol Genet* 10:1317–1324.
- Roberson ED, Halabisky B, Yoo JW, Yao J, Chin J, Yan F, Wu T, Hamto P, Devidze N, Yu G-Q, Palop JJ, Noebels JL, Mucke L (2011) Amyloid- /Fyn-induced synaptic, network, and cognitive impairments depend on Tau levels in multiple mouse models of Alzheimer's disease. *J Neurosci* 31:700–711.

- Roberson ED, Scearce-Levie K, Palop JJ, Yan F, Cheng IH, Wu T, Gerstein H, Yu G-Q, Mucke L (2007) Reducing endogenous Tau ameliorates Amyloid beta-induced deficits in an Alzheimer's disease mouse model. *Science* (80-) 316:750–754.
- Rosén C, Hansson O, Blennow K, Zetterberg H (2013) Fluid biomarkers in Alzheimer's disease - current concepts. *Mol Neurodegener* 8:20.
- Rui Y, Tiwari P, Xie Z, Zheng JQ (2006) Acute impairment of mitochondrial trafficking by beta-Amyloid peptides in hippocampal neurons. *J Neurosci* 26:10480–10487.
- Runz H, Rietdorf J, Tomic I, de Bernard M, Beyreuther K, Pepperkok R, Hartmann T (2002) Inhibition of intracellular cholesterol transport alters presenilin localization and amyloid precursor protein processing in neuronal cells. *J Neurosci* 22:1679–1689.
- Sadleir KR, Eimer WA, Cole SL, Vassar R (2015) A β reduction in BACE1 heterozygous null 5XFAD mice is associated with transgenic APP level. *Mol Neurodegener* 10:1.
- Sadleir KR, Kandalepas PC, Buggia-Prévot V, Nicholson DA, Thinakaran G, Vassar R (2016) Presynaptic dystrophic neurites surrounding amyloid plaques are sites of microtubule disruption, BACE1 elevation, and increased A β generation in Alzheimer's disease. *Acta Neuropathol* 132:235–256.
- Sanchez-Varo R, Trujillo-Estrada L, Sanchez-Mejias E, Torres M, Baglietto-Vargas D, Moreno-Gonzalez I, De Castro V, Jimenez S, Ruano D, Vizuete M, Davila JC, Garcia-Verdugo JM, Jimenez AJ, Vitorica J, Gutierrez A (2012) Abnormal accumulation of autophagic vesicles correlates with axonal and synaptic pathology in young Alzheimer's mice hippocampus. *Acta Neuropathol* 123:53–70.
- Sandoval I. ., Bakke O (1994) Targeting of membrane proteins to endosomes and lysosomes. *Trends Cell Biol* 4:292–297.
- Sannerud R, Annaert W (2009) Trafficking, a key player in regulated intramembrane proteolysis. *Semin Cell Dev Biol* 20:183–190.
- Satoh J, Tabunoki H, Ishida T, Saito Y, Arima K (2013) Ubiquilin-1 immunoreactivity is concentrated on Hirano bodies and dystrophic neurites in Alzheimer's disease brains. *Neuropathol Appl Neurobiol* 39:817–830.
- Saunders AM, Strittmatter WJ, Schmechel D, George-Hyslop PH, Pericak-Vance MA, Joo SH, Rosi BL, Gusella JF, Crapper-MacLachlan DR, Alberts MJ (1993) Association of apolipoprotein E allele epsilon 4 with late-onset familial and sporadic Alzheimer's disease. *Neurology* 43:1467–1472.
- Sawaya MR, Sambashivan S, Nelson R, Ivanova MI, Sievers SA, Apostol MI, Thompson MJ, Balbirnie M, Wiltzius JJW, McFarlane HT, Madsen AØ, Riek C, Eisenberg D (2007) Atomic structures of amyloid cross- β spines reveal varied steric zippers. *Nature* 447:453–457.
- Schweers O, Schönbrunn-Hanebeck E, Marx A, Mandelkow E (1994) Structural studies of tau protein and Alzheimer paired helical filaments show no evidence for beta-structure. *J Biol Chem* 269:24290–24297.
- Selkoe DJ (2001) Alzheimer's disease :genes, proteins, and therapy. *Physiol Rev* 81:741–766.
- Selkoe DJ, Wolfe MS (2007) Presenilin:running with scissors in the membrane. *Cell* 131:215–221.
- Serneels L et al. (2009) γ -Secretase heterogeneity in the aph1 subunit: Relevance for Alzheimer's disease. *Science* (80-) 324:639–642.
- Seward ME, Swanson E, Norambuena A, Reimann A, Cochran JN, Li R, Roberson ED, Bloom GS (2013) Amyloid- β signals through tau to drive ectopic neuronal cell cycle re-entry in

- Alzheimer's disease. *J Cell Sci* 126:1278–1286.
- Shah TM, Gupta SM, Chatterjee P, Campbell M, Martins RN (2017) Beta-amyloid sequelae in the eye: a critical review on its diagnostic significance and clinical relevance in Alzheimer's disease. *Mol Psychiatry*:1–11.
- Shi Q, Ge Y, Sharoar MG, He W, Xiang R, Zhang Z, Hu X, Yan R (2014) Impact of RTN3 Deficiency on Expression of BACE1 and Amyloid Deposition. *J Neurosci* 34:13954–13962.
- Shi Q, Prior M, He W, Tang X, Hu X, Yan R (2009) Reduced amyloid deposition in mice overexpressing RTN3 is adversely affected by preformed dystrophic neurites. *J Neurosci* 29:9163–9173.
- Shilling D, Muller M, Takano H, Daniel Mak D-O, Abel T, Coulter DA, Foskett JK (2014) Suppression of InsP3 receptor-mediated Ca²⁺ signaling alleviates mutant Presenilin-linked familial Alzheimer's disease pathogenesis. *J Neurosci* 34:6910–6923.
- Shipton OA, Leitz JR, Dworzak J, Acton CEJ, Tunbridge EM, Denk F, Dawson HN, Vitek MP, Wade-Martins R, Paulsen O, Vargas-caballero M (2011) Tau protein is required for Amyloid beta-induced impairment of hippocampal long-term potentiation. *J Neurosci* 31:1688–1692.
- Sohal VS, Zhang F, Yizhar O, Deisseroth K (2009) Parvalbumin neurons and gamma rhythms enhance cortical circuit performance. *Nature* 459:698–702.
- Sokolow S, Henkins KM, Bilousova T, Gonzalez B, Vinters H V., Miller CA, Cornwell L, Poon WW, Gyls KH (2015) Pre-synaptic C-terminal truncated tau is released from cortical synapses in Alzheimer's disease. *J Neurochem* 133:368–379.
- Sontag E, Nunbhakdi-Craig V, Lee G, Brandt R, Kamibayashi C, Kuret J, White CL, Mumby MC, Bloom GS (1999) Molecular interactions among protein phosphatase 2A, tau, and microtubules. Implications for the regulation of tau phosphorylation and the development of tauopathies. *J Biol Chem* 274:25490–25498.
- Sontag J-M, Sontag E (2014) Protein phosphatase 2A dysfunction in Alzheimer's disease. *Front Mol Neurosci* 7:16.
- Spillantini MG, Goedert M (2013) Tau pathology and neurodegeneration. *Lancet Neurol* 12:609–622.
- Spires TL, Meyer-Luehmann M, Stern EA, McLean PJ, Skoch J, Nguyen PT, Bacskai BJ, Hyman BT (2005) Dendritic spine abnormalities in Amyloid Precursor Protein transgenic mice demonstrated by gene transfer and intravital multiphoton microscopy. *J Neurosci* 25:7278–7287.
- Stalder M, Deller T, Staufenbiel M, Jucker M (2001) 3D-Reconstruction of microglia and amyloid in APP23 transgenic mice: no evidence of intracellular amyloid. *Neurobiol Aging* 22:427–434.
- Stamer K, Vogel R, Thies E, Mandelkow E, Mandelkow E-M (2002) Tau blocks traffic of organelles, neurofilaments, and APP vesicles in neurons and enhances oxidative stress. *J Cell Biol* 156:1051–1063.
- Steiner H, Haass C (2000) Intramembrane proteolysis by presenilins [Review]. *Nat Rev Mol Cell Biol* 1:217–224.
- Stokin GB, Raman R, Davies P, Masliah E (2005) Axonopathy and transport deficits early in the pathogenesis of Alzheimer's disease. *Science* (80-) 307:1282–1288.
- Su JH, Cummings BJ, Cotman CW (1993) Identification and distribution of axonal dystrophic neurites in Alzheimer's disease. *Brain Res* 625:228–237.

- Su JH, Cummings BJ, Cotman CW (1998) Plaque biogenesis in brain aging and Alzheimer's disease. II. Progressive transformation and developmental sequence of dystrophic neurites. *Acta Neuropathol* 96:463–471.
- Suberbielle E, Sanchez PE, Kravitz A V, Wang X, Ho K, Eilertson K, Devidze N, Kreitzer AC, Mucke L, Francisco S, Francisco S, Francisco S, Francisco S (2013) Physiological brain activity causes DNA double strand breaks in neurons — exacerbation by Amyloid- β . *Nat Neurosci* 16:613–621.
- Suzuki M, Kimura T (2017) Microtubule-associated tau contributes to intra-dendritic trafficking of AMPA receptors in multiple ways. *Neurosci Lett* 653:276–282.
- Takahashi RH (2004) Oligomerization of Alzheimer's beta-Amyloid within processes and synapses of cultured neurons and brain. *J Neurosci* 24:3592–3599.
- Takahashi RH, Milner TA, Li F, Nam EE, Edgar MA, Yamaguchi H, Beal MF, Xu H, Greengard P, Gouras GK (2002) Intraneuronal Alzheimer A β 42 accumulates in multivesicular bodies and is associated with synaptic pathology. *Am J Pathol* 161:1869–1879.
- Tashiro K, Hasegawa M, Ihara Y, Iwatsubo T (1997) Somatodendritic localization of phosphorylated tau in neonatal and adult rat cerebral cortex. *Neuroreport* 8:2797–2801.
- Terwel D, Dewachter I, Van Leuven F (2002) Axonal transport, Tau protein, and neurodegeneration in Alzheimer's disease. *NeuroMolecular Med* 2:151–166.
- Thal DR, Rub U, Orantes M, Braak H (2002) Phases of A β -deposition in the human brain and its relevance for the development of AD. *Neurology* 58:1791–1800.
- Trabzuni D, Wray S, Vandrovцова J, Ramasamy A, Walker R, Smith C, Luk C, Gibbs JR, Dillman A, Hernandez DG, Arepalli S, Singleton AB, Cookson MR, Pittman AM, de Silva R, Weale ME, Hardy J, Ryten M (2012) MAPT expression and splicing is differentially regulated by brain region: relation to genotype and implication for tauopathies. *Hum Mol Genet* 21:4094–4103.
- Tsai J, Grutzendler J, Duff K, Gan W-B (2004) Fibrillar amyloid deposition leads to local synaptic abnormalities and breakage of neuronal branches. *Nat Neurosci* 7:1181–1183.
- Tu H, Nelson O, Bezprozvanny A, Wang Z, Lee SF, Hao YH, Serneels L, De Strooper B, Yu G, Bezprozvanny I (2006) Presenilins form ER Ca²⁺ leak channels, a function disrupted by familial Alzheimer's disease-linked mutations. *Cell* 126:981–993.
- Tucker KL, Meyer M, Barde YA (2001) Neurotrophins are required for nerve growth during development. *Nat Neurosci* 4:29–37.
- Tyler SJ, Dawbarn D, Wilcock GK, Allen SJ (2002) α - and β -secretase: Profound changes in Alzheimer's disease. *Biochem Biophys Res Commun* 299:373–376.
- Ubelmann F, Burrinha T, Salavessa L, Gomes R, Ferreira C, Moreno N, Guimas Almeida C (2017) Bin1 and CD2AP polarise the endocytic generation of beta-amyloid. *EMBO Rep* 18:102–122.
- Ulery PG, Beers J, Mikhailenko I, Tanzi RE, Rebeck GW, Hyman BT, Strickland DK (2000) Modulation of beta-amyloid precursor protein processing by the low density lipoprotein receptor-related protein (LRP). Evidence that LRP contributes to the pathogenesis of Alzheimer's disease. *J Biol Chem* 275:7410–7415.
- Vanderweyde T, Apicco DJ, Youmans-Kidder K, Ash PEA, Cook C, Lummertz da Rocha E, Jansen-West K, Frame AA, Citro A, Leszyk JD, Ivanov P, Abisambra JF, Steffen M, Li H, Petrucelli L, Wolozin B (2016) Interaction of tau with the RNA-Binding Protein TIA1 Regulates tau Pathophysiology and Toxicity. *Cell Rep* 15:1455–1466.
- Vassar R (2004) BACE1: The β -Secretase Enzyme in Alzheimer's Disease. *J Mol Neurosci* 23:105–

114.

- Vassar R, Kuhn P-H, Haass C, Kennedy ME, Rajendran L, Wong PC, Lichtenthaler SF (2014) Function, therapeutic potential and cell biology of BACE proteases: current status and future prospects. *J Neurochemistry* 130:4–28.
- Vossel KA, Zhang K, Brodbeck J, Daub AC, Sharma P, Finkbeiner S, Cui B, Mucke L (2010) Tau reduction prevents Abeta-induced defects in axonal transport. *Science* 330:198.
- Wagner T, Pietrzik CU (2012) The role of lipoprotein receptors on the physiological function of APP. *Exp Brain Res* 217:377–387.
- Walsh DM, Klyubin I, Fadeeva J V., Cullen WK, Anwyl R, Wolfe MS, Rowan MJ, Selkoe DJ (2002) Naturally secreted oligomers of amyloid β protein potently inhibit hippocampal long-term potentiation in vivo. *Nature* 416:535–539.
- Wang J, Tanila H, Puoliväli J, Kadish I, van Groen T (2003) Gender differences in the amount and deposition of amyloidbeta in APPswe and PS1 double transgenic mice. *Neurobiol Dis* 14:318–327.
- Wang Y, Martinez-Vicente M, Krüger U, Kaushik S, Wong E, Mandelkow EM, Cuervo AM, Mandelkow E (2009) Tau fragmentation, aggregation and clearance: The dual role of lysosomal processing. *Hum Mol Genet* 18:4153–4170.
- Willnow TE, Andersen OM (2013) Sorting receptor SORLA – a trafficking path to avoid Alzheimer disease. *J Cell Sci* 126:2751–2760.
- Wilson CA, Murphy DD, Giasson BI, Zhang B, Trojanowski JQ, Lee VM-Y (2004) Degradative organelles containing mislocalized α - and β -synuclein proliferate in presenilin-1 null neurons. *J Cell Biol* 165:335–346.
- Wolfe DM, Lee J hyun, Kumar A, Lee S, Orenstein SJ, Nixon RA (2013) Autophagy failure in Alzheimer’s disease and the role of defective lysosomal acidification. *Eur J Neurosci* 37:1949–1961.
- Woodhouse A, Vickers JC, Adlard PA, Dickson TC (2009) Dystrophic neurites in TgCRND8 and Tg2576 mice mimic human pathological brain aging. *Neurobiol Aging* 30:864–874.
- Yamazaki H, Bujo H, Kusunoki J, Seimiya K, Kanaki T, Morisaki N, Schneider WJ, Saito Y (1996) Elements of neural adhesion molecules and a yeast vacuolar protein sorting receptor are present in a novel mammalian low density lipoprotein receptor family member. *J Biol Chem* 271:24761–24768.
- Yan P, Bero AW, Cirrito JR, Xiao Q, Hu X, Wang Y, Gonzales E, Holtzman DM, Lee J-M (2009) Characterizing the appearance and growth of amyloid plaques in APP/PS1 mice. *J Neurosci Off J Soc Neurosci* 29:10706–10714.
- Yan R, Gurney ME, Bienkowski MJ, Shuck ME, Miao H, Tory MC, Pauley AM, Brashler JR, Stratman NC, Mathews WR, Buhl AE, Carter DB, Tomasselli AG, Parodi LA, Heinrichson RL (1999) Membrane-anchored aspartyl protease with Alzheimer’s disease beta-secretase activity. *Nature* 402:533–537.
- Yan R, Shi Q, Hu X, Zhou X (2006) Reticulon proteins: Emerging players in neurodegenerative diseases. *Cell Mol Life Sci* 63:877–889.
- Yang L-B, Lindholm K, Yan R, Citron M, Xia W, Yang X-L, Beach T, Sue L, Wong P, Price D, Li R, Shen Y (2003) Elevated β -secretase expression and enzymatic activity detected in sporadic Alzheimer disease. *Nat Med* 9:3–4.
- Yang YS, Strittmatter SM (2007) The reticulons: A family of proteins with diverse functions.

- Genome Biol 8:234.
- Ye W, Zhou J-N, Hu X-Y, Liu J-W, He J-H, Tang X-W (2003) Reconstruction of the three-dimensional structure of senile plaques in Alzheimer disease. *Sheng Wu Hua Xue Yu Sheng Wu Wu Li Xue Bao (Shanghai)* 35:449–453.
- Ye X, Cai Q (2014) Snapin-mediated BACE1 retrograde transport is essential for its degradation in lysosomes and regulation of app processing in neurons. *Cell Rep* 6:24–31.
- Ye X, Feng T, Tammineni P, Chang Q, Jeong YY, Margolis DJ, Cai H, Kusnecov A, Cai Q (2017) Regulation of synaptic Amyloid- β generation through BACE1 retrograde transport in a mouse model of Alzheimer's disease. *J Neurosci* 37:2639–2655.
- Yoshida H, Goedert M (2002) Molecular cloning and functional characterization of chicken brain tau: isoforms with up to five tandem repeats. *Biochemistry* 41:15203–15211.
- Yuan A, Kumar A, Peterhoff C, Duff K, Nixon RA (2008) Axonal transport rates in vivo are unaffected by Tau deletion or overexpression in mice. *J Neurosci* 28:1682–1687.
- Zempel H, Luedtke J, Kumar Y, Biernat J, Dawson H, Mandelkow E, Mandelkow E-M (2013) Amyloid- β oligomers induce synaptic damage via Tau-dependent microtubule severing by TLL6 and spastin. *EMBO J* 32:2920–2937.
- Zhan SS, Kamphorst W, Van Nostrand WE, Eikelenboom P (1995) Distribution of neuronal growth-promoting factors and cytoskeletal proteins in altered neurites in Alzheimer's disease and non-demented elderly. *Acta Neuropathol* 89:356–362.
- Zhang X, Li Y, Xu H, Zhang Y-W (2014) The γ -secretase complex: from structure to function. *Front Cell Neurosci* 8:427.
- Zhang X, Song W (2013) The role of APP and BACE1 trafficking in APP processing and amyloid- β generation. *Alzheimers Res Ther* 5:46.
- Zhao J, Fu Y, Yasvoina M, Shao P, Hitt B, O'Connor T, Logan S, Maus E, Citron M, Berry R, Binder L, Vassar R, O'Connor T, Logan S, Maus E, Citron M, Berry R, Binder L, Vassar R (2007) β -Site Amyloid Precursor Protein cleaving enzyme 1 levels become elevated in neurons around Amyloid Plaques: implications for Alzheimer's Disease pathogenesis. *J Neurosci* 27:3639–3649.
- Zhong Q, Congdon EE, Nagaraja HN, Kuret J (2012) Tau isoform composition influences rate and extent of filament formation. *J Biol Chem* 287:20711–20719.
- Zhou L, McInnes J, Wierda K, Holt M, Herrmann AG, Jackson RJ, Wang YC, Swerts J, Beyens J, Miskiewicz K, Vilain S, Dewachter I, Moechars D, Strooper B De, Spires-Jones TL, Wit J De, Verstreken P (2017) Tau association with synaptic vesicles causes presynaptic dysfunction. *Nat Commun* 8:1–13.
- Zou C, Shi Y, Ohli J, Schüller U, Dorostkar MM, Herms J (2016) Neuroinflammation impairs adaptive structural plasticity of dendritic spines in a preclinical model of Alzheimer's disease. *Acta Neuropathol* 131:235–246.

